


 Cite this: *RSC Adv.*, 2020, **10**, 24893

Applications of Cu(0) encapsulated nanocatalysts as superior catalytic systems in Cu-catalyzed organic transformations

Majid M. Heravi, * Bahareh Heidari, Vahideh Zadsirjan * and Leila Mohammadi

Recently, Cu nanoparticles (NPs) encapsulated into various materials as supports (e.g., zeolite, silica) have attracted much devotion due to their unique catalytic properties such as high catalytic activity, intensive reactivity and selectivity through highly protective properties. Nowadays, the superior catalytic activity of Cu-NPs, encapsulated onto zeolite, silica and different porous systems, is extensively investigated and now well-established. As a matter of fact, Cu-NPs are protected from deactivation by this kind of encapsulation. Thus, their exclusion proceeds smoothly, and their recyclability is significantly increased. Cu-NPs have been used as potential heterogeneous catalysts in different chemical transformations. In this review, we try to show the preparation and applications of Cu(0) encapsulated nanocatalysts in zeolite and silica as superior catalytic systems in Cu-catalyzed organic transformations. In addition, the catalytic activity of these encapsulated Cu-NPs in different important organic transformations (such as hydrogenation, oxidation and carbon–carbon bond formations) are compared with those of a variety of organic, inorganic and hybrid porous bearing a traded metal ion. Moreover, the results from the TGA/DTA analysis and optical properties of Cu-complexes are demonstrated. The inherited characteristic merits of the encapsulated Cu-NPs onto zeolite and silica, such as their low leaching, catalytic activity, reusability economic feasibility and originality are critically considered.

 Received 12th March 2020
 Accepted 10th June 2020

 DOI: 10.1039/d0ra02341h
rsc.li/rsc-advances

1. Introduction

The art of organic synthesis has overgrown a captivating transformation over the past few decades. The applications of various transition-metal species as effective catalysts in catalytic processes have permitted the rapid and effective synthesis of both simple and structurally complex molecules. This is achieved using commercially available or easily accessible starting materials under mild and green reaction conditions.¹ The importance of transition-metal catalysis on the art of organic synthesis may be evaluated by the broad range and wide spectrum of molecules that have been synthesized. These molecules extend from simple ones, such as biaryls, to rather complex pharmaceutical intermediates, medication, and very complex structures.² Transition-metal-catalyzed catalysis has been divided into two major classes. They are homogeneous and heterogeneous catalysis, and both have their own merits and drawbacks. This classification, especially in practice, has given researchers in both academia and industry an opportunity to expand their choices.^{2b,3} Homogeneous catalysis has been developed as an influential synthetic tool due to the well-definite nature of the catalysts. Thus, the catalytic processes

can be studied from mechanistic and kinetic points of view. These developments have led the wide variety of commercial processes to use homogeneous catalysts as the chief catalytic species.⁴ In this regard, several industrial processes, such as, the important Ziegler–Natta polymerization, Wacker process, the Monsanto carbonylation process hydroformylation (Otto Roelen oxo process) and the SHOP process (Shell higher olefin process), use homogeneous catalysis.^{4c,d,5} The main drawback related to homogeneous catalysis is the problem of catalyst separation thus, an improvement strategy to circumvent this problem was found by anchoring the catalytic species to a solid support.⁶ A literature survey disclosed a plethora of reports over the past decade, underscoring the commanding nature of homogeneous catalysis in catalyzing such transformations.⁷ Transition metal complexes, having unique physio-chemical and structural properties, showed high catalytic activities under mild reaction conditions. Although they have been used as oxidizing agents of organic compounds by alchemists in the early age of chemistry as a science, they have been found to be useful as selective oxidation catalysts in the past five decades. Thus, transition metal complexes have attracted much interest from the chemical community.⁸ Cu(II), in particular, is well known as an appropriate and powerful oxidizing agent for various organic substrates. They show the merits of high selectivity. Thus, they can be considered as mild and compatible oxidizing agents, being found to exist in the 0, 1⁺, 2⁺, and 3⁺

Department of Chemistry, School of Science, Alzahra University, P. O. Box 1993891176, Vanak, Tehran, Iran. E-mail: mmheravi@alzahra.ac.ir; mmh1331@yahoo.com; z_zadsirjan@yahoo.com; Fax: +98 21 88041344; Tel: +98 21 88044051



oxidation states.⁹ The catalytic-selective oxidation reaction of aromatic compounds in the presence of heterogeneous and reusable catalysts under mild (nearby ambient) and green reaction conditions using “clean oxidants”, such as molecular oxygen and hydrogen peroxide, has been an overgrowing field of investigation in recent years.¹⁰ The oxidation and hydroxylation reactions of aromatic compounds by O₂ extensively take place in nature. In this regard, the homogeneous copper-(N-base)-O₂ systems have been selected as a model for biological processes of Cu-bearing proteins, including tyrosinase and hemocyanin.¹¹ For example, the copper-pyridine-O₂ system, has been found as an active homogeneous catalyst for the efficient oxidative coupling of aromatic acetylenes,¹² phenols¹³ and amines.¹⁴ In recent years, different homogeneous catalysts have been converted to their heterogeneous counterparts with the well-known advantages over homogeneous catalysts, such as the ease of separation from the reaction mixture, effective reusability for several times and being utilized in continuous flow processes.¹⁵ It is worth mentioning that heterogeneous catalysts often show limited activity and selectivity.¹⁶ Different methods for the heterogenization of homogeneous catalytic systems to render the catalyst and the product(s) are known. The homogeneous catalyst can be immobilized onto different solid supports.¹⁷ In general, immobilization comprises the interaction of two entities known as the biomaterial (as an immobilizer) and an immobilization agent. Various immobilization methods are expected to have a bright future in the field of pharmacy, medicine or industry. Biocatalyst re-usage will significantly decrease the costs. Immobilization in nanodelivery systems may soon dominate the field of medical sciences. The vast problem of civilization diseases is the difficulty in the administration of medication, either due to the size of the drug or the inaccessibility of the treated site. The method chosen for immobilization depends on the suitability of both entities to react, and it forms a stable and appropriate immobilized phase. Characteristically, the biomaterials employed as an immobilizer are an insoluble matrix, which is inactive with the neighboring and also its immobilized agent. An immobilized system is provided to attain its specific objective, for example, to achieve a supporting immobilization, to enhance agent reusability, purification, process control or as sequential immobilization either to enhance the rate of release or prolong it.¹⁸ Different immobilization methods were developed and reported.^{17a} These techniques were classified into two main distinct physical and chemical immobilizations. This classification is based on its preparation method. Nevertheless, nowadays, immobilization can be achieved by combining multiple disparities of immobilizations.

1.1. Supporting materials

1.1.1. Zeolite. The need for a novel and sophisticated synthetic strategy gives rise to a rapidly and increasingly development of a collection of solid supports.¹⁹ Several solid supports, including composite materials and functionalized surfaces, are suitable for such purpose.²⁰ In the process of selecting the proper support, it is important to consider the

optimal performance during solid-phase synthesis.²¹ To this purpose, mesoporous materials have been extensively used.²² Mesoporous materials contain pores with diameters between 2 and 50 nm.²³ They are extensively used as adsorbents,²⁴ catalysts,²⁵ and supports of active centers or host-guest²⁶ for different kinds of molecules. One of the most versatile types of mesoporous materials is porous silica with its well-defined pore sizes, which have a wide range of applications due to its biocompatibility.²⁷ In addition, different kinds of zeolites can be used as microporous solid supports.²⁸ Aluminosilicate minerals are also commonly employed as commercial adsorbents, catalysts and supports.²⁹ The term zeolite was formerly coined by the Swedish Mineralogist, Axel F. Cronstedt, in 1756.³⁰

Zeolites are also useful as catalysts, sorbents and solid supports. Their well-defined pore structure and variable acidity make them very active catalysts in the catalysis of a wide range of organic transformations.³¹ Zeolites are crystalline microporous aluminosilicates, which are made from corner-sharing SiO₄⁻ and AlO₄⁻ tetrahedra. These porous materials are generated in nature as a result of volcanic activity. Nowadays, a collection of zeolites can be easily prepared in the standard chemistry laboratory. To date, about 300 different kinds of zeolites have been prepared and fully characterized. The homogeneous Cu-pyridine system has been immobilized onto zeolites, converting it into a heterogeneous catalyst with the same active species. The intracrystalline cages or channel structures of zeolites were prepared. After full characterization, they were successfully employed as a heterogeneous catalyst in organic transformation.³²

Moreover, the mechanically stable beaded gel resins can be used as support. Several metal catalysts have been immobilized onto resins, and polymers were used as heterogeneous catalysts in different chemical transformations. This led to the selective oxidation of alcohols into the corresponding carbonyl compounds,³³ and the construction of different heterocyclic systems.³⁴ Different metal nanoparticles (MNPs) can also be loaded to different supports to effectively act as heterogeneous catalysts.³⁵ In such heterogeneous catalysts, the metal particle size and oxidation state are considered for selecting an appropriate oxidation catalyst. Furthermore, it is well-recognized that the reactivity and selectivity of monodisperse metal NPs can be improved by changes in their size and shape.³⁶

Yuji and co-workers successfully fixed a Cu-pyridine derivative complex on silica. It was subjected to a reversible redox cycle between copper(II) and copper(I), and applied successfully as a catalyst for the oxidative coupling reaction of methyl-acetylene.^{12,37} The design and improvement of an eco-friendly catalytic method is of urgent significance. The immobilization of homogeneous metal complexes on solid supports (including alumina, silica and polymers) has been investigated widely in order to provide heterogeneous catalysts with the desirable structure to act effectively, and show other advantages expected from a heterogeneous catalysts.

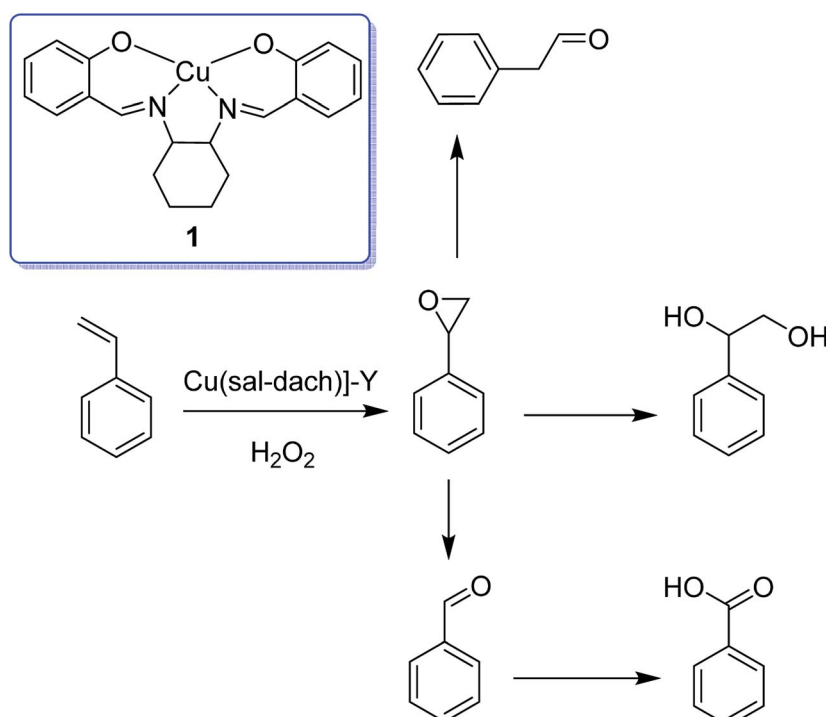
1.1.2. Silica. Silicon dioxide, as an oxide of silicon with the chemical formula SiO₂, was also found to be a suitable support as silica. It is known in nature as quartz and present in different



Table 1 Aerobic oxidation reaction of *p*-xylene over zeolite-encapsulated copper salens^a

Catalyst	Products (wt%)					4-Carboxy benzyl alcohol, 4-carboxy benzaldehyde and traces of terephthalic acid
	<i>p</i> -Xylene conversion (%)	TOF (h ⁻¹)	<i>p</i> -Toluic acid	<i>p</i> -Tolualdehyde	<i>p</i> -Tolualcohol	
CuSal-X	45.1	182 285	46.3	29	13.5	11.1
CuCl ₂ Sal-X	48.9	92 200	37.8	33.3	14.7	14.1
CuBr ₂ Sal-X	47.9	28 829	39.6	35	13.3	11.9
Cu(NO ₃) ₂ Sal-X	50.9	5238	38.7	29.6	19.4	12.2

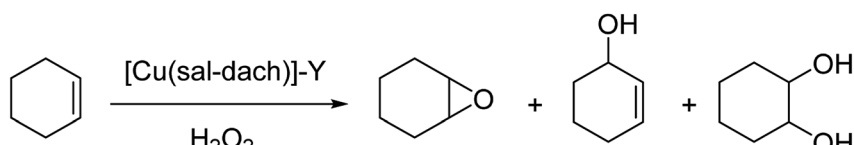
^a Reaction conditions: *p*-xylene, catalyst, 0.5 g TBHP, 403 K, 18 hours.



Scheme 1 Oxidation reaction of styrene in the presence of [Cu(sal-dach)]-Y as an efficient catalyst.

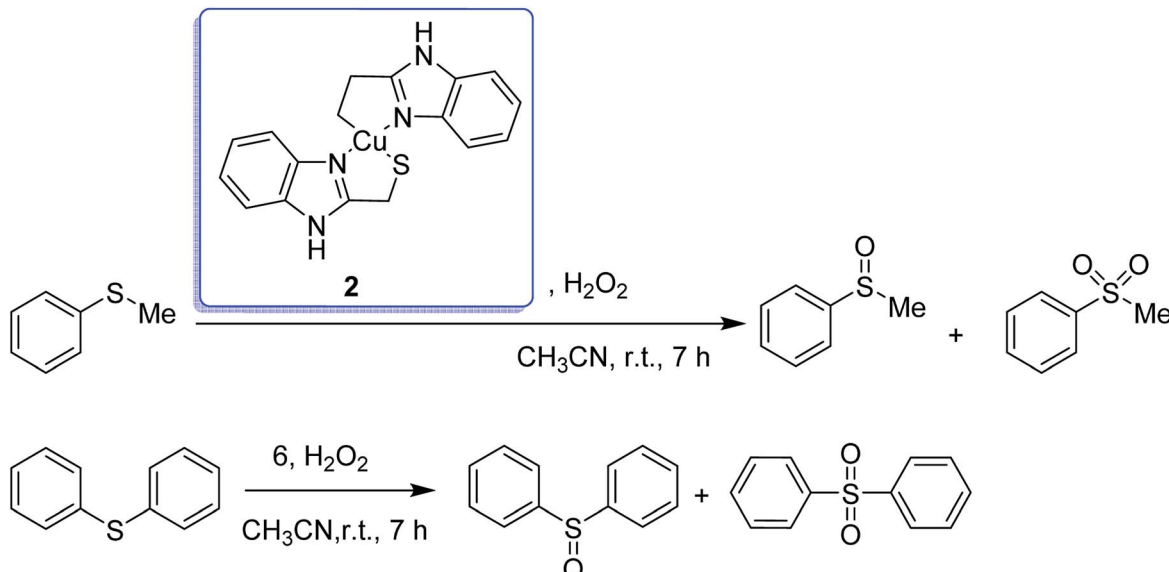
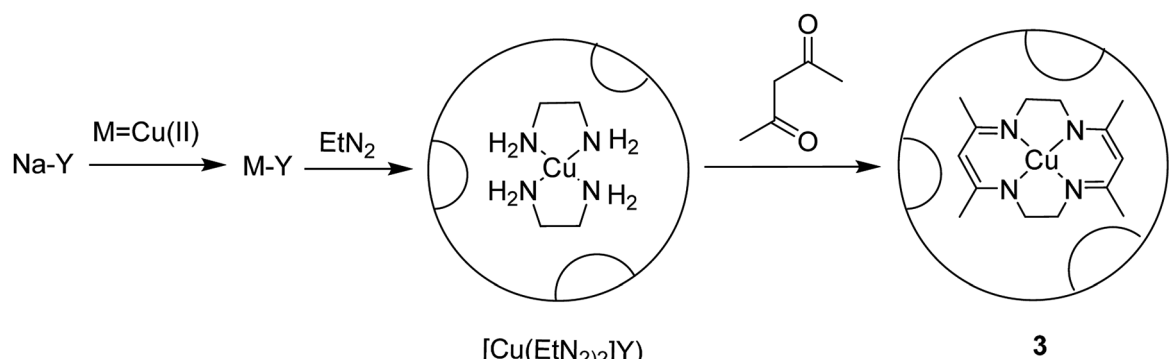
living organisms.³⁸ Silica-based materials are one of the most studied and applied systems for the immobilization of NPs.³⁹ The supreme structural properties of silica as supports are their appropriate pore (channel) size, pore volume, and surface area, making the encapsulated Cu species into the stable and highly active heterogeneous catalysts. Thus, a series of various sorts of silica materials have been employed for the encapsulation of various NPs, which were successfully used as effective catalysts

in various organic transformations.⁴⁰ Apart from the above-mentioned strategy for the heterogenization of a homogeneous catalyst, encapsulation can be used. The prepared metal encapsulated materials can be employed as effective catalysts in a wide variety of organic transformations. In chemistry, molecular encapsulation involves the confinement of an individual metal within a larger molecule. We are interested in heterogeneous catalyzed organic transformations.⁴¹ Recently,



Scheme 2 Oxidation reaction of cyclohexene in the presence of [Cu(sal-dach)]-Y as an efficient catalyst.



Scheme 3 Oxidation products of methyl phenyl sulfide and diphenyl sulfide in the presence of $[\text{Cu}(\text{tmbmz})_2]\text{-Y}$.

Scheme 4 Synthesis of Y-encapsulated Cu complex (3).

our group reported the catalytic applications of a Pd-encapsulated species in organic transformations. We underscored the applications of the Pd(0) encapsulated species as efficient and reusable catalysts in C-C bond formations.⁴² In recent years, our group has been engaged in heterogeneous copper-catalyzed organic transformations.^{33,34,43} In continuation of these interests in the applications of heterogeneous Cu species catalyzed reactions, we try to highlight in this review the applications of Cu-encapsulated species on organic transformations. We also try to reveal their advantages in comparison with naked Cu species as superior heterogeneous catalysts.

2. Applications of Cu(0) encapsulated nanocatalysts as superior catalytic systems in Cu-catalyzed organic transformations

2.1. Zeolite-encapsulated Cu NPs

2.1.1. Oxidation reactions. Principally, two main approaches have been reported in transition metal complexes that were encapsulated in zeolites, including the flexible ligand methods (FLM) and zeolite synthesis (ZS).⁴⁴ In the zeolite

Table 2 Epoxidation reaction of styrene using $[\text{CuMe}_4\text{[Et]}_2\text{[14]tetraeneN}_4]\text{-Y}$ (3)

Catalyst	Metal content Cycle (mmol g ⁻¹)	Styrene conversion (%)	Product selectivity (mol%)		
			TOF (h ⁻¹)	styrene oxide, benzaldehyde, benzoic acid, phenyl acetaldehyde	
$[\text{CuMe}_4\text{[Et]}_2\text{[14]tetraeneN}_4]\text{-Y}$ 1	0.110	68	154.5	40.0, 54.5, 5.0	
$[\text{CuMe}_4\text{[Et]}_2\text{[14]tetraeneN}_4]$ 1	1.581	27	4.3	35.4, 39.3, 25.3	



Table 3 The effect of various catalysts in the aerobic oxidation reaction of styrene

Entry	Catalyst	M (mmol g ⁻¹) total	Styrene conversion (%)	TOF (h ⁻¹)	Product		Selectivity (%)
					Styrene oxide	Benzaldehyde	
1	Fe-Y	0.204	60.6	74.3	30.1	61.7	8.2
2	FeQ ₃	2.048	80.1	89.4	43.2	56.8	0
3	FeQ ₃ -Y	0.224	83.4	93.1	24.5	58.2	17.3
4	FeQ ₃ -Y (2nd)	0.217	74.2	85.5	37.4	60.7	1.9
5	Fe-Y + FeQ ₃ d	0.518	66.5	74.7	45.1	51.5	3.4
6	Co-Y	0.080	63.3	197.8	33.2	58.5	8.3
7	CoQ ₂	2.880	51.0	117.0	46.2	53.0	0.8
8	CoQ ₂ -Y	0.109	56.7	130.0	39.2	59.6	1.2
9	Cu-Y	0.065	54.2	208.5	30.8	62.8	6.4
10	CuQ ₂	2.840	61.8	441.4	40.4	59.6	0
11	CuQ ₂ -Y	0.045	89.3	637.9	31.0	59.0	10.0

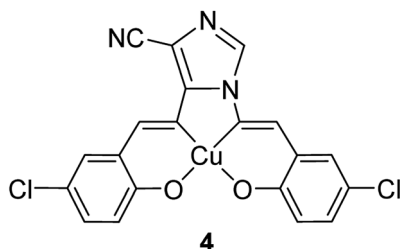
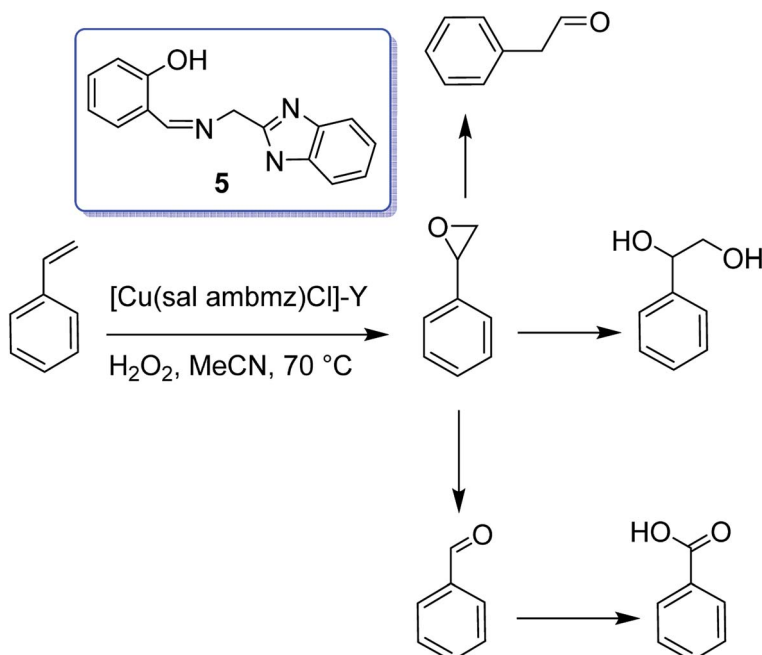


Fig. 1 Molecular structure of complex 4.

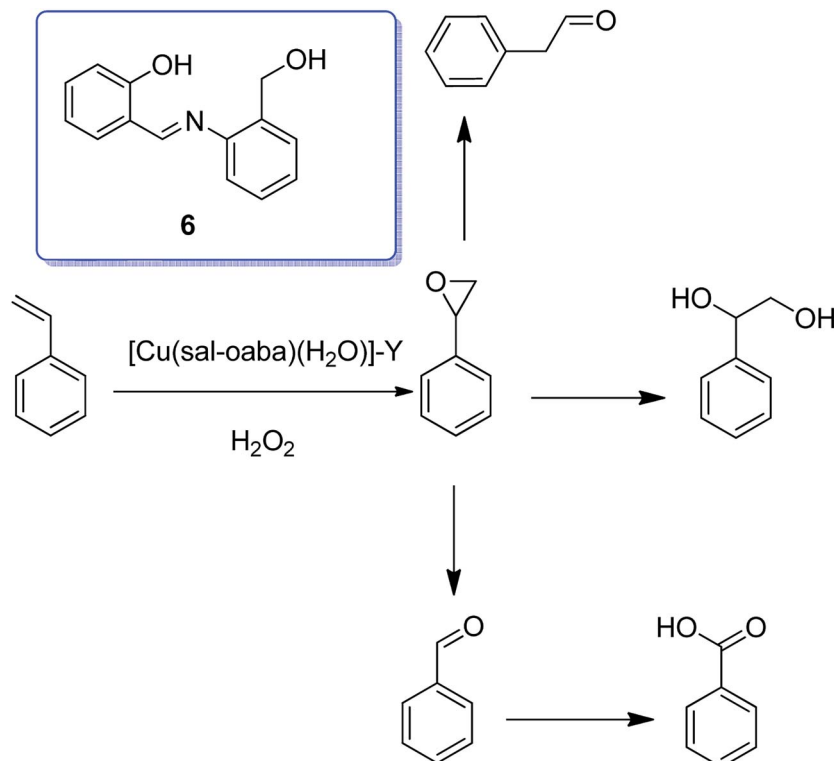
synthesis method, transition metal complexes, which are stable under the conditions of zeolite synthesis (such as high pH and elevated temperatures) are included in the synthesis mixture. It

is noteworthy that transition metal complexes were placed into the voids of the resultant zeolites. The phthalocyanines of Fe and Cu encapsulated in zeolites X and Y give instances of these types of catalysts.⁴⁵ In the FL method, a flexible ligand is able to diffuse easily through the zeolite pore complexes with a formerly exchanged metal ion. The resultant complex is very huge and breaks off to escape the cages. Notably, this method is appropriate for the encapsulation of metal-salen complexes as the salen ligand affords the expected flexibility. Thus, various Co, Mg, Fe, Rh and Pd salen complexes were provided *via* flexible ligand method in the Y-faujasite supercages.⁴⁶ In 1998, Ratnasamy and coworkers demonstrated the encapsulation of the Cu (X₂-salen) complex, in which salen²⁺ = *N,N'*-ethylene bis(salicylideneaminato) and X = H, Cl, Br or (NO₂) in the



Scheme 5 The oxidation reaction of styrene.



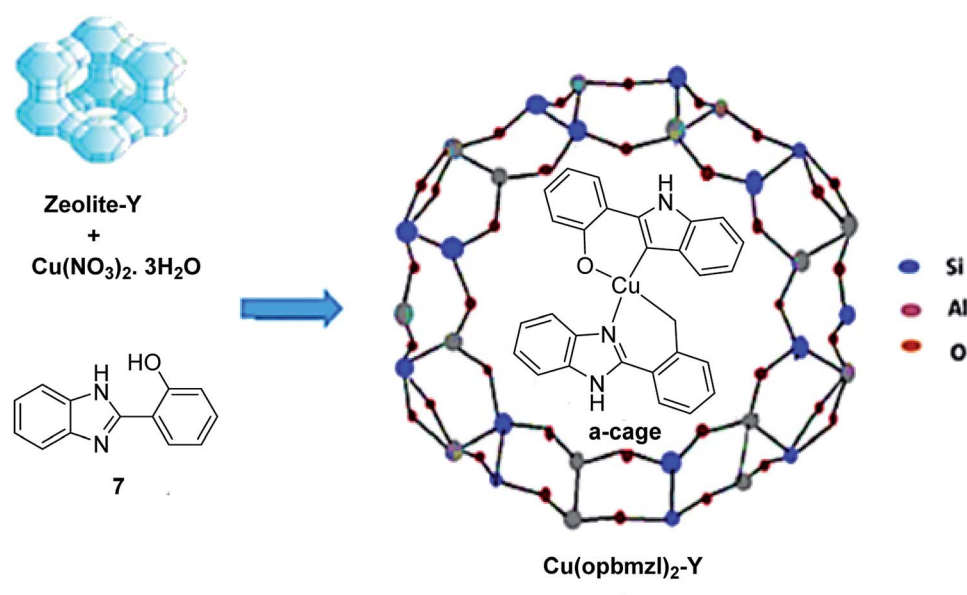


Scheme 6 Oxidation reaction of styrene in the presence of $[\text{Cu}(\text{sal-oaba})(\text{H}_2\text{O})]\text{-Y}$ using hydrogen peroxide.

cavities of zeolites NaX and NaY.⁴⁷ The thermal degradation pattern for CuSal-Y(FL) exhibits a two-step loss; the first is related to the removal of four intrazeolite water molecules and the second is related to the decomposition of the chelate scaffold. In comparison with the free chelate (550 K), the

decomposition of the zeolite-encapsulated chelate structure happens at an increased temperature (700 K).

Notably, the substitution of the aromatic hydrogen atoms in the salen ligand with electron-withdrawing groups (including $-\text{Br}$, $-\text{Cl}$, and NO_2 groups) have two main influences: the



Scheme 7 Schematic illustration of the preparative pathway for $\text{Cu}(\text{opbmzl})_2\text{-Y}$ **8** via flexible ligand method. Reprinted from (ref. 56) with permission of the Royal Society of Chemistry.

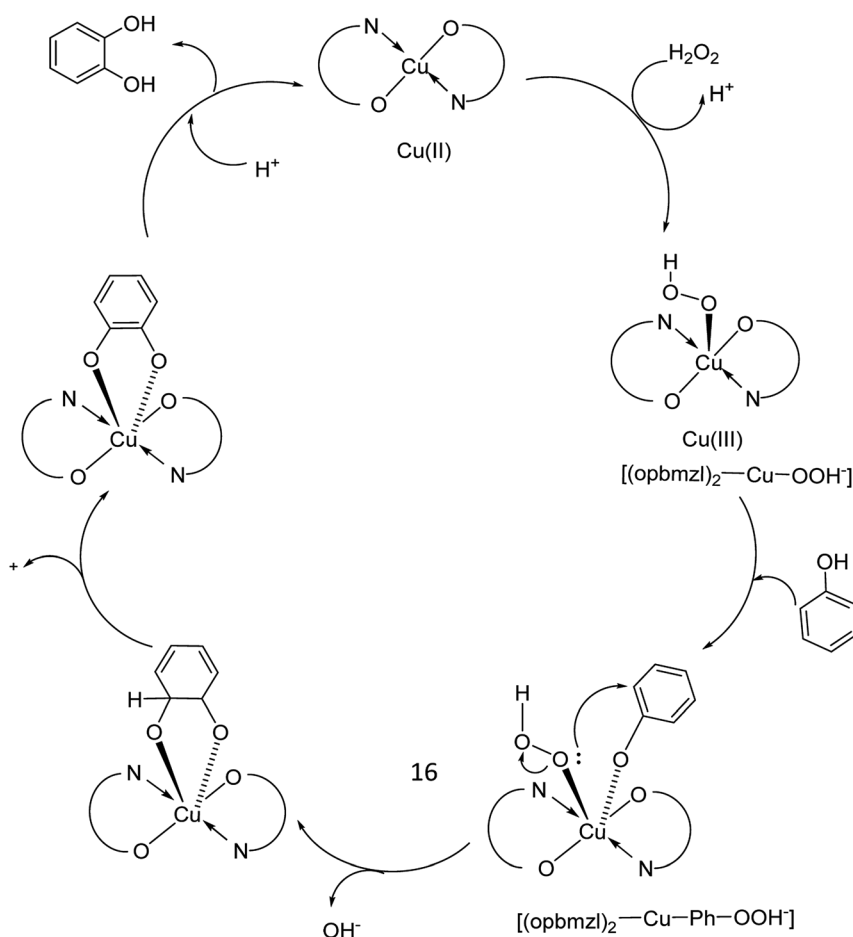


retention and concentration of the Cu complex in the zeolite cavities are improved (due to the larger size of the groups), and the spectral properties of the encapsulated complex are also changed. Remarkably, the catalytic activity of the encapsulated copper salen in the decomposition of hydrogen peroxide, *tert*-butyl hydroperoxide (TBHP) and also the peroxidative oxidation of styrene, phenol and *para*-xylene were examined. For the oxidation of styrene under this condition, the major products benzaldehyde, phenyl acetaldehyde and styrene oxide were provided with the minor quantities of benzene-1,2-ethane diol and benzoic acid. In addition, hydrogen peroxide catalyzed the peroxidative oxidation of phenol (to hydroquinone and catechol), which is related linearly (major) to the catalytic efficacy of the encapsulated copper salens. The major products of oxidation of *p*-xylene are *p*-toluic acid, *p*-toluyl alcohol and also *p*-tolualdehyde (Table 1).

The zeolite-Y encapsulated metal complex, $[\text{Cu}(\text{sal-dach})]\text{-Y}$, was synthesized by the reaction of *N,N*-bis(salicylidene) cyclohexane-1,2-diamine ($\text{H}_2\text{sal-dach}$) and Cu(II) exchanged zeolite-Y under reflux condition in methanol. Outstandingly, this encapsulated complex catalyzed the oxidation reaction of styrene, cyclohexane and cyclohexene using H_2O_2 (ref. 48) (Schemes 1 and 2). Under the optimal conditions, the oxidation reaction of styrene catalyzed by (1) gave 21.7% conversion with

four products, including benzaldehyde (69.0%), styrene oxide (12.9%), phenyl acetaldehyde (12.0%) and benzoic acid (7.1%). Based on this method, the conversion of cyclohexene to cyclohexene oxide, 2-cyclohexene-1-one, 2-cyclohexene-1-ol, and cyclohexane-1,2-diol as major products with $[\text{Cu}(\text{sal-dach})]\text{-Y}$ was 18.1%. A maximum of 78.1% of cyclohexane with $[\text{Cu}(\text{sal-dach})]\text{-Y}$ was produced in which the selectivity of three main products follows the sequence: cyclohexanol > cyclohexane-1,2-diol > cyclohexanone.

The encapsulation of the copper(II) complex of monobasic bidentate NS donor ligand, 2-mercaptopethylbenzimidazole (Htmbmz) (2) in the cavity of zeolite-Y was achieved *via* flexible ligand method. $[\text{Cu}(\text{tmbmz})_2]\text{-Y}$ was used as a catalyst in the oxidation of styrene, diphenyl sulfide and methyl phenyl sulfide.⁴⁹ Under the optimized condition, the conversion of styrene in the presence of $[\text{Cu}(\text{tmbmz})_2]\text{-Y}$ has poor efficiency (36.9%). It should be mentioned that four products (including benzaldehyde, styrene oxide, benzoic acid and phenyl-acetaldehyde) were produced. Outstandingly, this catalyst is very active in the oxidation of diphenyl sulfide and methyl phenyl sulfide (Scheme 3). The oxidation of diphenyl sulfide was achieved in the presence of at least hydrogen peroxide to diphenyl sulfide in a molar ratio of 3 : 1 to give 91.7% conversion in 7 hours. However, 94.3% conversion of methyl phenyl



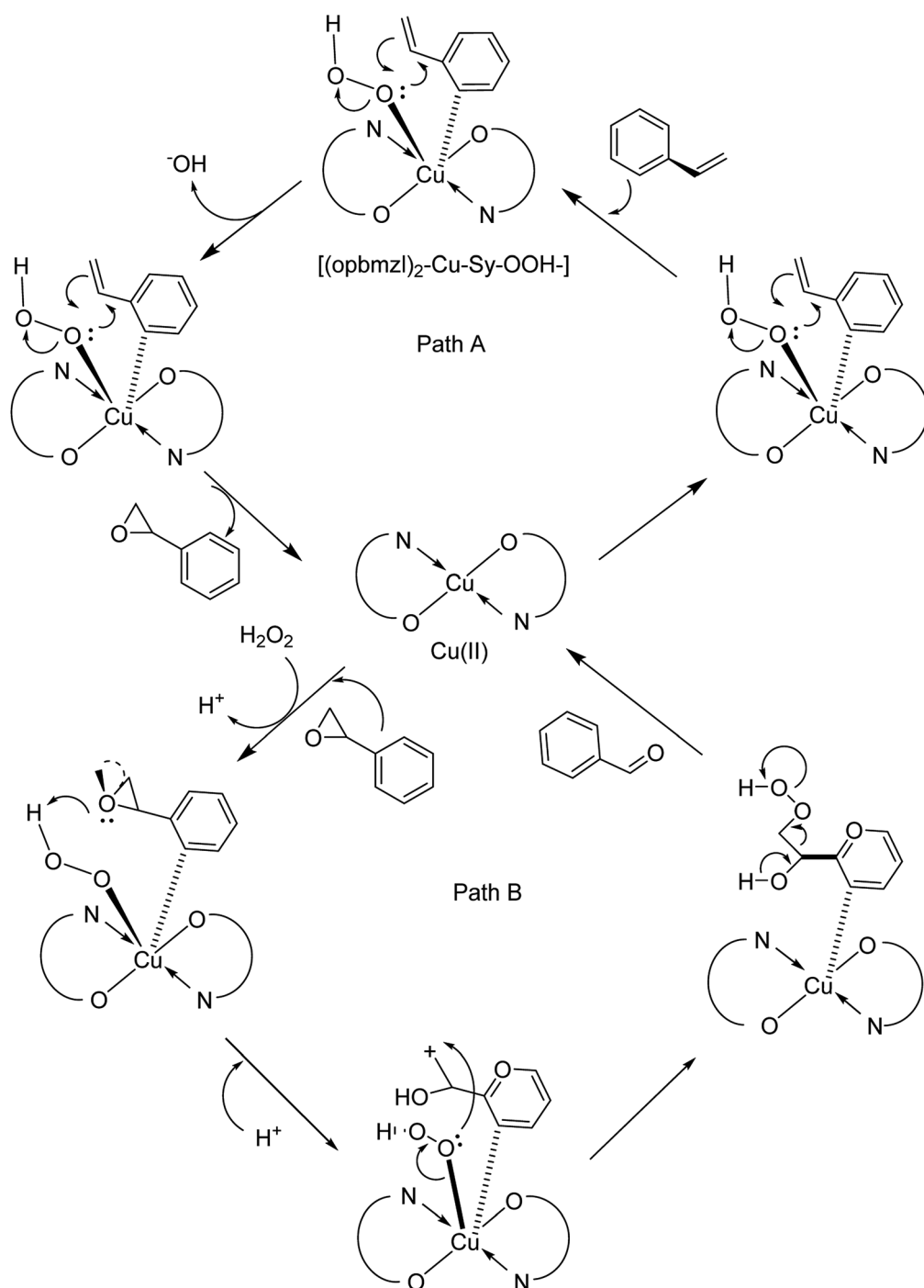
Scheme 8 Suggested probable mechanistic route for the oxidation of phenol.



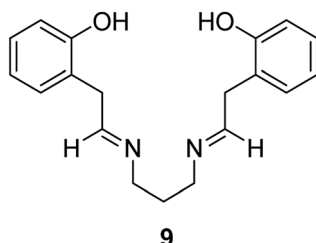
sulfide was obtained in 3 hours of contact time at a precursor to hydrogen peroxide molar ratio of 1 : 1.

The tetraazamacrocyclic complex of copper(II) encapsulated into zeolite-Y $[(\text{CuMe}_4)_2[14]\text{tetraNe}_4]_Y$ (3) was synthesized and used as a heterogeneous catalyst for the aerobic oxidation of styrene (Scheme 4).⁵⁰ This complex was constructed *via* a ship-in-a-bottle method in which the transition metal cations were ion-exchanged into zeolite-Y and reacted with ethylenediamine, and subsequently by acetylacetone.

In this method, to synthesize Na-Y, sodium hydroxide and NaAlO_2 were dissolved in water and silica sol was gradually added to it at ambient temperature. The desired Na-Y product was obtained. For the synthesis of the M^{n+} -exchanged-Y zeolites, Na-Y was then added to a solution of $[\text{Cu}(\text{OAc})_2]$ in water, and the mixture was refluxed at 90 °C. The formation of the $[\text{Cu}(\text{EtN}_2)_2]$ -Y catalyst was adapted depending on the usual method, and ethylenediamine was added to the resulting Cu-Y in MeOH at 80 °C. Acetylacetone was added to a suspension of



Scheme 9 Suggested probable mechanistic route for the oxidation of styrene

Fig. 2 The formation of transition metal complexes of ($H_2\text{salpn}$) 9.

$[\text{Cu}(\text{EtN}_2)_2]\text{Y}$ in MeOH at 80 °C. Lastly, the desired Cu-encapsulated catalyst was successfully synthesized (Scheme 4).

$[(\text{CuMe}_4)_2[14]\text{tetraeneN}_4]\text{Y}$ (3) was used as heterogeneous catalyst for the aerobic oxidation of styrene. The recoverability and stability of $[\text{Cu}(\text{Me}_4\text{Et})_2[14]\text{tetraeneN}_4]\text{Y}$ was explored. The results demonstrated that the catalyst could be effectively recycled three times without reducing the efficacy and selectivity.

In addition, to explore the heterogeneity of this catalytic method, a leaching examination was accomplished. For this purpose, the catalyst was eliminated using filtration at the reaction temperature (80 °C). Subsequently, the filtrated catalyst was known to transform styrene at only a very low rate. The quantity of Cu in the filtrate was known to be insignificant using ICP-AES. Therefore, the majority of the catalysis is actually heterogeneous.

It should be mentioned that, the homogeneous complex $\text{CuMe}_4(\text{Et})_2[14]\text{tetraeneN}_4$ exhibited lower activity in comparison with the relevant heterogeneous complexes under the analogue conditions (Table 2).

The encapsulation of copper(II) complexes of 8-quinolinol into the supercages of zeolite-Y (CuQ_nY) was achieved *via* the flexible ligand method.⁵¹ In this route, the transition metal cations were initially ion-exchanged into zeolite-Y and subsequently complexed by an 8-quinolinol ligand. Next, the catalytic activity of the metal-exchanged zeolites, metal complexes encapsulated into zeolite-Y and non-encapsulated homogeneous catalysts were examined in the aerobic oxidation of styrene. Strikingly, it was found that the encapsulated complexes constantly demonstrated greater activity in comparison with their corresponding non-encapsulated counterparts. Table 3 illustrates the results for the aerobic oxidation of styrene in the presence of various catalysts. It should be mentioned that except for Na-Y, all metal-exchanged zeolites and metal complexes either encapsulated or did not exhibit catalytic activity. This shows that the active sites were replaced metal ions and encapsulated metal complexes. Indeed, based

on the elemental analysis, most of the replaced transition metals in MQ_nY are linked with 8-quinolinol, namely 88.9% for CuQ_2Y . This demonstrates that the performance of MQ_nY is mostly performed with the encapsulated metal complexes and not with the replaced metal ions. CuQ_2Y is more active than its corresponding metal exchanged zeolites and neat metal complexes. Remarkably, the encapsulated metal complexes show different advantages in comparison with their homogeneous equivalents. Notably, the catalytic activity of MQ_nY is greater in comparison with its corresponding nonencapsulated complexes (Table 3, entries 10 and 11), which is due to the site-isolation of the metal complexes.⁵²

Two heterogeneous catalysts based on the copper(II) complexes bearing the 1,5-bis((E)-5-chloro-2-hydroxybenzylideneamino)-1*H*-imidazole-4-carbonitrile ($H_2\text{-imida-salen}$) ligand (4) (Fig. 1) were considered as candidates in the styrene oxidation reaction.⁵³ In this route, the non-encapsulated and encapsulated copper complexes were applied as catalysts in the oxidation of styrene using *tert*-butylhydroperoxide as the oxygen source and CH_3CN as the solvent. Under the optimized reaction conditions, the catalysts exhibited good activity with greater selectivity to benzaldehyde. It is noteworthy that no Cu leaching was detected during the reaction cycle.

Interaction of the copper(II) exchanged zeolite-Y with the Schiff base produced from 2-aminomethylbenzimidazole ($H\text{-salambmz}$) (5) and salicylaldehyde afforded the encapsulated copper(II) complex $[\text{Cu}(\text{sal ambmz})\text{Cl}]\text{Y}$.⁵⁴ Under optimal reaction conditions, about 42% conversion of phenol was provided in the presence of this catalyst in which the selectivity of catechol changed in the order (73.9% and 56.7% conversion of styrene), and also the oxidation of styrene gave benzaldehyde,

Table 4 Oxidation of phenol using *tert*-butyl hydroperoxide in the presence of metal pyrrolylazine complexes^a

Entry	Run	Catalyst	T^b (h)	%C ^c	CAT		Others		
					%S	%Y	%S ^d	%Y ^e	
1	1	NaY	48	4	—	—	—	—	—
2	1	$\text{Cu}_2\text{L}@\text{Y}_B$	6	86	61	53	39	33	
3	2		24	67	100	67	0	0	
4	1	$\text{Cu}_2\text{L}@\text{Y}_A$	24	34	50	17	50	17	
5	2		<24	38	100	29	0	0	

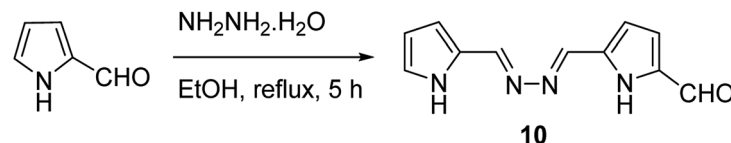
^a Reaction conditions: PhOH, 1 : 3 PhOH : *t*BuOOH, heterogeneous catalyst.

^b Reaction time at which the PhOH conversion starts to become constant.

^c Reaction runs under homogeneous conditions.

^d Equivalent 100 mg of $\text{Fe}_2\text{L}@\text{Y}$.

^e Equivalent 100 mg of $\text{Fe}_2\text{L}@\text{Y}_B$.



Scheme 10 Synthesis of the pyrrolyl-azin derivative.



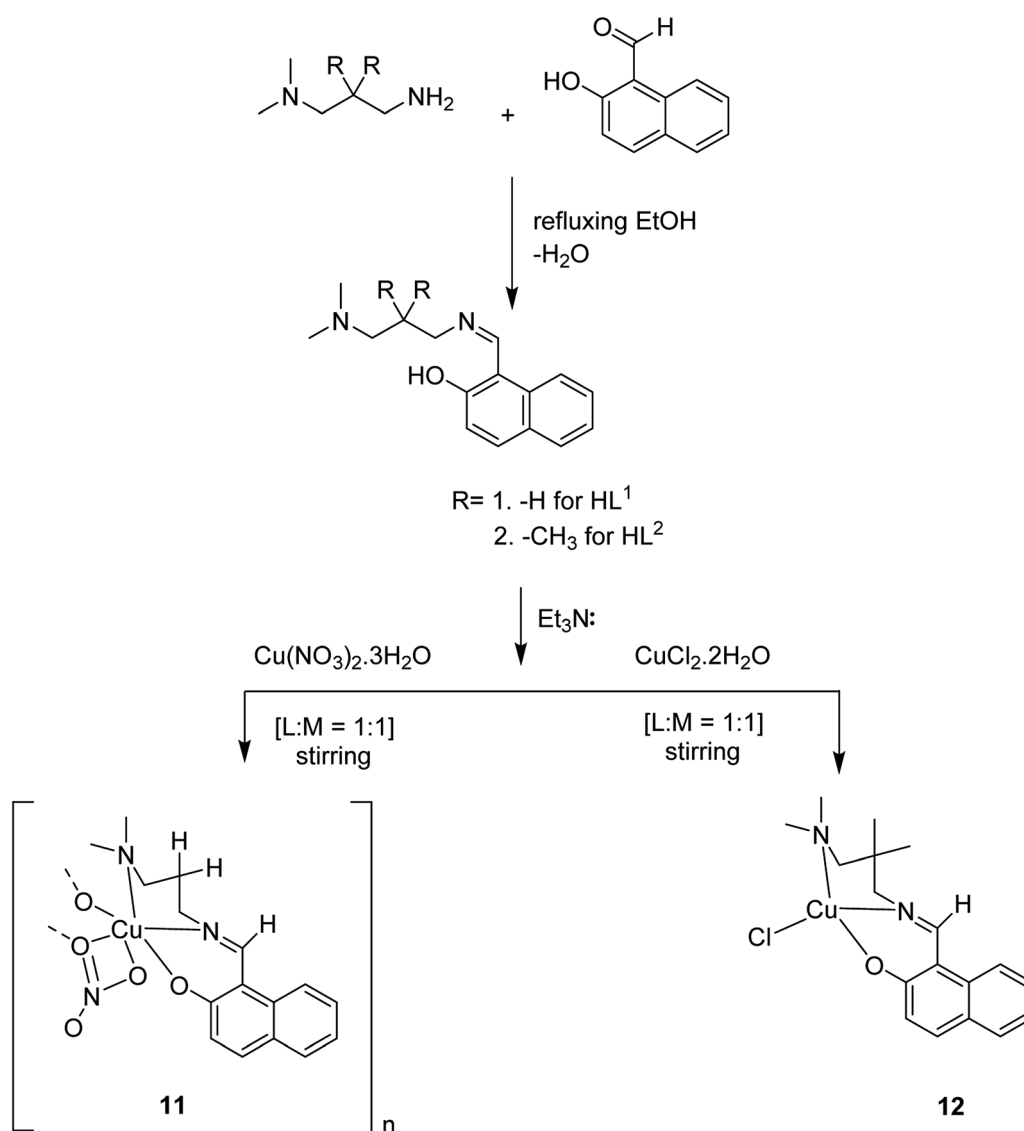
phenylacetaldehyde, styrene oxide, benzoic acid, and 1-phenylethane-1,2-diol as major products (Scheme 5).

The copper(II) complex of the Schiff base generated from the reaction of *o*-aminobenzyl alcohol and salicylaldehyde ($\text{H}_2\text{sal-oaba}$) was encapsulated into the nanopores of zeolite-Y through the flexible ligand method.⁵⁵ The TGA results for $[\text{Cu}(\text{sal-oaba})(\text{H}_2\text{O})]\text{-Y}$ demonstrated its decomposition in three stages. The exothermic elimination of only trapped H_2O of *ca.* 4.7% happened up to 150 °C, although an exothermic weight loss of *ca.* 8.0% related to the elimination of intra-zeolite water happened in the temperature range from 150 °C to 350 °C. The encapsulated complex had one or more coordinated water molecules, and their elimination in this stage was also anticipated. In addition, the third stage included the slow exothermic weight loss of *ca.* 15.6% in a wider temperature range because of the decomposition of the metal complex. A low weight loss percentage in the higher temperature range is in agreement

with the low percentage of metal content obtained for the encapsulated complexes.

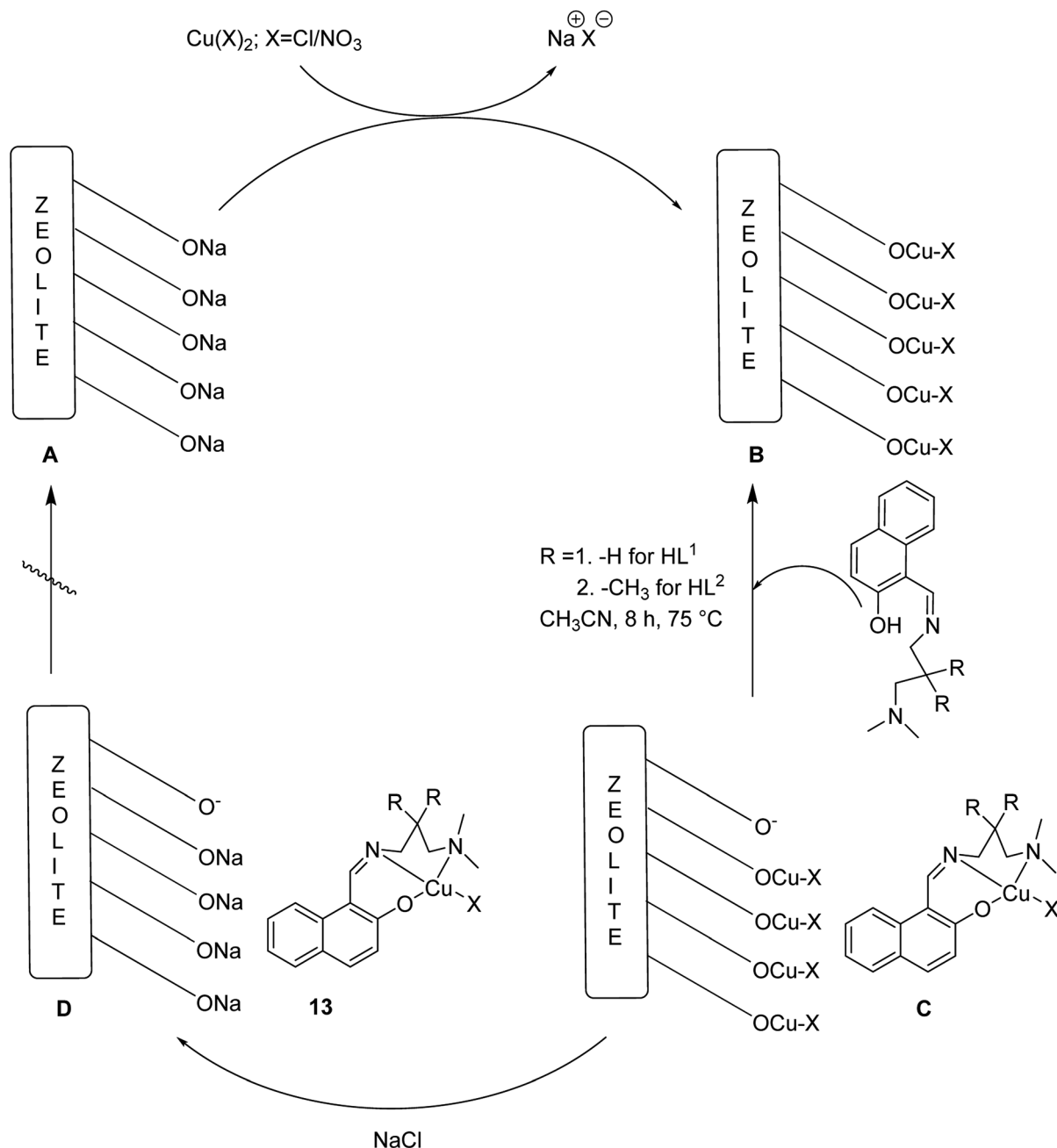
Notably, the encapsulated complex $[\text{Cu}(\text{sal-oaba})(\text{H}_2\text{O})]\text{-Y}$ catalyzed the oxidation of cyclohexane and styrene using H_2O_2 as oxidant. Styrene in the presence of $[\text{Cu}(\text{sal-oaba})(\text{H}_2\text{O})]\text{-Y}$ (6) as catalyst gave five reaction products, including styrene oxide, benzaldehyde, phenylacetaldehyde, benzoic acid and 1-phenylethane-1,2-diol (Scheme 6). It is noteworthy that styrene oxide was produced only in poor yield, while the yield of benzaldehyde was the maximum. This catalyst, using *tert*-butylhydroperoxide, gave styrene oxide in the main yield. However, the overall conversion was low (10–30%). Using $[\text{Cu}(\text{sal-oaba})(\text{H}_2\text{O})]\text{-Y}$ with 45.8% conversion of cyclohexane, the selectivity of the two products follow the sequence: cyclohexanone (50.7%) > cyclohexanol (44.8%).

In 2016, Gayathri and co-workers reported the formation of a copper complex of 2-(2'-hydroxyphenyl)benzimidazole (ohpbmzl) (7) encapsulated into the cavity of zeolite-Y (8) *via* the



Scheme 11 Construction of Schiff-base ligands HL^1 and HL^2 , and their Cu(II) complexes (11 and 12).

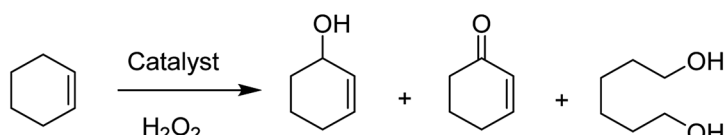




Scheme 12 Synthesis of heterogeneous catalysts via metal (M = Cu) incorporation followed by immobilization of the Schiff base ligands into the zeolite, NaY.

flexible ligand method (Scheme 7).⁵⁶ The catalytic activity of the non-encapsulated and encapsulated Cu-Y complex was explored in the oxidation reaction of phenol and styrene. Hydroquinone, catechol, and parabenoquinone were the only major products

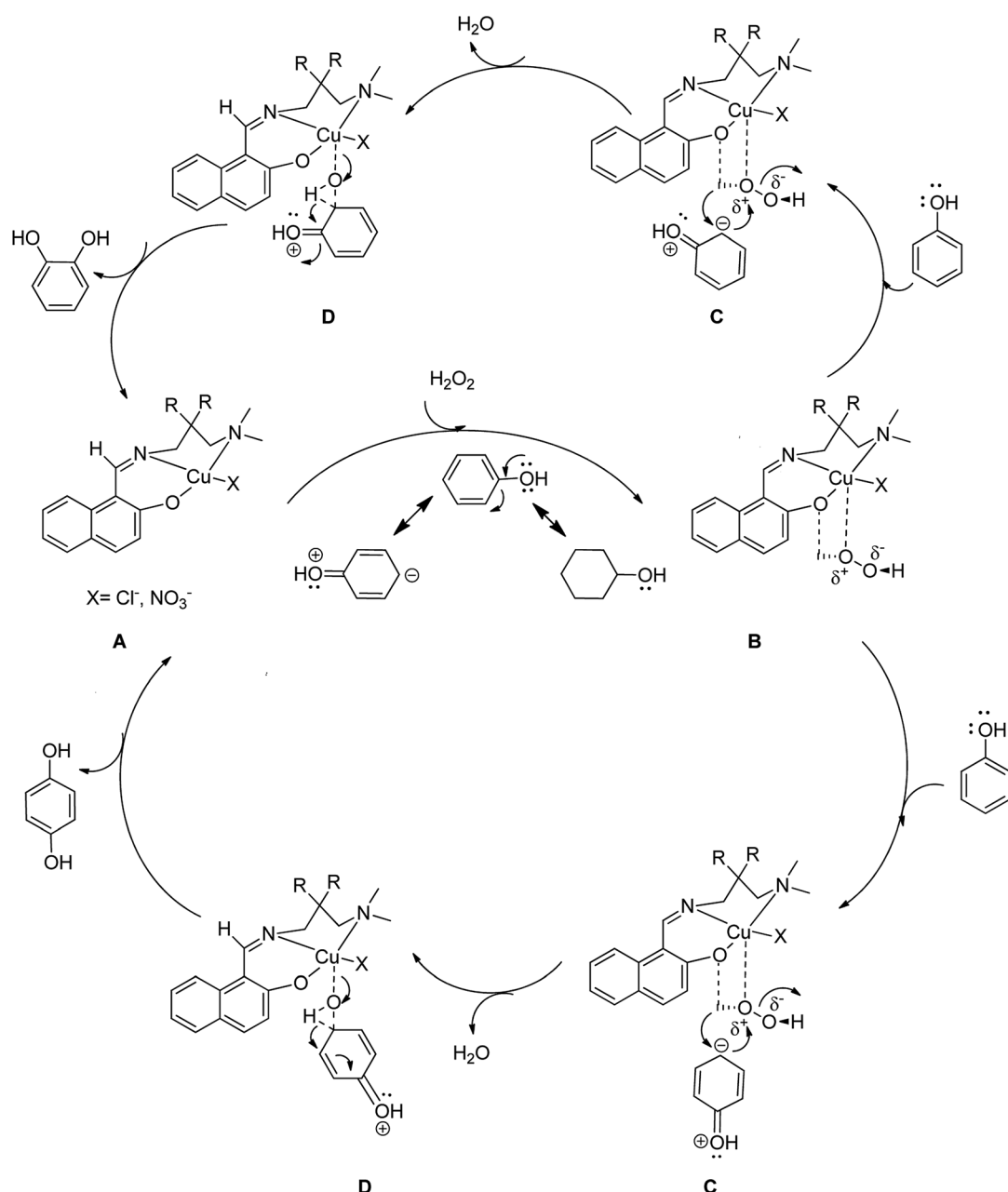
obtained in the oxidation reaction of phenol and parabenoquinone that were identified amongst the products using zeolites with moderately larger quantities of encapsulated CuCl_4Pc complexes (with 0.27 and 0.28 wt% of Cu,



Scheme 13 Different oxidation products of cyclohexene.

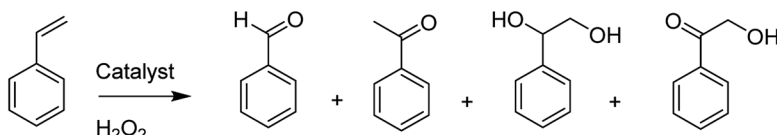
Table 5 The conversion and selectivity of cyclohexene oxidation products

Entry	Catalysts	Conversion (%)	Selectivity		Product Other	TOF (min ⁻¹)
			Cyol	Cyone		
1	Blank	1.91	—	100	—	—
2	[CuL ₁ NO ₃] _n	44.42	23.68	51.57	24.75	—
3	CuL ₂ Cl	35.24	28.63	65.32	6.05	—
4	NaY	9.84	29.47	70.42	—	—
5	Cu(II)@Y(NO ₃)	18.83	20.02	62.34	17.64	73.1
6	Cu(II)@Y(Cl)	15.84	22.09	69.93	8.28	70.6
7	CuL ₁ NO ₃ @Y	62.69	19.12	69.03	11.85	322.9
8	CuL ₂ Cl@Y	58.67	18.70	72.83	8.47	384.2

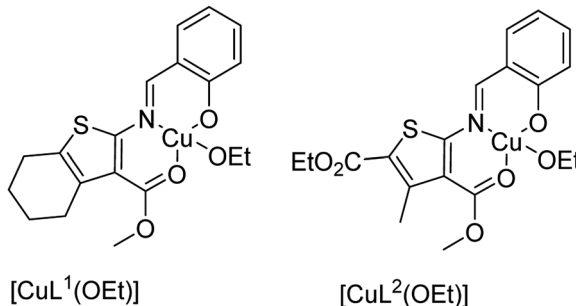


Scheme 14 Probable catalytic cycle for the phenol hydroxylation reaction to form catechol or/and hydroquinone as the major products.





Scheme 15 Various products in the oxidation of styrene.

Fig. 3 Proposed structure for free and encapsulated complexes $[\text{CuL}^1(\text{OEt})]$ and $[\text{CuL}^2(\text{OEt})]$.

respectively). The encapsulated complex showed greater catalytic activity and selectivity in comparison with the non-encapsulated complex. Notably, the catalytic activity of the catalysts in the phenol oxidation reaction surveyed the order: $\text{Cu}(\text{opbmzI})_2\text{-Y}$ (86.7%) > $\text{Cu}(\text{opbmzI})_2$ (70.6%) > Cu-Y (64.3%) > Na-Y (22.6%). However, the catalytic activity of the catalysts in their selectivity towards catechol was in the order: $\text{Cu}(\text{opbmzI})_2\text{-Y}$ (66.8%) > Cu-Y (51.2%) > $\text{Cu}(\text{opbmzI})_2$ (48.2%) > Na-Y (18.6%). Na-Y resulted in a lower phenol conversion (22.6%), exhibiting the importance of a transition metal in the zeolite cavity for greater catalytic activity. As a result, the reactions were accomplished without the plausibility of free radicals, and the probable mechanistic pathways based on the intermediate complexes and the Cu-oxygen species were proposed with some uncertainty (Schemes 8 and 9).

The effect of various factors on the catalytic activity of $\text{Cu}(\text{opbmzI})_2\text{-Y}$ was investigated by changing the phenol, solvents, temperature, catalyst dosage and H_2O_2 molar ratio. Initially, the reactions were examined with H_2O_2 and TBHP under the particular conditions. H_2O_2 was also selected as the desirable oxidant to attain the optimal conditions. Next, the influence of the temperature on the phenol oxidation was explored by repeating the reaction in the temperature range

from 303 K to 343 K. It was noteworthy that this group proposed that the phenol conversion was very susceptible to temperature changes. The most promising temperature at which the reactant molecules would have the threshold energy to overcome the barrier to provide products was known to be 333 K at a reaction time of 6 hours. In addition, the solvent can either stabilize or destabilize the transition state. It changes the concentration and distribution of the intermediates generated throughout the reaction progress at the active site of the catalyst, and affects the reaction rate by dissolving the reactants and intermediates in the solution. Moreover, phenol oxidation was performed in several solvents such as MeOH , EtOH , MeCN , MeCOMe and tetrahydrofuran (THF). As a result, MeCN (4 mL) was selected as the best solvent.

It should be mentioned that AAS analysis demonstrated no sign of metal leaching into the reaction mixture. In addition, no further conversion was detected upon the elimination of the catalyst from the reaction mixture or extending the reaction time (up to 7 hours for the oxidation of styrene and 6 hours for the oxidation of phenol). Notably, this result is very important in highlighting the heterogeneous catalyst as a candidate for industrial usage.

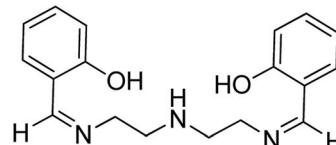
Maurya *et al.* in 2003 reported the encapsulation of transition metal complexes of *N,N'*-bis(salicylidene) propane-1,3-diamine (H_2salpn) (**9**) into zeolite-Y (Fig. 2). The catalytic activity of this catalyst was examined in the oxidation reaction of phenol.⁵⁷ In this pathway, *N,N'*-bis(salicylidene)propane-1,3-diamine copper(II), $[\text{Cu}(\text{salpn})]$ was encapsulated in the supercages of zeolite-Y.⁵⁸ The catalytic activity of $[\text{Cu}(\text{salpn})]\text{-Y}$ was examined in the oxidation of phenol to a mixture of hydroquinone and catechol using H_2O_2 as an oxidant. Based on the optimal reaction conditions, the selectivity towards catechol and hydroquinone formation was about 80 and 20%, respectively. Elevating the temperature from 50 to 80 °C in acetonitrile increased the percentage of hydroquinone formation from 12 to 27%. In addition, an analogous pattern was followed with CCl_4 as a solvent in which the hydroquinone selectivity increased

Table 6 Hydrooxidation of phenol using molecular dioxygen as the oxidant^a

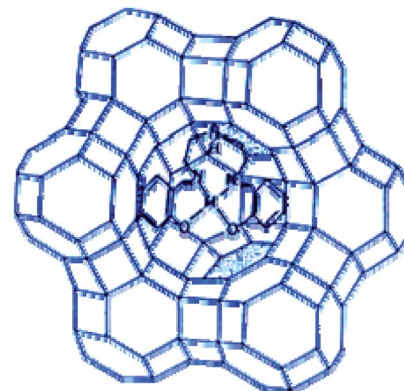
Catalyst	Phenol conv. (mol%)	BZQ (mol%)	Others (mol%)	TOF (h ⁻¹)
CuAc "neat"	5.1	4.9	0.2	3.6
CuAc-Y	11.5	11.5	—	60.9
CuClAc "neat"	1.0	1.0	—	0.9
CuClAc-Y	12.0	11.9	0.1	227.1

^a TON = turnover frequency (number of molecules of phenol converted per atom of Cu per hour). Reaction condition: pH = 6.5, 298 K, 19 hours.





14



15

Scheme 16 Suggested structure of $[M(\text{saldien})]-Y$ ($M = \text{Cu(II)}, \text{Ni(II)}$ and Zn(II)). Reprinted from (ref. 57) with permission of the Royal Society of Chemistry.

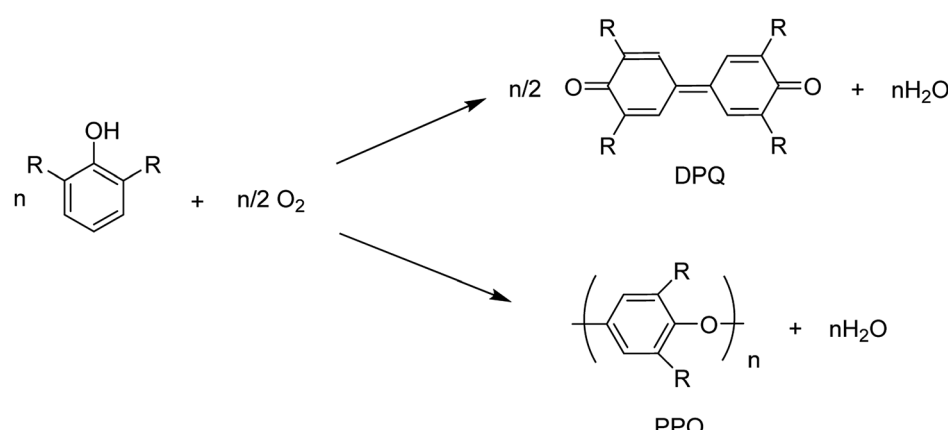
Table 7 Oxidation reaction of phenol using hydrogen peroxide in the presence of phthalocyanines^a

Catalyst	Cu (wt%)	TON (moles of phenol converted per mol of Cu in the catalyst)	Products <i>p</i> -benzoquinone catechol hydroquinone
$\text{CuCl}_{14}\text{Pc}$	—	2.1	2.0, 59.5, 38.5
$\text{Cu}(\text{NO}_2)_4\text{Pc}$	—	1.21	12.5, 0, 87.5
$\text{CuCl}_{14}\text{Pc-Na-Y}$	0.11	7.95	0, 65.8, 34.2
$\text{CuCl}_{14}\text{Pc-Na-Y}$	0.17	8.27	0, 63.1, 36.9
$\text{CuCl}_{14}\text{Pc-Na-Y}$	0.26	6.77	0, 50.9, 49.1
$\text{CuCl}_{14}\text{Pc-Na-Y}$	0.27	7.35	6.1, 49.1, 44.8
$\text{CuCl}_{14}\text{Pc-Na-X}$	0.14	8.25	0, 62.8, 37.2
$\text{CuCl}_{14}\text{Pc-Na-X}$	0.28	7.36	11.2, 46.4, 34.4
$\text{Cu}(\text{NO}_2)_4\text{Pc-Na-Y}$	0.09	7.40	0, 0, 100
$\text{Cu}(\text{NO}_2)_4\text{Pc-Na-Y}$	0.16	3.95	0, 0, 100
$\text{Cu}(\text{NO}_2)_4\text{Pc-Na-X}$	0.11	4.25	0, 0, 100
$\text{Cu}(\text{NO}_2)_4\text{Pc-Na-X}$	0.14	3.95	0, 0, 100

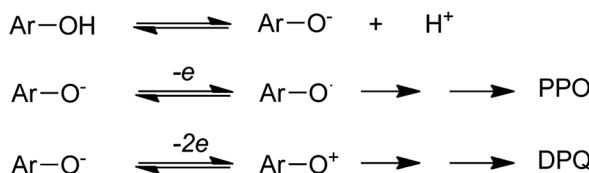
^a Reaction condition: catalyst, phenol/ H_2O : (3 : 1), 3 hours, 353 K.

from 20 to 32% on elevating the temperature from 50 to 80 °C. It is noteworthy that ethanol served quite differently as a solvent in which the selectivity towards catechol and hydroquinone construction was 85 and 15%, respectively.

It is noteworthy to mention that phenol was successfully oxidized using the heterogeneous catalysts based on Fe(II) or Cu(II) pyrrolylazine (**10**) complexes that were encapsulated into the NaY zeolite (Scheme 10).⁵⁹ Notably, the encapsulated metal



Scheme 17 The oxidative coupling reaction of 2,6-dimethylphenol using homogeneous Cu-amine catalysts.



Scheme 18 Dissociation of phenol to the phenolate anion.

pyrrolylazine complexes in the NaY zeolite increased the superior conversion of phenol into catechol (Table 4).

Crystalline copper(II) Schiff base complexes of $[\text{CuL}_1\text{NO}_3]_n$ **11** and $[\text{CuL}_2\text{Cl}]$ **12** (where $\text{HL}^1 = 1\text{-}[(3\text{-dimethylaminopropylimino})\text{-methyl}]\text{-naphthalen-2-ol}$ and $\text{HL}^2 = 3\text{-}[(3\text{-dimethylamino-2,2-dimethyl-propylimino})\text{-methyl}]\text{-naphthalen-2-ol}$) were constructed in 2018 by Mukhopadhyay *et al.* (Scheme 11).⁶⁰

Various solvents comprising diethyl ether, acetonitrile and methanol were used to purify the resultant products to eliminate the unexpected species or the species, which were adsorbed on the zeolite surfaces. The formation of the host-guest complexes into the zeolite supercages was further confirmed *via* the colour of the target product. Finally, anhydrous $[\text{CuL}_1\text{NO}_3]_n\text{@Y}$ or $[\text{CuL}_2\text{Cl}]_n\text{@Y}$ (**13**) was provided as a blue-violet powder (Scheme 12).

Thermogravimetric analysis (TGA) was used to attain information about the thermal stability of the neat and metal-exchanged zeolite NaY, and also the encapsulated complexes under static nitrogen atmosphere. Both pure and metal exchanged zeolite presented only distinct degradation at 192 °C, due to the loss of peripheral -OH moieties or loss of physically and chemically adsorbed water. Moreover, it exhibited minor mass reduction until 400 °C, which is apparent from the differential thermal analysis (DTG) profiles. The zeolite-

encapsulated complexes exhibited additional decomposition stages because of the loss of ligand molecules, and the relevant temperature range extended up to ~500 °C. This demonstrates the improvement in the thermal stability of the complexes after encapsulation in the zeolite framework. A slight mass loss (~4%, $n\text{CuL}_2\text{Cl}@Y$) obviously indicates the presence of slight quantities of metal complex in the supercages of zeolite, which is related to the low metal concentration estimated by ICP-MS analysis.

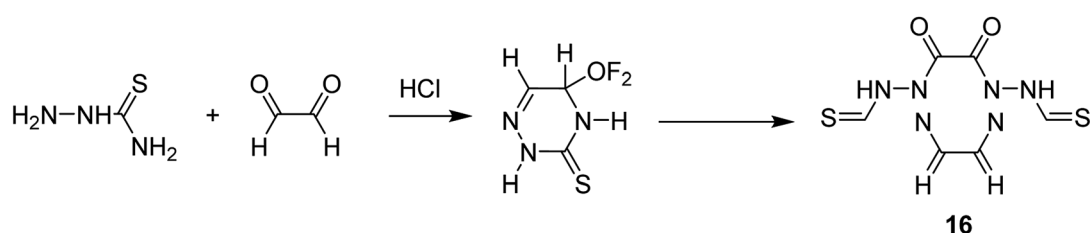
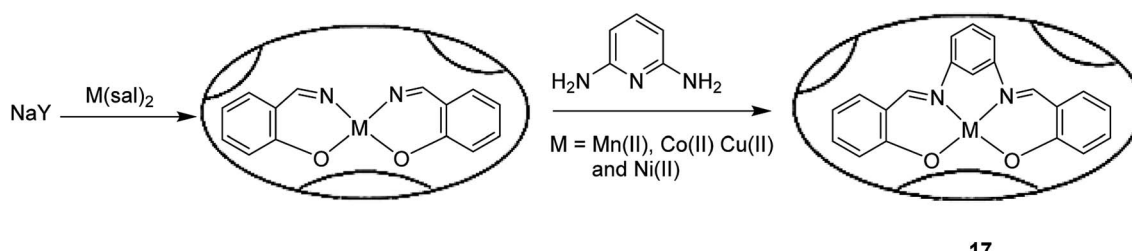
Notably, this method exhibits the advantageous of heterogeneous catalytic reactions for the stability of metal complexes in the supercages of zeolite-Y and the selective oxidation reaction of phenol, styrene, and cyclohexene using H_2O_2 . The catalytic activity of the zeolite entrapped Cu(II) complexes were compared with their homogeneous analogues as well. Catalytic hydroxylation of phenol gave two major products, including hydroquinone and catechol; however, it can be further oxidized to *para*-benzoquinone (Scheme 13).

Table 5 displays the percentage conversion of the oxidation products of cyclohexene using various catalysts and keeping other parameters fixed.

Scheme 14 displays the suggested possible mechanism for the oxidation of phenol in the presence of homogeneous complexes (by $[\text{CuL}_1\text{NO}_3]_n$; X = -NO₃ and R = -H and $[\text{CuL}_2\text{Cl}]$; X = -Cl and R = -CH₃) using H_2O_2 in which complex **13** gives the potent oxidative metal-hydroperoxide species.⁵¹

The catalytic oxidation of styrene provided benzaldehyde, 1-phenylethane-1,2-diol, acetophenone and 2-hydroxy-1-phenylethanone (Scheme 15).

Mobinikhaledi and co-workers in 2014 reported the encapsulation of copper(II) complexes of methyl-2-(2-hydroxybenzylideneamino)-4,5,6,7-tetrahydrobenzo[b]thiophene-3-carboxylate (HL^1) and 2-ethyl-4-methyl 5-(2-hydroxybenzylideneamino)-3-methylthiophene-2,4-dicarboxylate (HL^2) (Fig. 3) into the

Scheme 19 Preparation of **16**.

Scheme 20 The encapsulation of transition metal complexes in the supercages of a NaY zeolite.



Table 8 Oxidation of cyclohexene using TBHP in the presence of $[\text{Cu}(\text{H}_4\text{C}_6\text{N}_6\text{S}_2)]\text{-NaY}$ as the catalyst

Catalyst	Conversion (%)	Selectivity (%)		
		2-Cyclohexene-1-one	2-Cyclohexene-1-ol	1-(<i>Tert</i> -butylproxy)-2-cyclohexene
$[\text{Cu}(\text{H}_4\text{C}_6\text{N}_6\text{S}_2)]\text{-NaY}$	40.1	65.5	22.0	12.5

supercages of zeolite NaY *via* the flexible ligand method.⁶² The neat and encapsulated complexes were used as catalysts in the oxidation reaction of phenol and benzyl alcohol. Remarkably, the encapsulated complexes were both more stable and reactive catalysts in comparison with the desired free complexes. It should be mentioned that the complex of HL^2 in both free and encapsulated modes illustrated greater activity in comparison to the complex of HL^1 . This is related to the electron-withdrawing groups that decrease the electron density of the copper(II) centers, and so they increase their Lewis acidity.

The catalytic activity of CuAc-Y and CuClAc-Y, CuAc and CuC1Ac in the oxidation of phenol to *o*-benzoquinone was examined (Table 6). Some features are mentioned in which the hydroxylation reaction does not occur in the absence of any catalyst. Both CuClAc-Y and CuAc-Y selectively oxidize phenol to *o*-benzoquinone. In addition, the turnover frequency for oxidation is remarkably increased upon encapsulation of the complexes in zeolite-Y for both CuC1Ac and CuAc. Finally, the particular catalytic activity of CuClAc-Y is greater than that of CuAc-Y at analogous levels of phenol conversion.

The reaction between excess *N,N'*-bis(salicylidene)diethylenetriamine (H₂saldien) (14) and copper(II) exchanged zeolite-Y at *ca.* 90 °C resulted in the encapsulation of the ligand in the supercages of zeolite. This was followed by the complexation with the metal ion (15) (Scheme 16).⁵⁷ The encapsulated complex was used as the significant catalyst for the decomposition of hydrogen peroxide, and for the oxidation reaction of phenol to a mixture of hydroquinone and catechol using H₂O₂ as an oxidant. Based on the optimal condition in the presence of $[\text{Cu}(\text{saldien})]\text{-Y}$ as the catalyst and using hydrogen peroxide in MeCN, the oxidation reaction of phenol at 80 °C gave the maximum conversion of phenol. Based on these conditions, the catalytic activity of $[\text{Cu}(\text{saldien})]\text{-Y}$ is 45% upon 24 hours.

The selective oxidation reaction with O₂ and hydrogen peroxide of *n*-hexane, phenols and naphthalene in the presence

Table 10 Oxidation of cyclohexene with *tert*-butylhydroperoxide catalyzed in the presence of metal complexes in CH₂Cl₂

Catalyst	Conversion (%)	Selectivity (%)	
		Ketone ^a , alcohol ^b , peroxide ^c	
$[\text{Cu}(\text{Sal-2,6-py})]\text{-NaY}$	47.2	71.9, 20.7, 7.4	

^a 2-Cyclohexene-1-one. ^b 2-Cyclohexene-1-ol. ^c 1-(*Tert*butylperoxy)-2-cyclohexene.

of Cu complexes was demonstrated in 1996 by Raja and co-workers.⁶³ The copper complexes included copper acetate ($\text{Cu}(\text{CH}_3\text{COO})_2$), copper phthalocyanine ($\text{C}_{32}\text{H}_{16}\text{CuN}_8$), copper nitrophthalocyanine ($\text{C}_{32}\text{H}_{16}\text{CuN}_9\text{O}_2$) and copper chlorophthalocyanine ($\text{C}_{32}\text{H}_{17}\text{ClCuN}_8$), and were encapsulated in molecular sieves (X, Y, MCM-22 and VPI-5). The oxidation of phenols to hydroquinone and catechol was achieved with high yields in the presence of Cu-phthalocyanines encapsulated into the zeolites Na-X or Na-Y.

Zeolite NaX or Na-Y with changed loadings of $\text{Cu}(\text{NO}_2)_4\text{Pc}$ or $\text{CuCl}_{14}\text{Pc}$ were provided successfully. The oxidation of phenol using hydrogen peroxide in the presence of CuPc-based catalysts was achieved (Table 7). Notably, both $\text{Cu}(\text{NO}_2)_4\text{Pc}$ and $\text{CuCl}_{14}\text{Pc}$ are active catalysts for the oxidation reaction of phenol to catechol/hydroquinone using H₂O₂ as the oxidant. Table 7 demonstrates the effect of the Cu content (and, therefore the concentration of the Cu complex) in the zeolite on the rate of oxidation of phenol and in the product distribution. Herein, the noticeable aspects are as follows: (i) the catalytic activity (turnover number) of the Cu ions is greater in the encapsulated state in comparison with the “neat” complex; (ii) the Cl complex is

Table 9 The oxidation reaction of cyclohexane in the presence of the physical mixtures of Cu(salen)/Y and Fe(salen)/Y^a

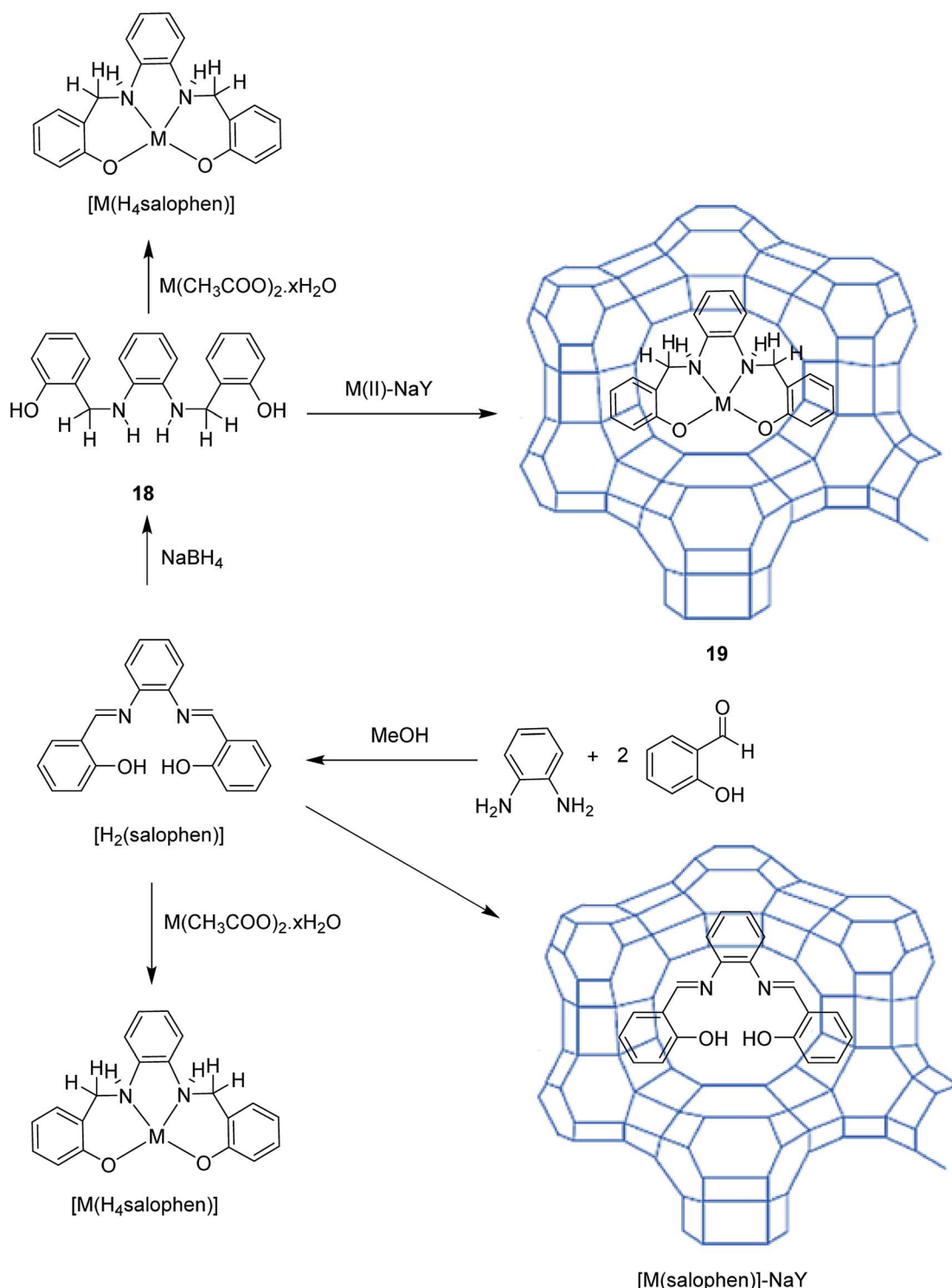
Catalyst	Amounts of Cu ²⁺ and Fe ³⁺ cations (mmol)	$\text{Cu}^{2+}/\text{Fe}^{3+}$ (mol mol ⁻¹)	Selectivity (%)		
			TON	Cyclohexanol	Cyclohexanone
Cu(salen)/Y + Fe(salen)/Y	0.013	2.80	89	50.5	49.5
Cu(salen)/Y + Fe(salen)/Y	0.013	1.93	85	56.8	43.2
Cu(salen)/Y + Fe(salen)/Y	0.013	0.6	70	55.9	44.1
Cu(salen)/Y + Fe(salen)/Y	0.013	0.21	62	57.3	42.7

^a Reaction conditions: the designed amount of catalyst, 10 mL of CH₃CN, 18.5 mmol of substrate, 19.5 mmol of H₂O₂ (30% in aqueous solution), 60 °C, 2 hours.



also more potent than the NO_2 complex; (iii) the TON does not change considerably with Cu content, suggesting that the Cu complexes are well separated from each other (the conversion of phenol, obviously, improves with the concentration of the Cu complex into the zeolite); (iv) parabenoquinone hydroquinone

and catechol are the only main products generated in the oxidation of phenol. It should be mentioned that the quantity of 'tar' products is low (less than 1%). Notably, the resultant product was almost colourless. In addition, parabenoquinone is detected between the products having zeolites with



Scheme 21 Encapsulation of Mn(II), Co(II), Ni(II) and Cu(II) complexes of salophen nanopores of zeolite. Reprinted from (ref. 70) with permission of the Royal Society of Chemistry.



Table 11 Oxidation of cyclohexane using H_2O_2 in the presence of salophen and tetrahydrofuran salophen transition metal complexes in CH_3CN

Catalyst	Conversion (%)	Selectivity (%)	
		Cyclohexanol	Cyclohexanone
$[Cu(salphen)]^a$	43.2	36.4	63.6
$[Cu(H_4salphen)]^a$	48.7	42.3	57.7
$[Cu(H_4salphen)]^b$	26.8	60.9	39.1
$[Cu(H_4salphen)]^c$	42.1	38.9	61.1
$[Cu(H_4salphen)]^d$	18.6	31.4	68.6

^a Reaction condition: time (2 hours), cyclohexane (10 mmol), catalyst (1.02×10^{-5} mol), H_2O_2 (20 mmol), CH_3CN (5 mL). ^b A similar procedure as system was carried out with 0.5×10^{-5} mol catalyst instead of 1.02×10^{-5} . ^c A similar procedure as system was carried out with 2.04×10^{-5} mol catalyst. ^d A similar procedure as system was carried out with 4.08×10^{-5} mol catalyst.

comparatively larger quantities of encapsulated $CuCl_{14}Pc$ complexes (having 0.27 and 0.28 wt% copper, respectively).

The copper(II)-pyridine complex was encapsulated into the supercage of the Y zeolite. The complex was simply reduced to Cu(I) at 200 °C under vacuum and re-oxidized to Cu(II) upon exposure to molecular oxygen in its reduced state. The oxidative coupling reaction of 2,6-dimethylphenol was selected as a model reaction.¹² This reaction was explored in the presence of homogeneous copper-amine catalysts in solution using O_2 .¹³ Two corresponding products, diphenoxquinone (DPQ) and polyphenylene oxide (PPO) were prepared through C-C and C-O coupling reactions, respectively (Scheme 17).⁶⁴

The results demonstrate that Cu-Py-NaY affords extraordinary selectivity to PPO in comparison with $CuCl^+P$, in spite of its low catalytic activity. Although various probable reaction mechanisms were proposed, Oyama and co-workers (1987)⁶⁵ and Waters (1971)⁶⁶ recommended in their homogeneous investigations that PPO or DPQ is produced *via* different intermediates (Scheme 18). Initially, the dissociation of phenol into a phenolate anion occurs using bases. Next, PPO is generated *via* an intermediate ArO^\bullet radical or DPQ *via* an ArO^+ cation, in which a one- or two-electron transfer occurs from the phenolate anion to Cu(II) ion, respectively. To provide the catalytic reaction, the reduced copper(I) ions should be reoxidized to Cu(II) ions with O_2 . It was found that Cu-Py-NaY favors the C-O coupling since the catalytically active species for it is separated in the zeolite supercage, and must subsequently admit only one electron from a phenolate anion.

Salavati-Niasari and co-workers in 2008 reported the encapsulation of $[M(H_4C_6N_6S_2)]$ ($H_6C_6N_6S_2 = 1,2,5,6,8,11$ -hexaazacyclododeca-7,12-dithione-2,4,8,10-tetraene) (**16**) into the nanocavity of zeolite-Y *via* the flexible ligand method (Scheme 19).⁶⁷

Based on this method, an ethanolic solution of thiosemicarbazide in the presence of HCl was added to an ethanolic solution of glyoxal. Then, an ethanolic solution of $CuCl_2$ was added to an ethanolic suspension of the intermediate ligand, 6-ethoxy-4-thio-2,3,5-triazine to provide 1,2,5,6,8,11-

hexaazacyclododeca-7,12-dithione-2,4,8,10-tetraene. Next, a hot ethanolic solution of relevant metal acetate was added to a hot ethanolic suspension of the 12-membered macrocyclic ligand under reflux to form the desired complex. $M(II)-NaY$ was synthesized using the ion-exchange approach. Then, NaY was added to the solution of manganese acetate in water. It is noteworthy that the encapsulated complex was produced *via* FLM. For this purpose, $M(II)-NaY$ and $H_6C_6N_6S_2 = 1,2,5,6,8,11$ -hexaazacyclododeca-7,12-dithione-2,4,8,10-tetraene were mixed and heated at 250 °C. The melted ligand served as the solvent and as reactant. The resulting material was isolated using MeOH until the complex was free from the unreacted $H_6C_6N_6S_2$. The resulting zeolites were isolated with *N,N*-dimethylformamide (DMF) and with EtOH to eliminate excess unreacted diamine and any $M(II)$ complexes adsorbed onto the external surface of the zeolite crystallites.

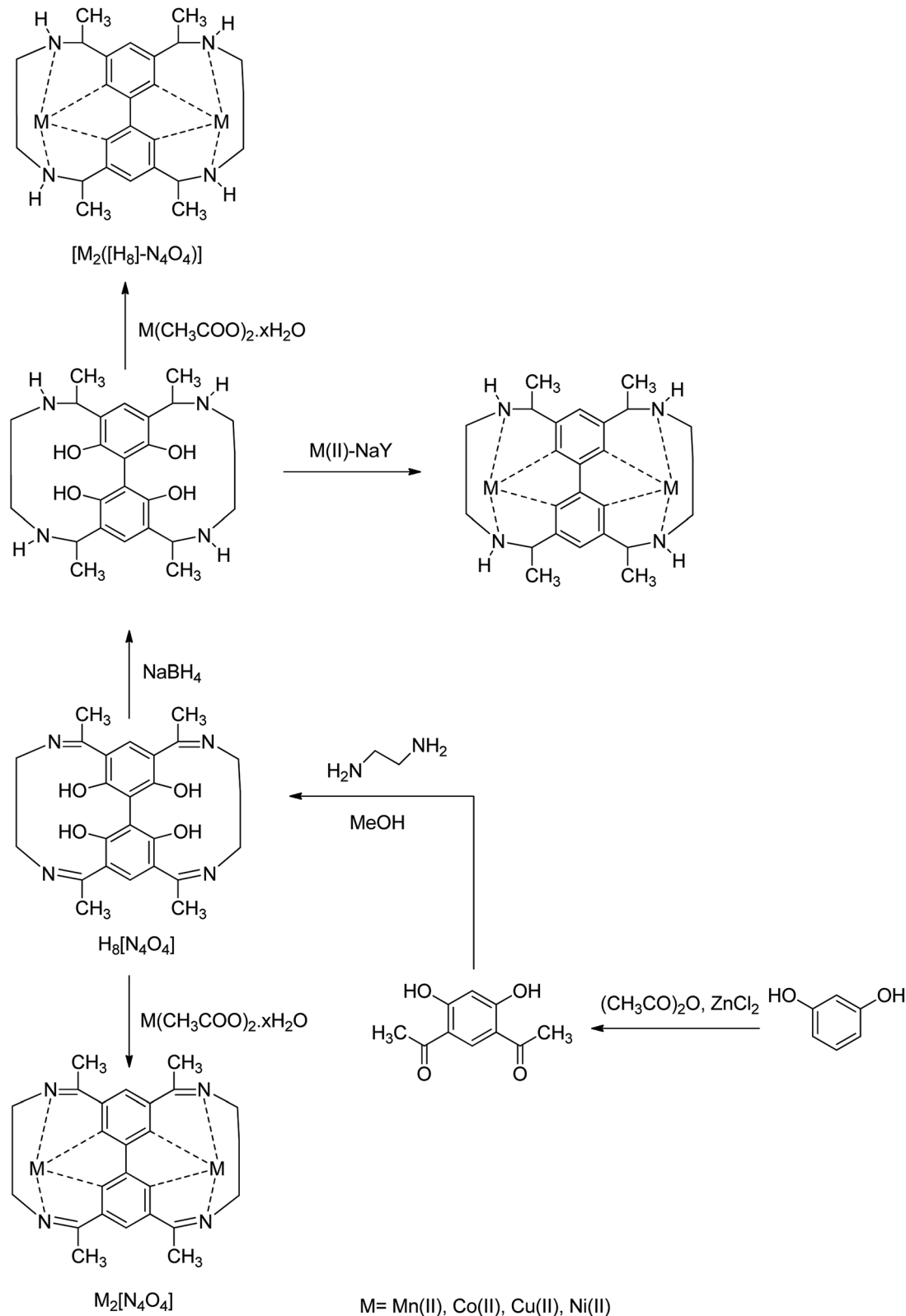
The activity of this catalyst was examined in the oxidation of cyclohexene. This complex exhibited significant activity in the oxidation of cyclohexene to 2-cyclohexene-2-ol, 2-cyclohexene-1-one, and 1-(*tert*-butylperoxy)-2-cyclohexene, where *tert*-butylhydroperoxide was provided as the product with the maximum yield (Table 8).

Iron and copper(II)salen complexes were spontaneously encapsulated into zeolite-Y *via* the flexible ligand method. Notably, this complex demonstrated considerable greater activity in comparison with the neat Fe(salen) and Cu(salen) in the oxidation reaction of cyclohexane with H_2O_2 .⁶⁸ It should be mentioned that the presence of a synergistic influence is the reason for this high activity. This synergistic influence may originate from the interaction of the adjacent moderately coordinated Fe(salen) and Cu(salen) complex molecules and/or the formation of the dinuclear salen complexes *via* the lattice oxygen of the zeolitic host. This reaction was achieved more rapidly on (Cu-Fe)(salen)/Y than on Cu(salen)/Y or Fe(salen)/Y. The optimal molar ratio of Cu^{2+} to Fe^{3+} in the resulting material is 1.93 : 1. This reaction was accomplished in the presence of a catalyst in CH_3CN with H_2O_2 at 60 °C. These catalysts exhibited considerably greater activity in comparison with the zeolite Y-encapsulated iron salen and zeolite Y-encapsulated copper(II) salen for the oxidation of cyclohexane with hydrogen peroxide (Table 9).

The Cu(II) complex having a pentadentate Schiff-base ligand, *N,N*-bis(salicylidene)-2,6-pyridinediaminato, and $H_2[sal-2,6-py]$, was encapsulated into the nanocavity of zeolite-Y (**17**) (Scheme 20).⁶⁹ The results demonstrated that the encapsulated Cu(II) complexes in the nanodimensional pores of zeolite-Y were different from those of the free complexes. These differences can arise from distortions provided by steric effects due to the presence of sodium cations, or from interactions with the zeolite matrix. The host-guest nanocomposite materials $[M(sal-2,6-py)]-NaY$ catalyzed the oxidation reaction of cyclohexene using TBHP.

As shown in Table 10, the activity of these catalysts in cyclohexene oxidation using different solvents decreases in the order: $CH_2Cl_2 > CH_3Cl > MeOH > CH_3CN$. Based on this method, only allylic oxidation occurred with the formation of 2-





Scheme 22 Schematic diagram exhibiting the construction of host–guest nanocomposites.

cyclohexene-1-ol, 2-cyclohexene-1-one, and 1-(*tert*-butylperoxy)-2-cyclohexene and 2-cyclohexene-1-one (as the major product).

Cu(II) complexes having tetrahydro-salophen (salophen = *N,N*-bis(salicylidene)-1,2-phenylenediamine; $H_2[H_4\text{salophen}] =$

2-(2-[(2-hydroxybenzyl)amino] anilinomethylphenol) (18) was encapsulated into the nanopores of zeolite-Y, $[M(H_4\text{salophen})]-NaY$ (19), *via* the flexible ligand method.⁷⁰ For the formation of the ligand, 1,2-phenylenediamine and salicylaldehyde were

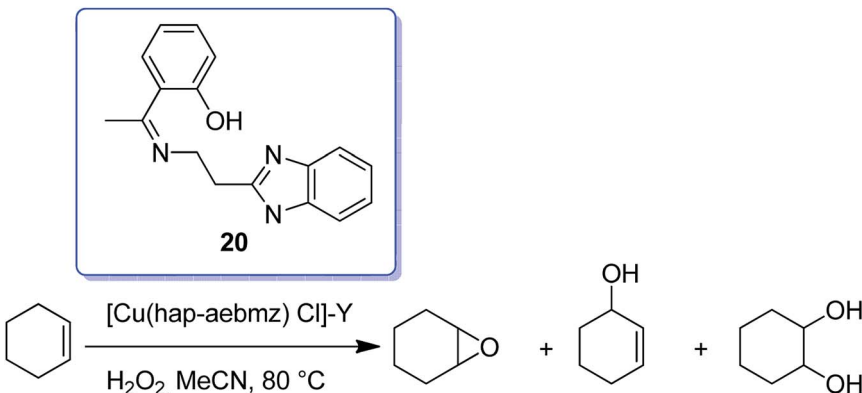
Scheme 23 Cyclohexene oxidation reaction in the presence of $[\text{Cu}(\text{hap-aebmz})\text{Cl}]$.

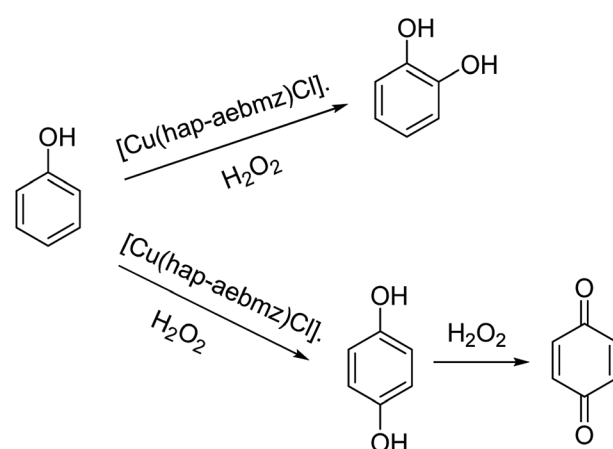
Table 12 Conversion of cyclohexene and selectivity of the different oxidation products upon 48 h of reaction time

Catalyst	Conversion (%)	Selectivity (%)			TON
		2-Cyclohexene-1-ol	2-Cyclohexene-1-one	1-Tert-butylperoxy-2-cyclohexene	
$[\text{Cu}(\text{PAN})\text{Cl}]$	26	—	32	68	83.4
$[\text{Cu}(\text{PAN})]\text{@Y}$	28	—	11	89	56.7

used. This method resulted in the encapsulation of Mn(II), Co(II), Ni(II) and Cu(II) complexes of salophen and tetrahydro-salophen ligands in the nanopores of zeolite (Scheme 21). The catalytic activity using host–guest nanocomposite complexes in the oxidation of cyclohexane was examined. This catalytic complex exhibited excellent activity in the oxidation of cyclohexane under mild conditions (Table 11). Therefore, zeolite-encapsulated systems increased the catalytic potential, particularly in comparison with the activity for limited oxidation and stability.

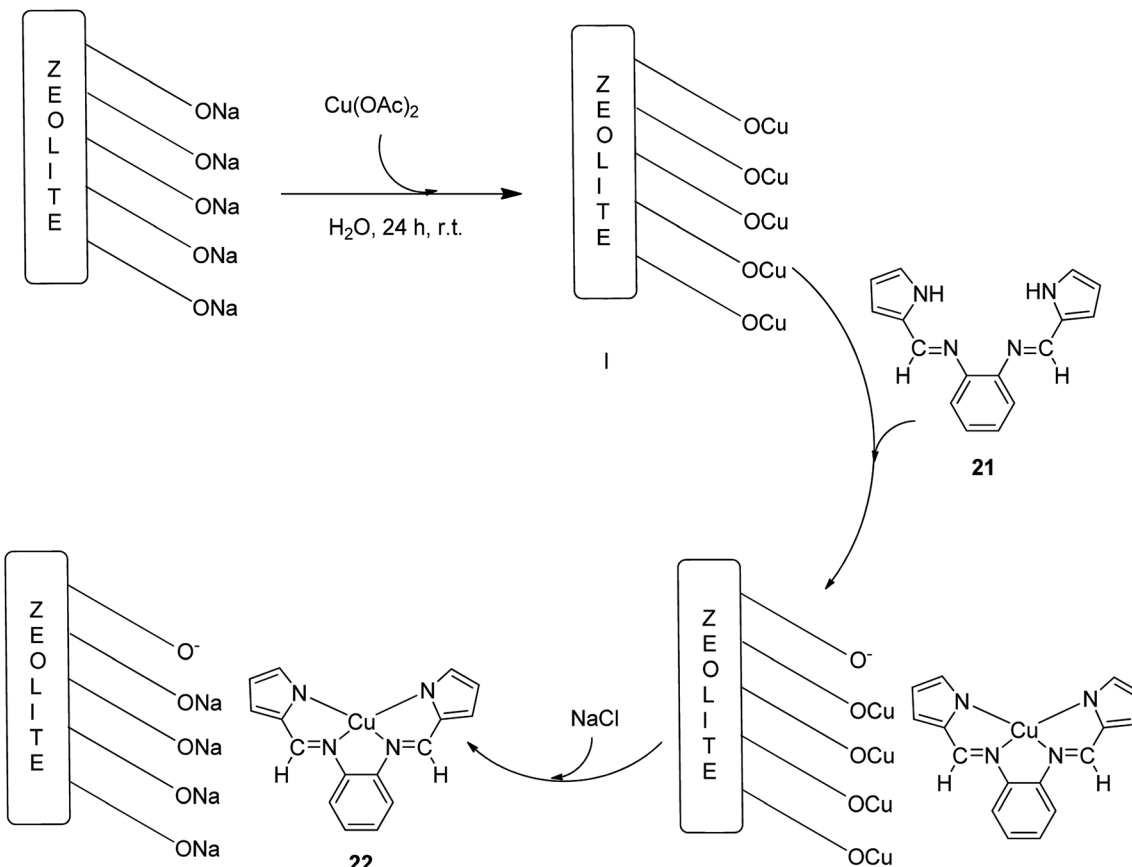
Cu(II) complexes bearing octahydro-Schiff base ($\text{H}_4\text{-N}_4\text{O}_4$) = 2,7,13,18-tetramethyl-3,6,14,17-tetraazatricyclo-[17.3.1.1]-tetracosa-1(23),2,6,8(24),9,11,13,17,19,21-decaene-9,11,20,22-tetraol, $\text{H}_4([\text{H}]_8\text{-N}_4\text{O}_4)$ = 2,7,13,18-tetramethyl-3,6,14,17-tetraazatricyclo-[17.3.1.1]-tetracosa-1(23),8(24),9,11,19,21-hexane-9,11,20,22-tetraol, were encapsulated into the nanopores of zeolite-Y, $[\text{M}([\text{H}]_8\text{-N}_4\text{O}_4)]\text{@NaY}$, via the flexible ligand method (Scheme 22). The zeolite-encapsulated octahydro-Schiff base copper(II) complex, $[\text{Cu}([\text{H}]_8\text{-N}_4\text{O}_4)]\text{@NaY}$, demonstrated high activity in the cyclohexane oxidation.⁷¹ It is noteworthy that the catalytic activity of these complexes are influenced by the steric environment of the active site and by their geometry.

These complexes are also more active than the relevant neat complexes, $[\text{Cu}([\text{H}]_8\text{-N}_4\text{O}_4)]$. Remarkably, the encapsulation of the Schiff base complexes found as the most widely explored in the investigation arena of ship-in-a-bottle materials in this kind of complex has a flexible conformation with different geometries, namely stepped configurations, planar, and umbrella-type. As a result, they could provide various active site environments for several oxidations. However, the amount of the encapsulated Schiff base complex is very limited due to the existence of a comparatively severe C=N bond. On the other hand, the hydrogenation reaction of C=N to C–N would increase the nitrogen basicity and make the conformation of the complex more flexible, leading to the more readily accessible

Table 13 Oxidation reaction of cyclohexanol to cyclohexanone using *t*-BuOOH in the presence of the guest–host catalyst

Catalyst	Time (h)	Conversion (%)	Yield (%)	TON
$[\text{Cu}(\text{PAN})]\text{@Y}$	3	46	46	2722

Scheme 24 Oxidation of phenol using $[\text{Cu}(\text{hap-aebmz})\text{Cl}]$.

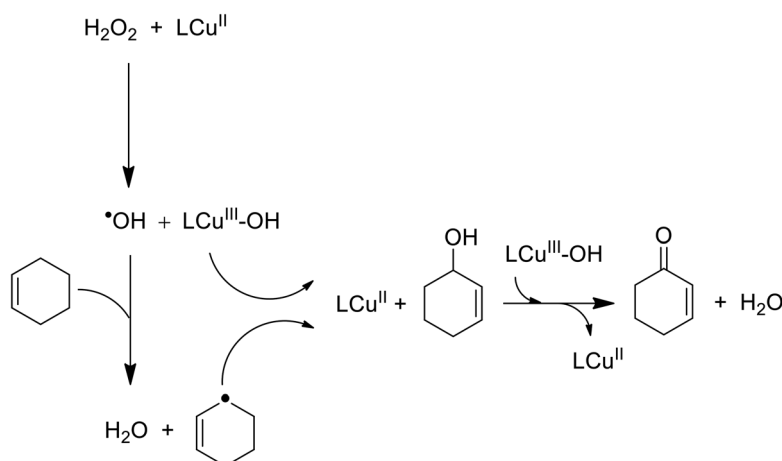


Scheme 25 Encapsulation of Cu(II) into NaY (metal exchanged Y-zeolite).

coordination to the metal centers in a folded method. Hence, this results in the inclusion of more transition metal complexes or active sites without rigid blockage of the channels in the zeolitic matrix. Moreover, the transition metal tetrahydro-salophen complex (M-[H₄]salophen) is considered to be more active than [Cu-salophen] in the homogeneous oxidation reaction of cyclohexane.⁷⁰ This resulted in [M-[H₄] salophen]-Y as

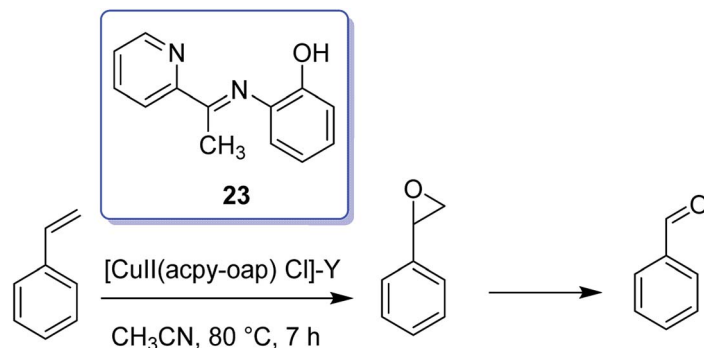
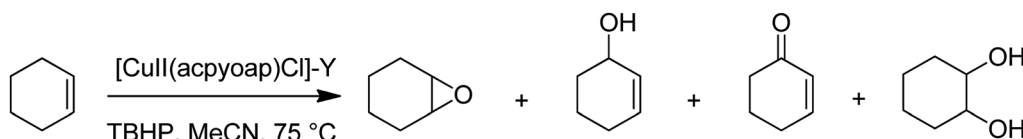
an active heterogeneous catalyst for the oxidation reaction of this type of organic substrates. As a result, this group demonstrated the formation of a wide range of [M([H]₈-N₄O₄)]-Y catalysts and the investigation of catalytic activities in the oxidation of cyclohexane.

The Cu(II) ion with the 1-(2-pyridylazo)-2-naphthol (PAN) ligand was encapsulated into supercages of the Y zeolite (host)



Scheme 26 Oxidation reaction of cyclooctene.

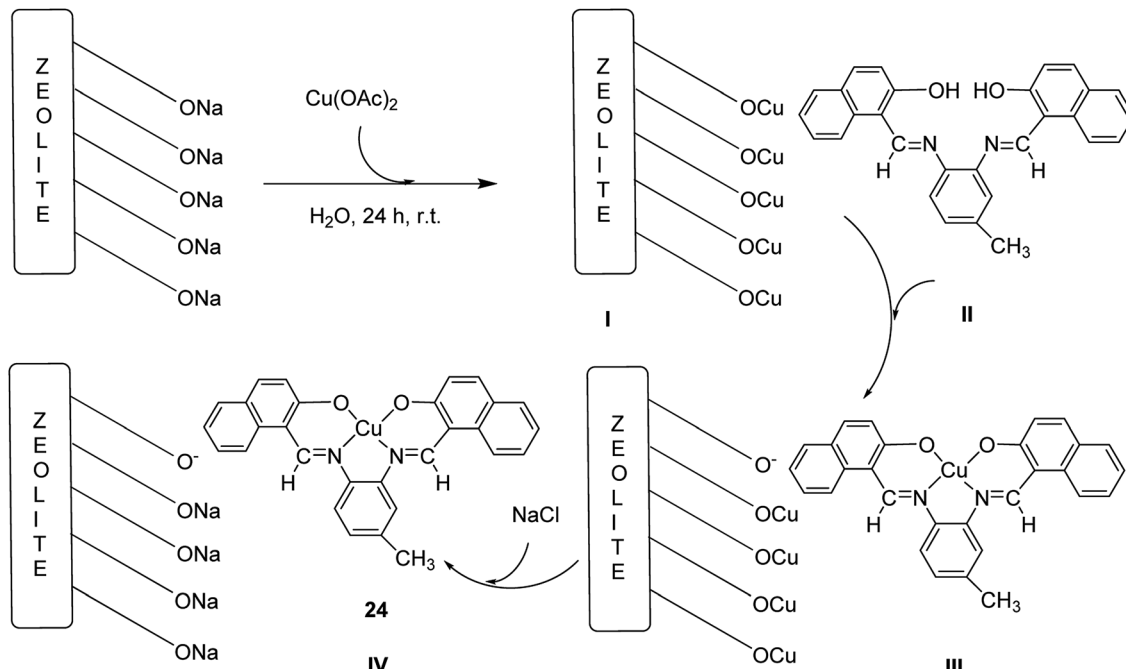


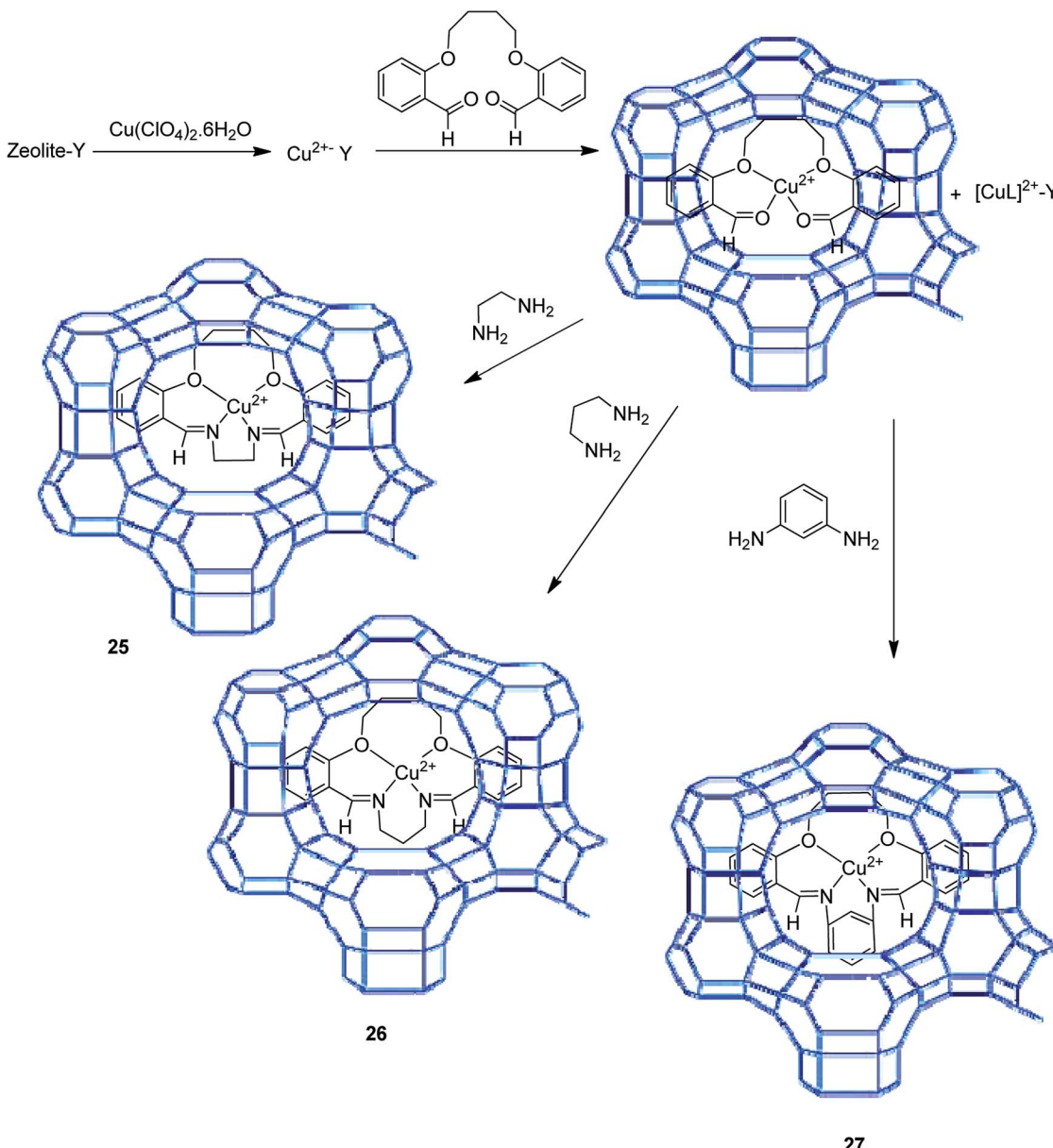
Scheme 27 The oxidation of styrene in the presence of $[\text{Cu}(\text{II})(\text{acpyoap})\text{Cl}]\text{-Y}$.Scheme 28 Oxidation of cyclohexene in the presence of $[\text{Cu}(\text{II})(\text{acpyoap})\text{Cl}]\text{-Y}$.

via the flexible ligand method. The catalytic activity of this catalyst was examined in liquid phase in the cyclohexanol and cyclohexene oxidations using *tert*-butylhydroperoxide as the oxidizing agent at 40 °C and 60 °C, respectively.⁷² Cyclohexene is appropriate for both allylic oxidation and epoxidation. To attain proof for or against a radical mechanism and to evaluate the catalyst selectivity, the oxygenation reaction of cyclohexene was achieved. The resultant products were identified as 2-cyclohexene-1-one, 2-cyclohexene-1-ol and 1-*tert*-butylperoxy-2-

cyclohexene.⁷³ The results for the oxidation of cyclohexene and cyclohexanol in the presence of this heterogeneous catalyst, $[\text{Cu}(\text{PAN})]\text{@Y}$, are shown in Tables 12 and 13, respectively.

The reaction between CuCl_2 and $(Z)\text{-2-(2-(1H-benzo}[d]\text{imidazol-2-yl)ethylimino)ethyl phenol(Hhap-aebmz)}$ (**20**) that was generated from 2-aminoethylbenzimidazole (aebmz) and *o*-hydroxyacetophenone (Hhap) gave $[\text{Cu}(\text{hap-aebmz})\text{Cl}]$. Next, $[\text{Cu}(\text{hap-aebmz})\text{Cl}]$ was encapsulated in the nanocavity of zeolite-Y through various physico-chemical approaches.⁷⁴ The

Scheme 29 The formation of Cu-NaY **24**.



Scheme 30 Encapsulation of Cu(II) complex nanoparticles of 16- and 17-membered diazadioxamacrocycles in nanopores of zeolite-Y. Reprinted from (ref. 78) with permission of the Royal Society of Chemistry.

encapsulated system was used as an efficient catalyst for the oxidation of cyclohexene and phenol using H_2O_2 (Schemes 23 and 24). With the approximately quantitative oxidation of cyclohexene, the selectivity of the oxidation products follows the

order: 2-cyclohexene-1-ol (44%) > 2-cyclohexene-1-one (40%) > cyclohexeneoxide (12%) > cyclohexane-1,2-diol (4%). Obviously, the best result for the oxidation of phenol was obtained in the presence of $[\text{Cu}(\text{II})(\text{hap-aebmz})\text{Cl}]\text{-Y}$, hydrogen peroxide at 80 °C.

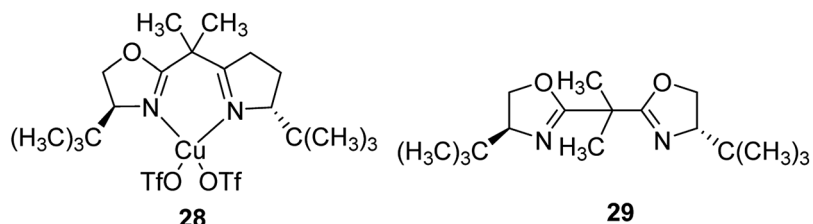
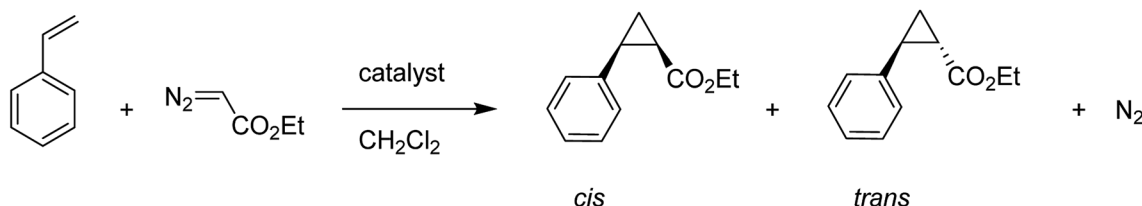


Fig. 4 Structure of the CuBox (28) and Box ligand (29).



Scheme 31 Cyclopropanation reaction of styrene with ethyldiazoacetate.

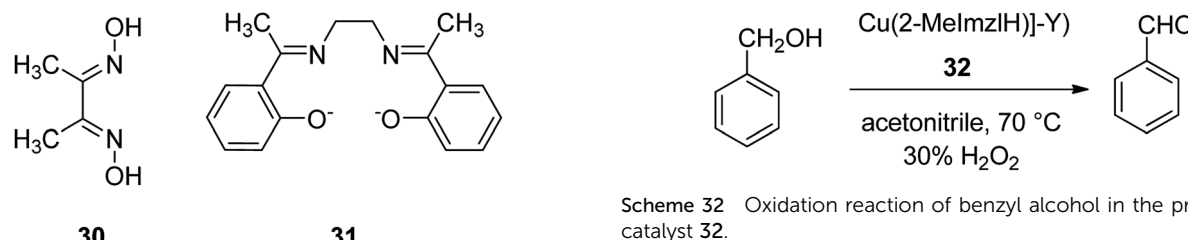


Fig. 5 Structure of compounds 30 and 31.

$[\text{Cu}(\text{hap-aebmz})\text{Cl}]\text{-Y}$ exhibited a conversion of 65.7% with selectivity of the main products, catechol (66.1%) and hydroquinone (32.9%).

The copper(II) complex of a Schiff base ligand (H_2L) (21) generated from *o*-phenylenediamine and pyrrolecarbaldehyde was encapsulated in the Y-zeolite matrix (22) (Scheme 25).⁷⁵ In this approach, for the synthesis of the ligand, pyrrolecarbaldehyde was added to an ethanolic solution of *o*-phenylenediamine. The reaction mixture was then heated to reflux. Then, for the formation of the copper(II) complex (CuL), the (H_2L) ligand was dissolved in EtOH and an ethanolic solution of $\text{Cu}(\text{CH}_3\text{COO})_2 \cdot \text{H}_2\text{O}$ was added to this solution under reflux. Next, the Na-Y zeolite was suspended in water containing $\text{Cu}(\text{NO}_3)_2$ and Cu-NaY (Scheme 25, I). For the immobilization of

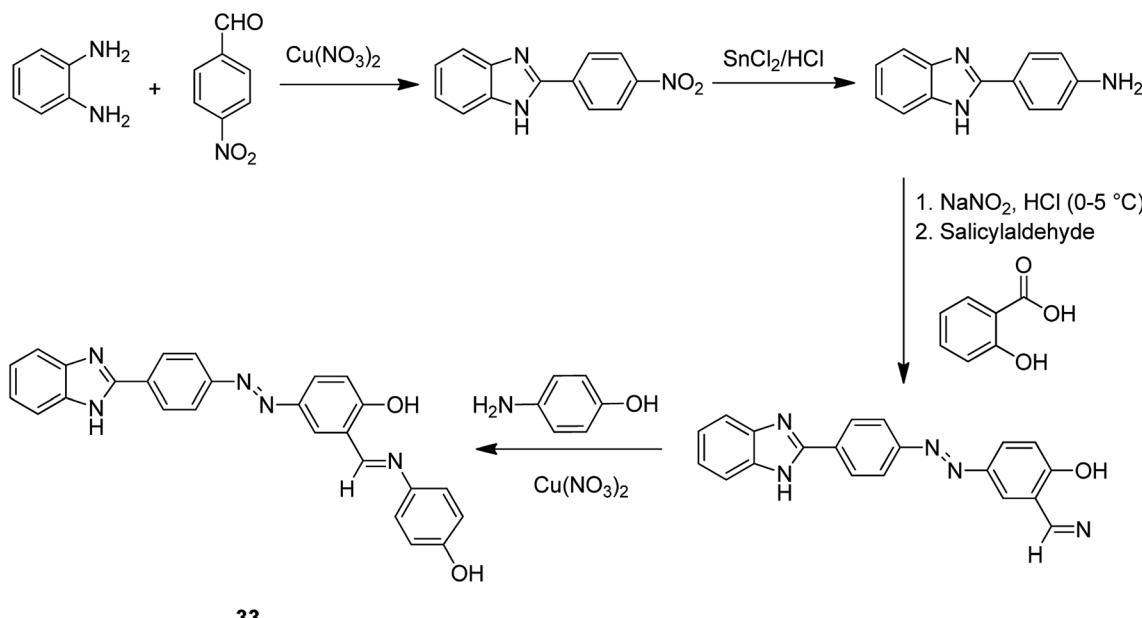
CuL in Cu-NaY, a quantity of Cu-NaY and MeCN solution of H_2L were mixed at 100 °C. The resultant material was isolated until the complex was free from the unreacted ligand. The non-complexed metal ions present in the zeolite were eliminated with an aqueous sodium chloride solution (Scheme 25). Finally, the desired encapsulated copper(II) catalyst was efficiently obtained.

The encapsulated copper(II) catalyst is an active catalyst for the oxidation of cyclohexene and cyclooctene using H_2O_2 as an oxidant. Notably, catalyst 22 gave 81% conversion of cyclohexene along with two main oxidation products, including 2-cyclohexenone and 2-cyclohexene-1-ol. In addition, 87% conversion of cyclooctene with 46% selectivity for epoxide construction was attained. Remarkably, the calcination of the

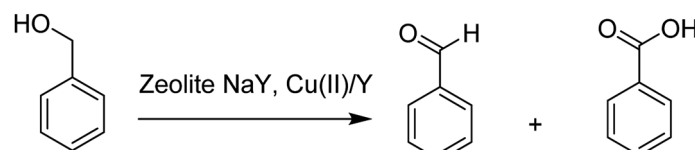
Table 14 Catalytic activity of zeolite copper(II) complexes

Sample	Substrate	Oxidant	Temperature (K)	Percent conversion (wt%)	TOF
$\text{YCu}(\text{dmgH})_2$	Benzyl alcohol	H_2O_2	323	30.0	90
			333	40.8	123
			343	52.6	158
	Ethylbenzene	H_2O_2	323	24.0	72
			333	33.6	101
			343	46.3	139
	Benzyl alcohol	O_2	323	18.6	56
			323	16.8	51
			323	14.2	43
$\text{YCuMe}_2\text{salen}$	Benzyl alcohol (poisoned)	H_2O_2	323	28.3	84
			333	36.8	109
			343	47.7	141
	Ethylbenzene	H_2O_2	323	23.1	68
			333	29.4	87
			343	39.2	116
	Benzyl alcohol	O_2	323	16.8	50
			323	11.1	33
			323	20.5	61





Scheme 33 Common method for the formation of complex 33.



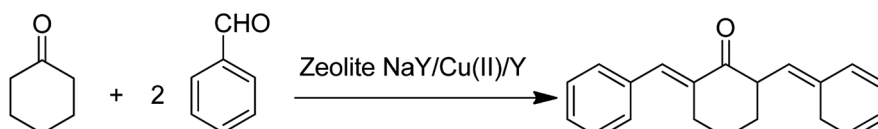
Scheme 34 The oxidation reaction of benzyl alcohol in the presence of zeolite NaY and Cu(II)/Y.

resultant copper(II)-incorporated zeolite was prevented from arresting the migration of copper(II) ions from the vicinity of the supercage (Scheme 25).

The oxidation reaction of cyclooctene in the presence of 22 as a catalyst using hydrogen peroxide and *tert*-butyl hydroperoxide (TBHP) afforded cyclooctene oxide as the major product, along with a minor quantity of the alcohol product. Two different oxidants containing H_2O_2 and *tert*-butylhydroperoxide were used for the oxidation of cyclooctene. The hexenyl radical reacted with $LCu^{(III)}OH$ to give 2-cyclohexene-1-ol demonstrated greater conversion and selectivity for epoxide formation. Then, 2-cyclohexene-1-ol reacted with another $LCu^{(III)}OH$ to afford 2-cyclohexenone (Scheme 26).

Hacpy-oap (23), an ONN donor, was used to form $[Cu^{(II)}(acpy-oap)Cl]$. The encapsulation into the supercages of zeolite-Y afforded $[Cu^{(II)}(acpy-oap)Cl]_Y$ (Scheme 27). The resultant encapsulated complex is active for the oxidation reaction of

cyclohexene and styrene.⁷⁶ The oxidation reaction of styrene gave 60.2% conversion with two major products, including styrene oxide (78.2%) and benzaldehyde (18.2%). In addition, the oxidation reaction of cyclohexene was accomplished to attain equilibrium with 61.3% conversion and selectivity: cyclohexane-1,2-diol (77.7%) > 2-cyclohexene-1-ol (11.1%) > cyclohexene epoxide (4.7%) > 2-cyclohexene-1-one (4.6%) (Scheme 28). In addition, the neat analogue $[Cu^{(II)}(acpy-oap)Cl]$ is active. However, it exhibits less conversion in comparison with the encapsulated complexes. The oxidation reaction of cyclohexene was accomplished using $[(HOO)-Cu^{(III)}(acpy-oap)Cl]$, formation, which was demonstrated with electronic absorption spectroscopy. The oxidation of styrene in the presence of $[Cu^{(II)}(acpy-oap)Cl]_Y$, was performed using 70% *tert*-butylhydroperoxide as an oxidant to afford benzaldehyde and styrene oxide, along with only minor amounts of unrecognized products.



Scheme 35 Aldol condensation of cyclohexanone and benzaldehyde using zeolite NaY, Cu(II)/Y.

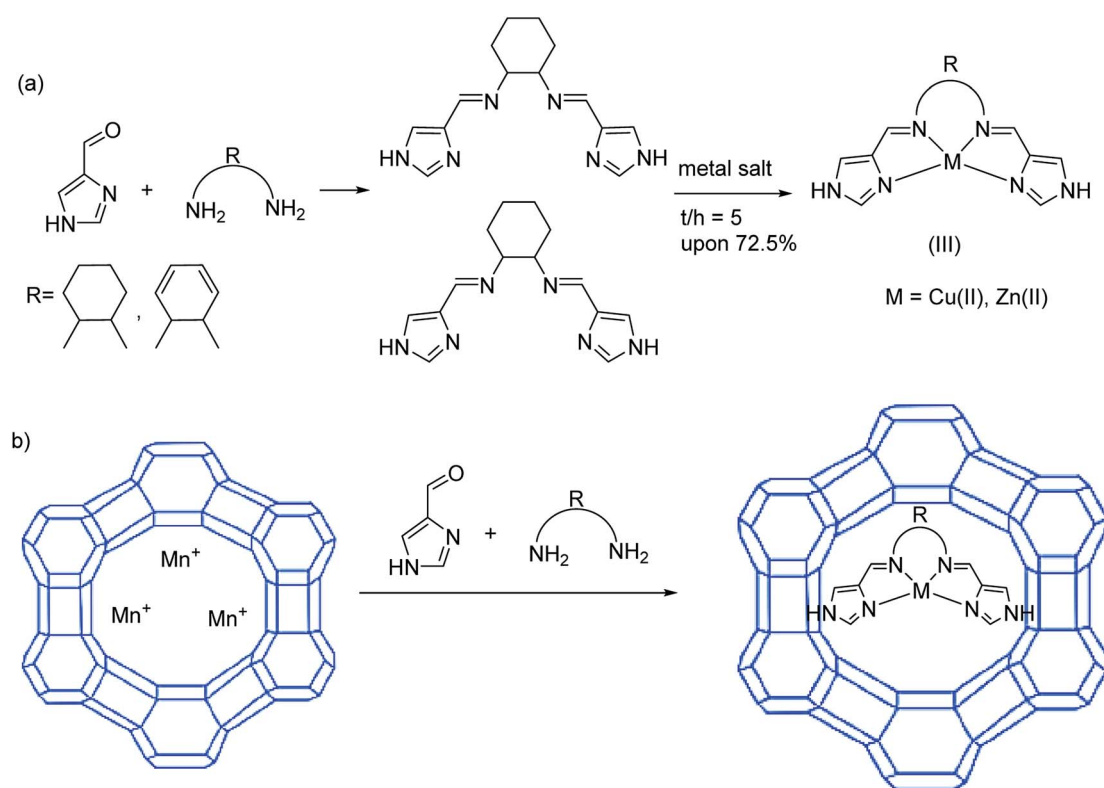


The copper(II) complex (CuL) (24), a Schiff base ligand provided from the reaction of 3,4-diaminotoluene and 2-hydroxy-naphthaldehyde, was encapsulated into the nanocavity of Y-zeolite (CuL–NaY) (Scheme 29).⁷⁷ Based on this method, 2-hydroxy-naphthaldehyde was added to an ethanolic solution of 4-methyl-*o*-phenylenediamine. The reaction mixture was heated to reflux (Scheme 29, II). The ligand (H₂L) was dissolved in EtOH and an ethanol solution of Cu(CH₃COO)₂·H₂O was added to this solution under reflux conditions (Scheme 29, III). Next, the Na-Y zeolite was suspended in water containing Cu(NO₃)₂, and Cu-NaY was provided after 24 h (Scheme 29, I). A quantity of Cu-NaY and MeCN solution of H₂L were then mixed and heated at 85 °C for 7 hours. In an oil bath, the resulting material was isolated until the complex was free from the unreacted ligand. Finally, the non-complexed metal ions in the zeolite were eliminated by exchange with aqueous sodium chloride solution (Scheme 29, IV).

The oxidation of olefins in the presence of CuL and CuL–NaY as an efficient catalyst using *tert*-butylhydroperoxide as an oxidant was achieved to provide the desired products in moderate yields. The oxidation of cyclooctene, methyl styrene, styrene and cyclohexene in the presence of CuL gave 83%, 84%, 81% and 56% conversion, respectively. In addition, the oxidation of cyclooctene, styrene, α -methyl styrene and cyclohexene in the presence of CuL–NaY gave 100%, 84%, 79% and 45% conversion, respectively.

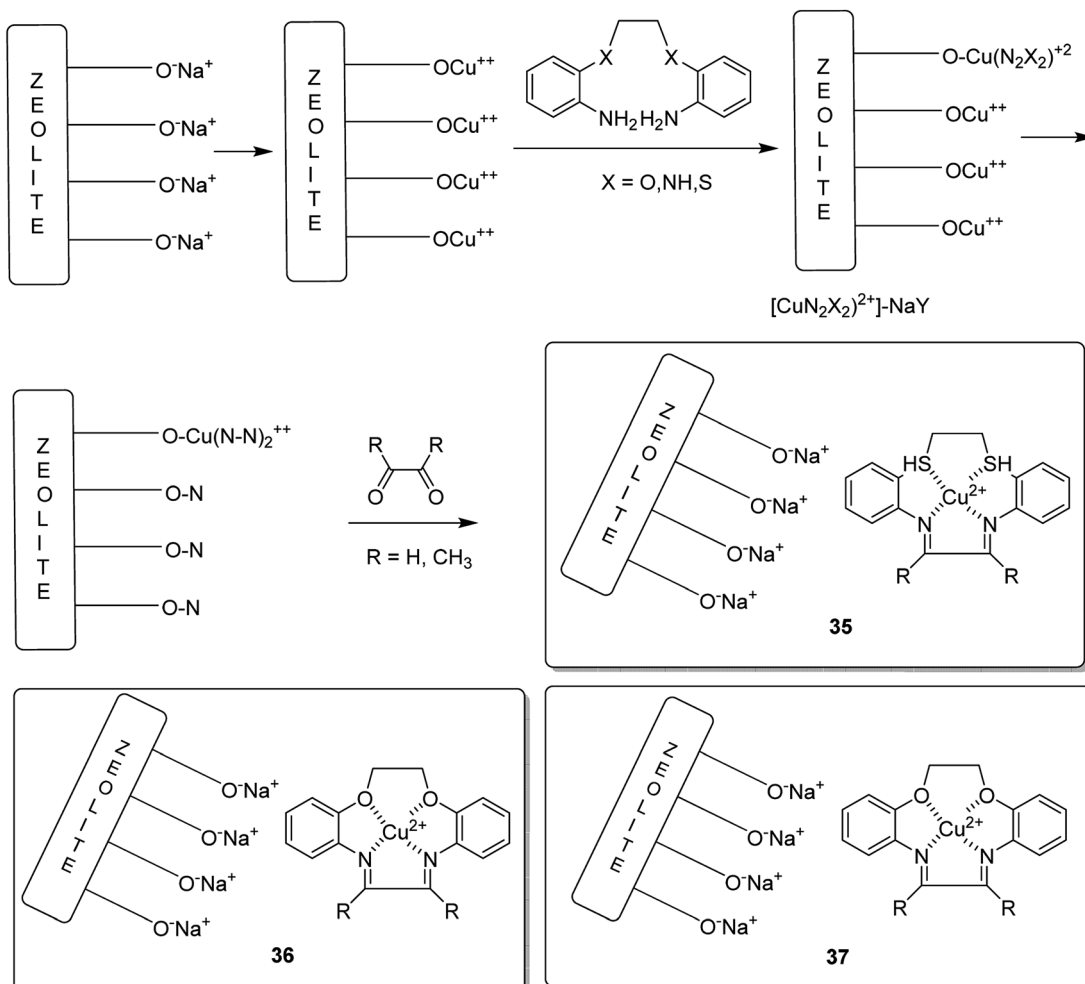
The copper(II) complexes of 16- and 17-membered diazadioxamacrocycles, [L₁]; 3,4,11,12-dibenzo-1,14-diaza-5,10-dioxacyclohexadecane-1,13-diene, [L₂]; 3,4,11,12-dibenzo-1,14-diaza-5,10-dioxacycloheptadecane-1,13-diene, and [L₃]; 3,4,11,12,15,16,17-tribenzo-1,14-diaza-5,10-dioxacycloheptadecane-1,13-diene, were encapsulated into the nanopores of zeolite-Y and synthesized through the template condensation reaction of diamine and 1,4-bis(2-carboxyaldehydephenoxy)butane [L']; Cu[L₁]²⁺·Y, Cu[L₂]²⁺·Y and Cu[L₃]²⁺·Y (Scheme 30).⁷⁸ The neat and encapsulated complexes were examined in the oxidation of cyclooctene with *tert*-butyl hydroperoxide as the oxidant using different solvents. The supported Cu[L₁]²⁺·Y showed a moderate 81.9% selectivity for epoxidation with 84.2% conversion.

A copper(II) C₂-symmetric bis(oxazoline), CuBox (28), was shown in two forms of marketable Y-zeolite: a sodium form (NaY) and an ultrastable form (NaUSY). CuBox was prepared *via* first partially replacing the sodium cations of both zeolites for copper(II), and then under reflux with the resultant precursors using a solution of bis(oxazoline) (Box) (29) (Fig. 4). Two different loadings were provided for each form of zeolite.⁷⁹ These complexes were all active in the cyclopropanation of styrene with ethyldiazoacetate at room temperature, and were diastereoselective toward *trans* cyclopropanes. Therefore, the CuBox encapsulated into NaUSY is a more active catalyst in the cyclopropanation reaction of styrene at ambient temperature



Scheme 36 Construction of the zeolite-encapsulated metal-salen complexes. Reprinted from (ref. 83) with permission of the Royal Society of Chemistry.





Scheme 37 The formation of Cu(II) complexes of the 12-membered macrocyclic ligand.

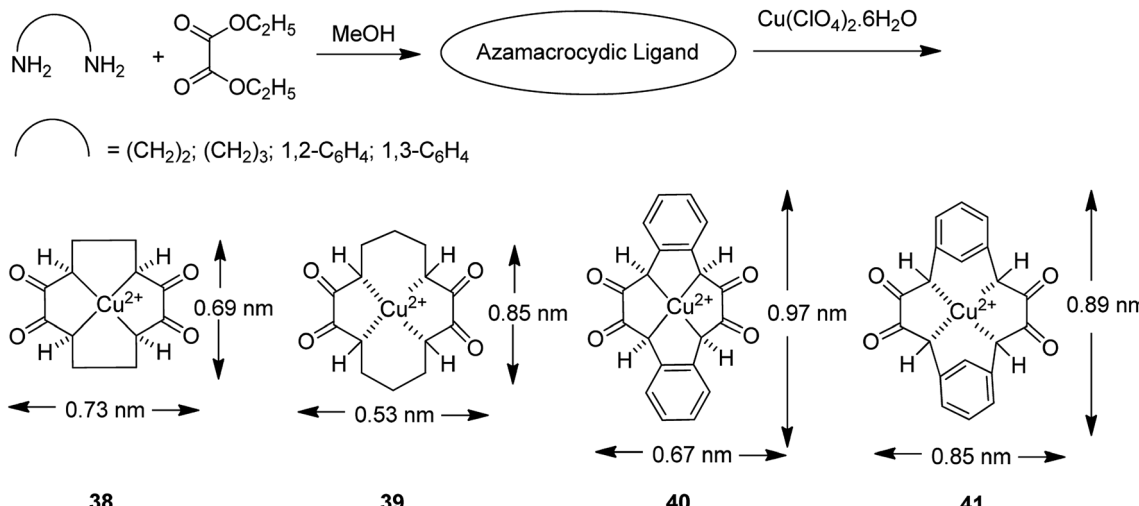
compared with NaY as the support. In addition, it was demonstrated that the catalytic activity increases with the amount of Box encapsulated. However, NaUSY showed greater activity in spite of the lower Box content, which can be identified with a stronger interaction of the zeolite and Box as a result of

dealumination reactions. The CuBox@Y₁, CuBox@Y₂, CuBox@USY₁ and CuBox@USY₂ complexes were examined as heterogeneous catalysts in the cyclopropanation reaction of styrene and ethyldiazoacetate at ambient temperature (Scheme 31). These complexes served as significant heterogeneous

Table 15 Oxidation reaction of ethylbenzene in the presence of host/guest nanocomposite materials^a

Catalyst	Conversion (%)	Selectivity (%)		
		Acetophenone	<i>o</i> - / <i>p</i> -Hydroxyacetophenone	Benzaldehyde, benzoic acid and 1-phenylethanol
Cu(II)-NaY, $[\text{Cu}([\text{H}]_2\text{-N}_4)]^{2+}$ -NaY, $[\text{Cu}([\text{H}]_2\text{-N}_4)]^{2+}$ -NaY, $[\text{Cu}([\text{H}]_2\text{-N}_4)]^{2+}$ -NaY, $[\text{Cu}([\text{CH}_3]_2\text{-N}_4)]^{2+}$ -NaY, $[\text{Cu}([\text{H}]_2\text{-N}_2\text{O}_2)]^{2+}$ -NaY, $[\text{Cu}([\text{CH}_3]_2\text{-N}_2\text{O}_2)]^{2+}$ -NaY, $[\text{Cu}([\text{H}]_2\text{-N}_2\text{S}_2)]^{2+}$ -NaY, $[\text{Cu}([\text{CH}_3]_2\text{-N}_2\text{S}_2)]^{2+}$ -NaY	30.7–58.2	62.7–97.3	2.7–9.8	40.5

^a Reaction condition: catalyst, TBHP, ethylenedichloride, CH₃CN, *T* = 333 K.

Scheme 38 Synthesis of $[\text{Cu}(\text{azamac.})]^{2+}$.

catalysts in the cyclopropanation of styrene, and a side-product from the ethyldiazoacetate dimerization, diethyl fumarate. In addition, the materials were diastereoselective toward the *trans* cyclopropanes and the *trans* for 3 hours of reaction. The Box involving CuBox@Y₂ and CuBox@USY₂ complexes exhibited enantioselectivity (ee) for both *trans* and *cis* cyclopropane isomers: 8% (*trans*) and 6% (*cis*) for NaY and 5% (*trans*) and 4% (*cis*) for USY. It is noteworthy that in the case of CuBox@USY₂, the enantioselectivity is dependent on the reaction time and is reduced with time. Therefore, the *cis* and *trans* cyclopropane ees are very poor in comparison with those that result once the reaction is performed in homogeneous cases based on the similar reaction conditions as the heterogeneous ones.

The Cu(II) complex of dimethylglyoxime (dmgH₂) **30** and *N,N*-ethylenebis(7-methylsalicylideneamine) (Me₂salen) **31** were encapsulated *in situ* into the Y-zeolite using the reaction of ion-exchanged metal ions through the flexible ligand method, which had diffused into the cavities (Fig. 5).⁸⁰ Data analysis exhibited the formation of complexes in the pores without influencing the zeolite framework structure, the absence of any unnecessary species and the geometry of the encapsulated complexes. The catalytic activity for hydrogen peroxide decomposition and the oxidation reaction of benzyl alcohol and ethylbenzene using zeolite complexes were examined. Of significance, the zeolite complexes were stable to be recycled and were appropriate to be employed as partial oxidation catalysts. The activity increases on elevating the reaction temperature from 323 to 343 K. The results demonstrated that YCu(dmgH)₂ experienced a higher degree of deactivation (53% loss in activity), while YCuMe₂salen exhibited improved poison-tolerance (Table 14). It is widely supposed that the stereochemical environment of the active site includes an extreme effect on the mobility of the molecules at the reaction center and therefore, on the poison-tolerance. Moderately superior activity of YCu(dmgH)₂ in comparison with YCuMe₂salen could be related to the increased mobility of the reactants at the active sites. The encapsulation of cobalt(II), nickel(II) and copper(II)

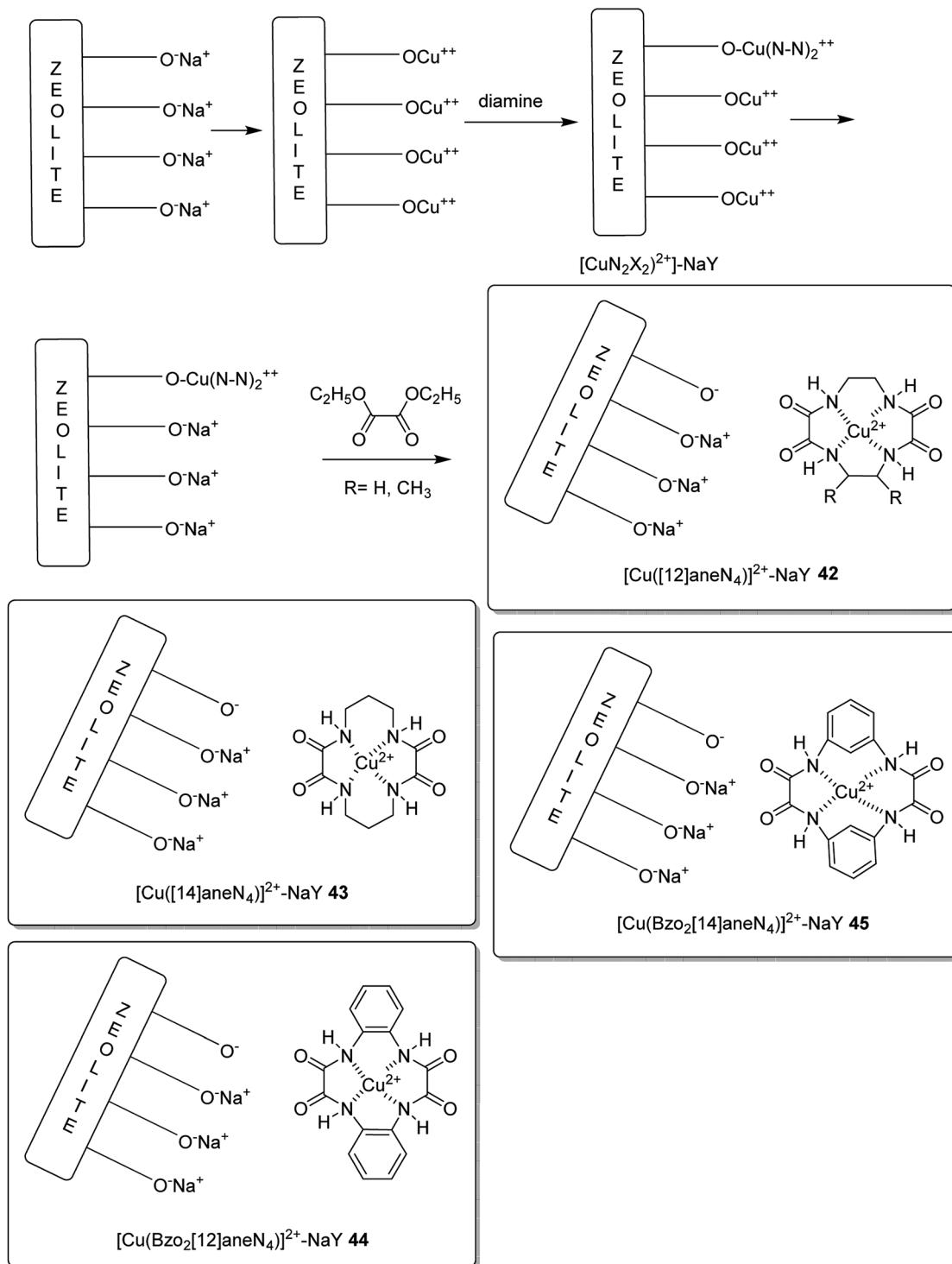
complexes of dmgH₂ and Me₂salen ligands was accomplished into the Y-zeolite *via* a flexible ligand method. The ligands, that are flexible enough to diffuse *via* the zeolite channels, react with the pre-exchanged metal ions in the supercage to yield the encapsulated complexes.

To mimic the structure and function of the enzyme, metal-imidazolesalen complexes were provided *in situ* in the cavities of the Y zeolite. Zeolite-encapsulated Cu salen II demonstrated appropriate catalytic activity in the selective oxidation reaction of benzyl alcohol. In particular, the efficacy and selectivity of the zeozyme were compared to those of the free copper-salen II complex in solution. The resultant zeozyme concurrently contains high activity and homogeneous catalysts. The copper(II), complex of 2-methylimidazole (2-MeImzIH) was encapsulated into the supercages of zeolite-Y ([Cu(2-MeImzIH)]-Y) **32** (Scheme 32).⁸¹ Oxidation of benzyl alcohol in the presence of these encapsulated complexes gave only benzaldehyde as the desired product. In addition, the oxidation of phenol was accomplished in the presence of [Cu(2-MeImzIH)]-Y as a significant catalyst using H₂O₂ as an oxidant in acetonitrile. The two products hydroquinone and catechol were identified in the reaction mixture with a mass balance of 95%.

The copper(II) complex of 4-(*E*)-4-(1Hbenzo[*d*]imidazol-2-yl)phenyl)diazenyl)-2-((*E*)-(4-hydroxyphenylimino)methyl)phenol (HL) **33** was encapsulated into zeolite NaY through the flexible ligand method (Scheme 33).⁸² The neat and encapsulated complexes were examined in the oxidation of benzyl alcohol and the aldol condensation reaction. Notably, the encapsulated complex was more stable and active than the relevant neat complex.

This reaction was demonstrated to be very dependent on the effect of the solvent. The results exhibited that once the reaction was performed in solvents having coordinative capability like EtOH and THF, the yield of the reaction exhibited an extreme reduction. This is possibly related to the strong coordination of the solvent *via* oxygen atoms to acidic sites of the catalyst. In addition, the polarity of CH₂Cl₂ is greater than CHCl₃. The



Scheme 39 Encapsulation of $[\text{Cu}(\text{azamac.})]^{2+}$ into the nanocavity of zeolite-Y.

mechanism of the reaction possibly also includes a polarized transition state. Consequently, it is not unreasonable that CH_2Cl_2 , in comparison to CHCl_3 , improved the yield and stability of the transition state. Thus, CH_2Cl_2 was found to be the optimal solvent in this reaction.

It is noteworthy that the leaching from the supercages of zeolite was not detected during the reactions with this encapsulated complex.

The activity of this type of catalyst was examined in the benzyl alcohol oxidation. The corresponding products of the benzyl alcohol oxidation are shown in Scheme 34. Zeolite NaY,

Table 16 Oxidation reaction of ethylbenzene using TBHP in the presence of copper(II) complexes^a

Catalyst	Conversion (%)	Selectivity (%)		
		Acetophenone	<i>o</i> -/p-Hydroxyacetophenone	Benzaldehyde
$[\text{Cu}([12]\text{aneN}_4)](\text{ClO}_4)_2$	31.9–56.5%	86.3%	22.7%	19.7%
$[\text{Cu}([12]\text{aneN}_4)](\text{ClO}_4)_2$, $[\text{Cu}(\text{BzO}_2[12]\text{aneN}_4)](\text{ClO}_4)_2$, $[\text{Cu}(\text{BzO}_2[12]\text{aneN}_4)](\text{ClO}_4)_2[\text{Cu}(\text{BzO}_2[12]\text{aneN}_4)](\text{ClO}_4)_2$, $[\text{Cu}(\text{BzO}_2[12]\text{aneN}_4)](\text{ClO}_4)_2[\text{Cu}(\text{BzO}_2[12]\text{aneN}_4)](\text{ClO}_4)_2$, $[\text{Cu}(\text{BzO}_2[12]\text{aneN}_4)](\text{ClO}_4)_2[\text{Cu}(\text{BzO}_2[12]\text{aneN}_4)](\text{ClO}_4)_2$				

^a Reaction condition: ethylbenzene in ethylenedichloride, catalyst, TBHP, acetonitrile, $T = 333$ K.

Table 17 Oxidation reaction of ethylbenzene using TBHP in the presence of a catalyst^a

Catalyst	Conversion (%)	Selectivity (%)		
		Acetophenone	<i>o</i> -/p-Hydroxyacetophenone	Benzaldehyde
$[\text{Cu}([12]\text{aneN}_4)]^{2+}\text{-NaY}$, $[\text{Cu}([12]\text{aneN}_4)]^{2+}\text{-NaY}$, $[\text{Cu}(\text{BzO}_2[12]\text{aneN}_4)]\text{-NaY}$, $[\text{Cu}(\text{BzO}_2[12]\text{aneN}_4)]\text{-NaY}$, $[\text{Cu}(\text{BzO}_2[12]\text{aneN}_4)]\text{-NaY}$, $[\text{Cu}(\text{BzO}_2[12]\text{aneN}_4)]\text{NaY}$, $[\text{Cu}(\text{BzO}_2[12]\text{aneN}_4)]\text{NaY}$	31.4–52.9%	99.0%	3.8%	40.5%

^a Reaction condition: ethylbenzene, catalyst, TBHP in ethylenedichloride, acetonitrile, $T = 333$ K.

$\text{Cu}(\text{II})/\text{Y}$, the encapsulated complex and free complex were applied and compared in this approach.

Moreover, the catalytic activity of the resultant complexes was explored in the acid-catalyzed aldol condensation. The reaction of benzaldehyde and cyclohexanone was achieved in the presence of zeolite $\text{NaY}/\text{Cu}(\text{II})/\text{Y}$ *via* aldol reaction (Scheme 35). Remarkably, the reactivity of the aldol reaction was intensely affected by the nature of the solvent, and the nature and quantity of catalyst.

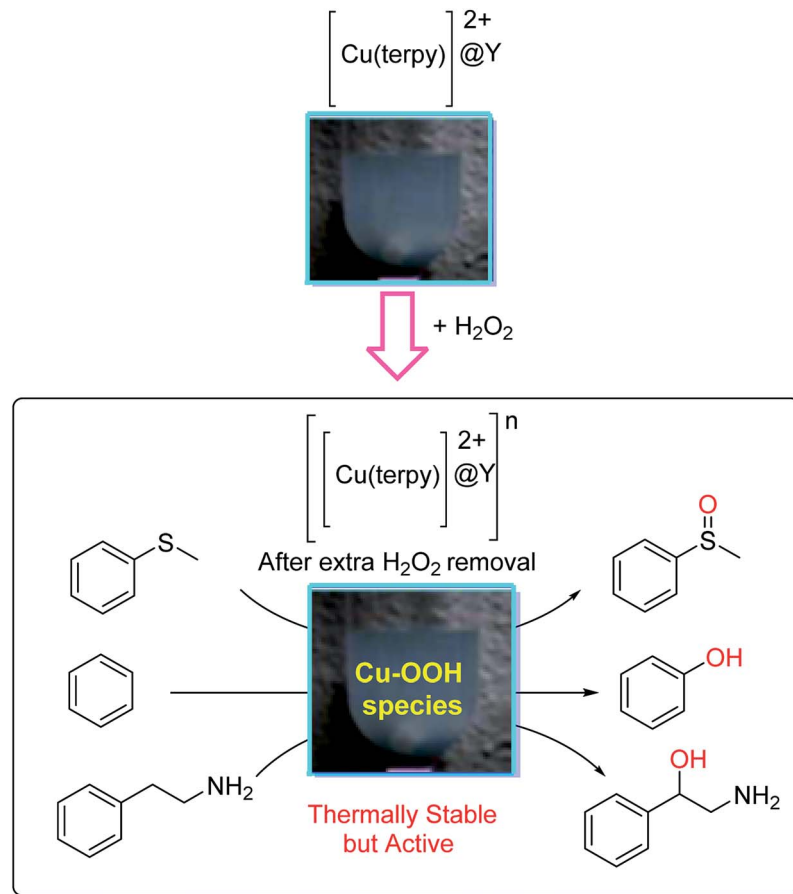
Metal-imidazole-salen complexes were encapsulated *in situ* in the cavities of Y zeolite by Song and co-workers 2018.⁸³ The zeolite- Y encapsulated metal-salen was designated as M-salen Y 34. The chemical structures and synthetic routes of the metal-salen-comprising samples are shown in Scheme 36. The catalytic activities of MY, M-salen and encapsulated M-salenIIY samples for the selective oxidation of benzyl alcohol were explored. The results demonstrated that the activity of the catalyst followed the order: Cu-salenII > Cu-salenI > Zn-salenII > Zn-salenI. For the similar ligand, copper(II)-salen complexes were more active than Zn salen. These results showed that the inherent properties of the M-salen complexes, including their electronic configuration and geometry, exhibited a key role in identifying their catalytic activities. In addition, the oxidation mechanism may be different for copper(II) and zinc(II)

complexes, with $\text{Zn}(\text{II})$ salen(I/II) catalysts containing a redox inactive central ion. Thus, Cu-salen(II), comprising lower oxidation state and a planar tetragonal structure, illustrated the highest benzyl alcohol oxidation activity.

Copper(II) complexes of the 12-membered macrocyclic ligands bearing three different donating atoms (N_2S_2 (35), N_2O_2 (36) and N_4 (37)) in the macrocyclic ring were encapsulated into the nanocavity of zeolite- Y *via* the flexible ligand method (Scheme 37).⁸⁴ It is noteworthy that the copper(II) complexes having macrocyclic ligands were entrapped in the nanocavity of zeolite- Y . Remarkably, the neat and encapsulated complexes exhibited satisfactory catalytic activity in the oxidation of ethylbenzene at 333 K, using *tert*-butylhydroperoxide (TBHP) as the oxidant. Moreover, acetophenone was the major product synthesized when using small amounts of *o*- and *p*-hydroxyacetophenones, showing that the carbon–hydrogen bond activation occurs both at the benzylidic and aromatic ring carbon atoms (Table 15). Noticeably, ring hydroxylation reaction was more over the neat complexes in comparison to over the encapsulated complexes.

The encapsulation of various copper(II) complexes including [12]ane N₄: 1,4,7,10-tetraazacyclododecane-2,3,8,9-tetraone [Cu([12]aneN₄)]²⁺ (38); [14]aneN₄: 1,4,8,11-tetraazacyclotetradecane-2,3,9,10-tetraone [Cu([14]aneN₄)]²⁺ (39); BzO₂[12]





Scheme 40 Reaction of $[\text{Cu}(\text{terpy})]^{2+}@\text{Y}$ and hydrogen peroxide to form the thermally stable, but active, $\text{Cu}^{\text{II}}\text{-OOH}$ species in $[\text{Cu}(\text{terpy})]^{2+}@\text{Y}$. Reprinted from (ref. 86) with permission of the Royal Society of Chemistry.



Scheme 41 Oxygenation reaction of enamines catalyzed by the $\text{Cu}(\text{Cl})\text{-X}$ zeolite.

aneN₄: dibenzo-1,4,7,10-tetraazacyclododecane-2,3,8,9-tetraone and $\text{BzO}_2[14]\text{aneN}_4$ $[\text{Cu}(\text{BzO}_2[12]\text{oneN}_4)]^{2+}$ (**40**) and dibenzo-1,4,8,11-tetraazacyclotetradecane-2,3,9,10-tetraone $[\text{Cu}(\text{BzO}_2[14]\text{oneN}_4)]^{2+}$ (**41**) into the nanopores of zeolite-Y (**42–45**) was achieved using the *in situ* one-pot condensation reaction (Schemes 38 and 39).⁸⁵

The neat and encapsulated complexes exhibited satisfactory catalytic activity in the oxidation of ethylbenzene using *tert*-butyl hydroperoxide (TBHP) as the oxidant at 333 K. Remarkably, acetophenone was the main product synthesized using small amounts of *o*- and *p*-hydroxyacetophenones, exhibiting that C–H bond activation occurs both at the aromatic and benzylic ring carbon atoms. The ring hydroxylation performed much better than the neat complexes, in comparison to its performance over that of the encapsulated complexes. Transformation for copper(II) complexes with different

azamacrocyclic ligands decreased in the order: $\text{BzO}_2[14]\text{aneN}_4 > [12]\text{aneN}_4 > \text{BzO}_2[14]\text{aneN}_4 > [14]\text{aneN}_4$ (for neat and encapsulated complexes). The encapsulated complexes demonstrated higher activity in comparison with the neat complexes (Tables 16 and 17).

The $[\text{Cu}(\text{terpy})]^{2+}$ complexes in the Na-Y zeolite ($[\text{Cu}(\text{terpy})]^{2+}@\text{Y}$) (terpy = 2,2':6',2''-terpyridine) were encapsulated and their catalytic activity was explored in the oxidation reaction of sulfides with hydrogen peroxide.⁸⁶ The oxidation of thioanisole, benzene and 2-phenethylamine in the presence of $[[\text{Cu}(\text{terpy})]^{2+}@\text{Y}]^*$, generated by the reaction of $[\text{Cu}(\text{terpy})]^{2+}@\text{Y}$ and hydrogen peroxide, was accomplished as shown in Scheme 40.

CuCl_2 complexes were easily prepared within the pores of zeolite X, with the modified zeolite found to serve as a heterogeneous catalyst for the oxygenation reactions of various

Table 18 The oxidative removal of enamines in the presence of the Cu-X zeolite as an efficient catalyst with molecular O₂^a

Substrate	t/h	Conversion (%)	Yield (%)		Products (%)	
			Amide	Ketone		
1-(2-Methylprop-1-en-1-yl)piperidine, 4-(2-methylprop-1-en-1-yl)morpholine, (<i>E</i>)-4-(2-methylpent-1-en-1-yl)morpholine, 4-(2-ethylbut-1-en-1-yl)morpholine, (cyclohexyldienemethyl)morpholine, 4-(2,2-diphenylvinyl)morpholine, 2,3-dimethyl-1 <i>H</i> -indole	5	91–100%	84–97%	66–97%		

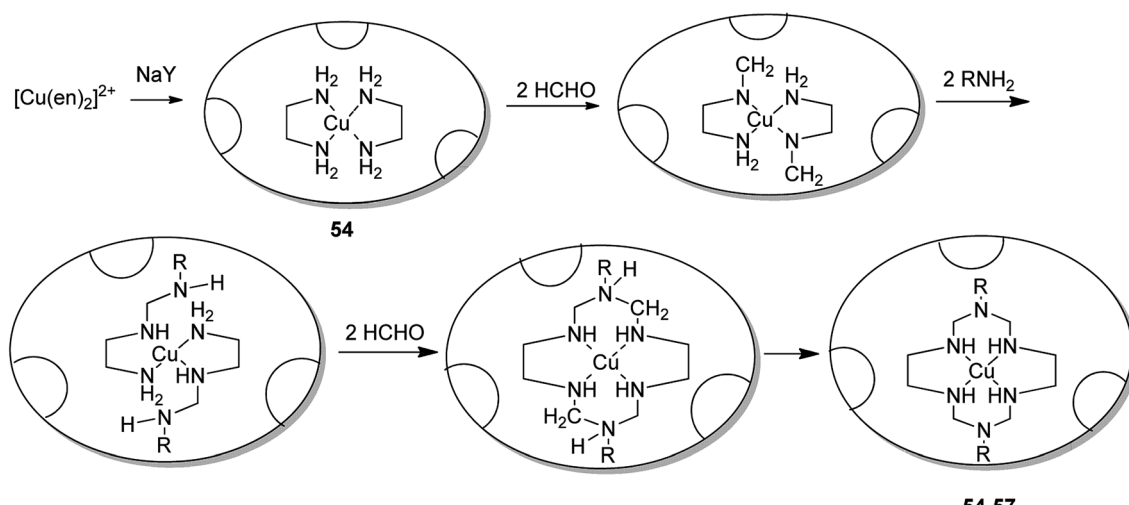
^a Reaction condition: CuX, MeCN, 50 °C, O₂ atmosphere.

Number	Complex
46	[Cu(en) ₂] (ClO ₄) ₂
47	[Cu((Me) ₂ [14] ane N ₆)] (ClO ₄) ₂
48	[Cu((Et) ₂ [14] ane N ₆)] (ClO ₄) ₂
49	[Cu((Bu) ₂ [14] ane N ₆)] (ClO ₄) ₂
50	[Cu((Benzyl) ₂ [14] ane N ₆)] (ClO ₄) ₂
51	NaY
52	Cu(II)-NaY
53	[Cu(en) ₂] ²⁺ -NaY
54	[Cu((Me) ₂ [14] ane N ₆)] ²⁺ -NaY
55	[Cu((Et) ₂ [14] ane N ₆)] ²⁺ -NaY
56	[Cu((Bu) ₂ [14] ane N ₆)] ²⁺ -NaY
57	[Cu((Benzyl) ₂ [14] ane N ₆)] ²⁺ -NaY

Scheme 42 The formation of Cu(II) complexes of the 14-membered hexaazamacrocyclic ligand.

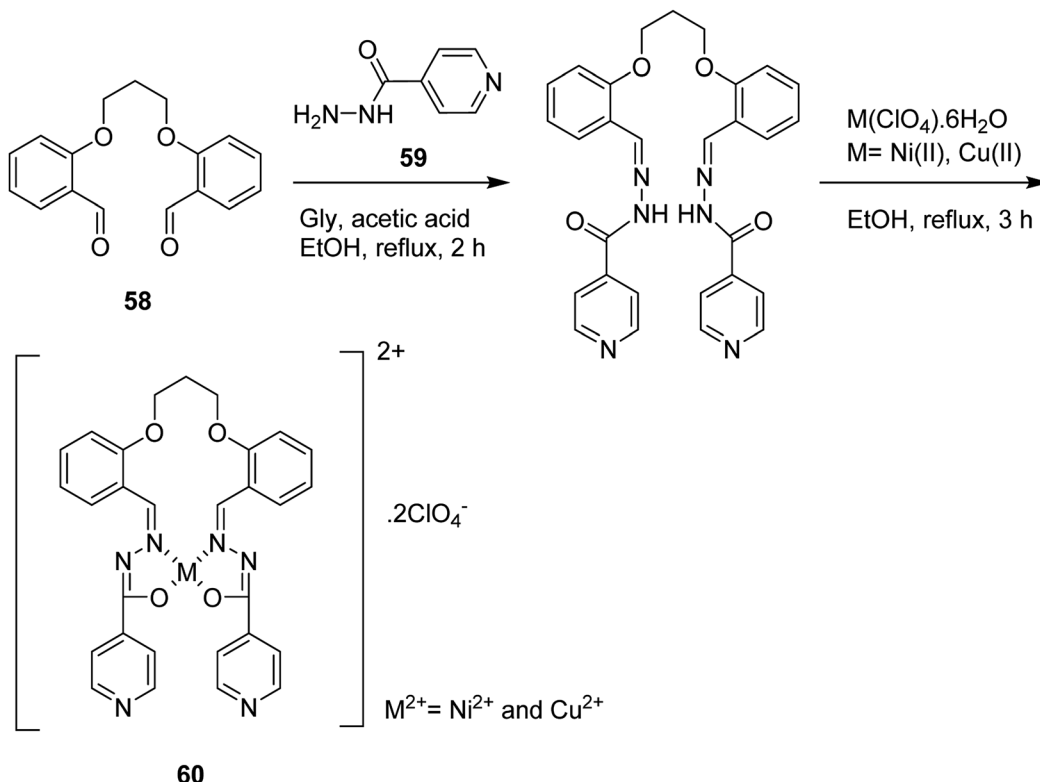
enamines using molecular oxygen (Scheme 41).⁸⁷ It is noteworthy that this catalyst can be recycled without leaching the Cu species, and the catalyst preserved its excellent catalytic activity and selectivity in this oxygenation reaction.

Kaneda and co-workers in 1982 demonstrated that the oxygenation reaction catalyzed by Cu(Cl)-X might contain a one-electron transfer from the enamine to molecular O₂ in a ternary Cu²⁺ complex attached to enamine and O₂, followed by the

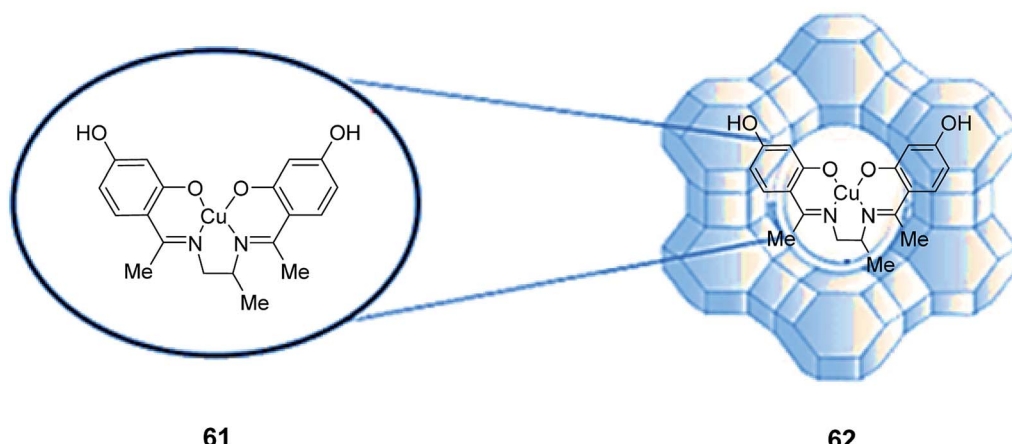


Scheme 43 The encapsulation of Cu(II) complexes of the hexaaza ligand inside the zeolite pore.





Scheme 44 The suggested probable mechanism of the nickel(II) and copper(II) complexes having a tetradentate N_2O_4 Schiff base moiety.



Scheme 45 Suggested scaffold structure of the zeolite-encapsulated metal Schiff base complexes. Reprinted from (ref. 91) with permission of the Royal Society of Chemistry.

formation of Cu^{2+} and a dioxetane intermediate.⁸⁸ These important results for the oxygenation reaction of enamines with Cu-X in MeCN-DCE are demonstrated in Table 18. The carbon double bonds of different enamines were easily eliminated to afford the corresponding ketones and amides. For bulky enamines (for instance, 1-(4-morpholino)-2,2-diphenylethene), the oxygenation rate with Cu-X was slower in comparison with that of a homogeneous copper(II) chloride catalyst. This different activity between the heterogeneous Cu-X and the homogeneous copper(II) chloride catalyst might be attributed to

a shape selective effect of the Cu^{2+} species in the three-dimensional zeolite pores. In addition, the Cu-X catalyst was active for the oxygenation reaction of 2,3-dimethylindole.

Salavati-Niasari and co-workers in 2003 demonstrated the formation of various copper(II) complexes of 14-membered hexaazamacrocyclic ligand “1,3,6,8,10,13-hexaazacyclotetradecane, 1,8-dimethyl-“ $[\text{Cu}((\text{Me})_2[14]\text{aneN}_6)](\text{ClO}_4)_2$ ” 47, 1,8-diethyl-“ $[\text{Cu}((\text{Et})_2[14]\text{aneN}_6)](\text{ClO}_4)_2$ ” 48, 1,8-dibutyl-“ $[\text{Cu}((\text{Bu})_2[14]\text{aneN}_6)](\text{ClO}_4)_2$ ” 49 and 1,8-dibenzyl-1,3,6,8,10,13-hexaaza cyclotetradecane “ $[\text{Cu}((\text{benzyl})_2[14]\text{aneN}_6)](\text{ClO}_4)_2$ ” 50”.⁸⁹

Table 19 Oxidation reaction of different sulfides with hydrogen peroxide catalyzed by CuL-Y^a

Substrates	CuL-Y	Conversion	Selectivity
		(%)	(%)
		(Sulfoxide)	(CuL-Y)
		100	100
		97	90
		100	100
		93	95
		55	100
		100	100
		100	100
		95	100
		100	100
		100	100

^a Reaction conditions: catalyst : sulfide : H₂O₂ : 1 : 80 : 800 at 25 °C for a 20 min reaction time.

Notably, these complexes were entrapped in the supercage of zeolite Y *via* a two-step route in the liquid phase, including the inclusion of a Cu(II) precursor complex, [Cu(en)₂]²⁺-NaY 53, and the spontaneous one-pot reaction of the copper(II) precursor complex using an amine and formaldehyde (Scheme 42). These complexes 55–57 were applied in the oxidation reaction of tetrahydrofuran using H₂O₂ as the oxygen donor. Remarkably, the resultant encapsulated complexes gave mostly THF-2-ol and

a slight quantity of THF-2-one. While using their homogenous counterparts, the selectivities to THF-2-one are better.

The 14-membered hexaazamacrocyclic Cu(II) encapsulated complexes in zeolite (54–57) were synthesized using a stepwise approach *via* flexible ligand method.⁹ As a result, the copper(II) complexes of hexaaza ligand encapsulated into the zeolite pore were synthesized efficiently (Scheme 43).

Schiff base ligand *O,O'*-trimethyl bis(salicylidene isonicotinoyl hydrazone) (H₂L) (60), synthesized by treatment of 1,3-bis(2-carboxyaldehydephenoxy) propane (SAL) (58) and isonicotinyl hydrazine (INH) (59) with Ni(II) and Cu(II) perchlorates (Scheme 44),⁹⁰ was encapsulated into the cavities of the zeolite *via* a fixed ligand method. Both free complexes and encapsulated complexes have been examined in the liquid phase oxidation reaction of benzhydrol/hydrogen peroxide, and the photodegradation of rhodamine-B (RhB) using UV/visible (H₂O₂) irradiation. The catalytic activities of the benzhydrol oxidation and rhodamine-B degradation were greater in comparison with those of the neat complexes and encapsulated complexes, respectively. It is noteworthy that in most cases, the copper(II) [Cu(II)L-Y, Cu(II)L₂ClO₄] complexes demonstrated greater activity in comparison with the nickel(II) complexes [Ni(II)L₂ClO₄, Ni(II)L-Y] in both benzhydrol and rhodamine-B degradation reactions.

The a tetradentate (N₂O₂) Schiff base ligand (H₂L) (61) and its related copper(II) complex (CuL) (62) were synthesized and encapsulated in the cavities of zeolite-Y *via* a fixed ligand method (Scheme 45).⁹¹

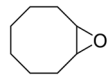
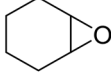
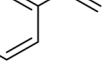
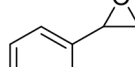
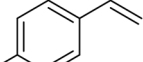
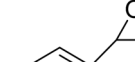
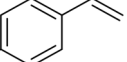
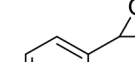
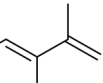
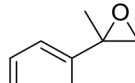
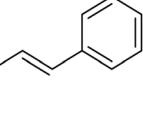
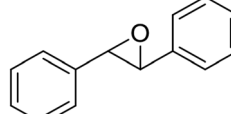
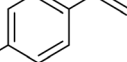
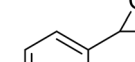
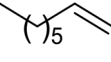
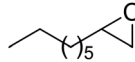
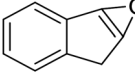
The catalytic and electrochemical activity of the synthesized encapsulated complex was examined in the oxidation of a wide range of olefins and sulfides using H₂O₂ in ethanol (Tables 19 and 20). The catalyst showed excellent activity in the oxidation of styrene in ethanol. Remarkably, various olefins afforded the epoxide products with high selectivity and conversion (Table 19).

Raja and Ratnasamy in 1997 explored the low temperature and selective oxidation of toluene, benzene, naphthalene and ethyl benzene over Cl- and NO₂-substituted phthalocyanine complexes of Cu encapsulated in zeolites X and Y, with molecular oxygen and aqueous H₂O₂ as the oxidants.¹⁰ It is noteworthy that the catalytic activity of the copper atoms is greater in the encapsulated state in comparison with the neat copper phthalocyanines. Once benzene was oxidized to phenol, both side chain oxidation and ring hydroxylation were identified in the case of the alkyl aromatics. Cl- and NO₂-substituted complexes of copper(II), cobalt(II) and iron encapsulated in molecular sieves are selective and favorable oxidation catalysts. Both ring hydroxylation of alkyl aromatics and side chain oxidation were identified in the oxidation of various aromatic substrates using CuCl₄Pc-Na-Y (0.17) with molecular oxygen or H₂O₂ as the oxidants (Table 21).

In the oxidation of benzene, catechol and hydroquinone were synthesized using the oxidation reaction of phenol. For toluene, the ring hydroxylation was the main reaction when molecular oxygen was used as the oxidant (80 wt%, yield of cresols). The oxidation reaction of the methyl group to



Table 20 Epoxidation reaction of olefins in the presence of CuL-Y as a catalyst and using H_2O_2 in EtOH^a

Substrate	Products	Conversion (%)		Epoxide selectivity (%)
		(CuL ₁ -Y)	(CuL ₁ -Y)	
		100		100
		100		100
		100		95
		98		94
		97		95
		100		90
				100
		100		98
		78		100
		100		100

^a The molar ratio of the catalyst : alkene : H_2O_2 was 1 : 50 : 500 in EtOH at 55 °C for a one-hour reaction time.

benzaldehyde, benzyl alcohol, and benzoic acid (total selectivity = 94.1% wt) predominated using H_2O_2 as the oxidant.

The liquid-phase direct catalytic oxidation reaction of benzene to phenol was performed using a copper(II) complex in a Faujasite-type zeolite with sucrose as a reducing agent and molecular oxygen as an oxidant.⁹² The construction of phenol using the copper(II) complex encapsulated in Y-zeolite was also examined using sucrose in the aqueous solution of acetic acid. Sucrose was an effective additive as a reducing agent since it was

hydrolyzed into two reducing sugars, including fructose and glucose. The results of the reusing experiments for CuPA-Y, CuQA-Y, CuPCA-Y and Cu-Y, using Cu/Y (Imp) as a reference, are shown in Table 22.

Nair and co-workers in 2016 examined the degradation of 4-chloro-3-methylphenol (PCMC) using zeolite-encapsulated copper(II) complexes of *N,N'*-disalicylidene-1,2-phenylenediamine as significant heterogeneous catalysts *via* a Fenton-type improved oxidation reaction (Scheme 46).⁹³ The

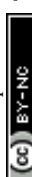


Table 21 Oxidation reaction of aromatic hydrocarbons using $\text{CuCl}_{14}\text{Pc-Na-Y}$ (0.17)^a

Substrate	Oxidant	Conversion (%)	Products (%, wt)
Benzene	H_2O_2	6.2	Phenol (95) (Cat + HQ)
	O_2	5.4	Phenol (100)
Toluene	H_2O_2	23.6	CH_2OH (68.6); CHO (8.8); COOH (16.5); cresols (5.9)
	O_2	22.9	CH_2OH (4.3), CHO (15.7), cresols (80)
Ethyl benzene	H_2O_2	31.6	COCH_3 (19.7), CHOCH_3 (20.9), <i>ortho</i> + <i>para</i> hydroxyl ethyl benzenes (58.3), <i>para</i> hydroxyl acetophenone (0.9)
	O_2	16.2	COCH_3 (80.2), CHOCH_3 (9.27), <i>ortho</i> + <i>para</i> hydroxyl ethyl benzenes (4.3), <i>ortho</i> + <i>para</i> hydroxyl acetophenone (6.2)
Naphthalene	H_2O_2	17.9	α -Naphthol (7.8), β -naphthol (53.6), naphthaquinone (1.1), phthalic anhydride (37.4)
	O_2	5.4	β -Naphthol (100)

^a Reaction condition: substrate/ H_2O_2 (3 mol), r.t., $t = 8$ h, acetonitrile, $T = 384$ K, catalyst = $\text{CuCl}_{14}\text{Pc-Na-Y}$ (0.17).

Table 22 The results of the reusing tests for the oxidation of benzene with the copper catalyst using sucrose as a reducing agent

Catalyst	Copper content (wt%)	Yield (%)	Phenol (%)
		Run 1	Run 2
Y-zeolite	0.0	n.d.	n.d.
Imp. Cu/Y	15.0	5.3	1.9
Cu-Y	6.18	4.6	1.7
CuPA-Y	7.00	7.0	4.4
CuQA-Y	6.00	7.4	5.2
CuPCA-Y	6.09	5.1	3.3

results demonstrated that at low acidic pH, nearly complete removal of 4-chloro-3-methylphenol was performed using the iron(III), nickel(II), and copper(II) catalysts with hydrogen peroxide. The Fe(III), Ni(II) and Cu(II)-*N,N'*-disalicylidene-1,2-phenylenediamine complexes were efficiently encapsulated *via* the ship-in-a-bottle approach into the zeolite Y supercage.

The reductions in the percentage degradation upon ten cycles for the Ni(II)-, and Cu(II)- and Fe(III)-based catalysts were 25%, 21%, and 14%, respectively. However, decreases in the catalytic activities were detected. The heterogeneous catalytic performances of the catalysts were not lost since the zeolite building block avoided leaching the metal-salophen complexes. Notably, these results demonstrated that these catalysts could be recycled at least three to five times without significant loss of activity.

Researchers worldwide have focused their interest on providing approaches for the removal of pollutants. These pollutants include dyes arising from various industries, such as

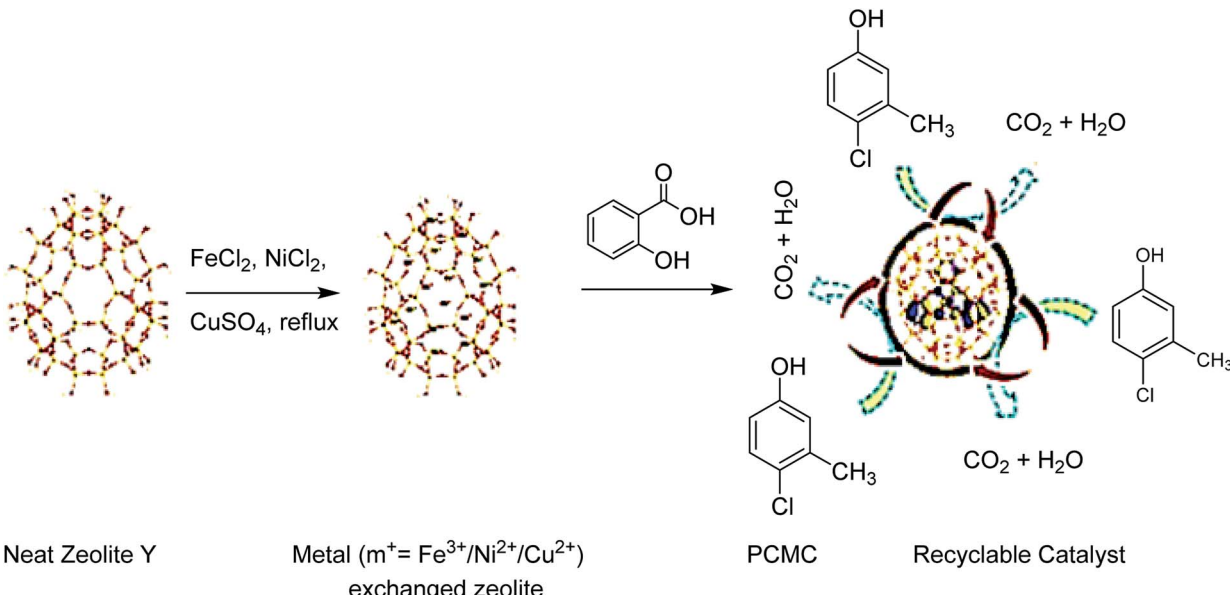
leather, textile and others. It is expected that about 1–15% of the dye is lost during the dyeing methods, and is released in wastewaters.⁹⁴ Removal of organic pollutants (such as dyes) with a Fenton reagent containing homogenous iron ions and H_2O_2 , was found to be very active.⁹⁵ Copper was found to undergo a Fenton-type reaction, and was used successfully to react with various organic pollutants.⁹⁶

The Fenton kind of process is a very favorable oxidation method in which wastewater is reacted with hydrogen peroxide in a non-pressurized reactor at low temperature with a catalyst, affording CO_2 and H_2O or other oxidation products.⁹⁷

The catalytic wet H_2O_2 oxidation reaction of an anionic dye was explored in this research. The copper(II) complex of *N,N'*-ethylene bis(salicylidene-aminato) (salenH₂) was encapsulated into supercages of zeolite-Y *via* flexible ligand method. The effect of various factors, including the catalyst, pH and hydrogen peroxide concentration, on the oxidation of dye were explored. Complete color removal is accomplished at 60 °C in less than 1 hour, using catalyst and hydrogen peroxide. Investigations on the marketable tannery wastewaters show that the catalyst acts well, even when using other chemicals in the processing.

The oxidation/decomposition of various organic materials using H_2O_2 is enhanced with the addition of a catalyst, as the latter activates the construction of 'OH from hydrogen peroxide. The reaction occurring in a Fenton method can be produced as follows: the restrictive stage in these types of oxidations is the construction of the hydroxyl radicals.⁹⁸ The 'OH species is generated, as shown in Scheme 47, and then attacks the organic substrates in the wastewater. This investigation was related to the construction and usage of a Cu salen-incorporated zeolite as a remarkable catalyst for the decolorization of a synthetic dye solution.





Scheme 46 The degradation of 4-chloro-3-methylphenol using the zeolite-encapsulated copper(II) complexes of *N,N'*-disalicylidene-1,2-phenylenediamine as the catalyst. Reprinted from (ref. 93) with permission of the Royal Society of Chemistry.



Scheme 47 The construction of hydroxyl radicals.

2.1.2. Hydroxylation. The dimeric copper(II) acetate and chloroacetate systems (CuAc and CuClAc, respectively) were encapsulated into zeolite-Y *via* the flexible ligand method.⁹⁹ These complexes catalyzed the *o*-hydroxylation of phenols to catechols, and the oxidation reaction to *o*-benzoquinone using molecular O₂. It is noteworthy that the turnover frequency for the phenol conversion increased remarkably after encapsulation. Due to the improved Cu–Cu binding after encapsulation, the strength and lability of the Cu–phenolate and Cu–dioxygen bonds are modified using a transaxial ligand influence, accounting for the increased reactivity of the encapsulated complex. A qualitative and preliminary view of the mechanism of oxidation reaction that arises from the investigations is that based on the conditions at pH 6.5,¹⁰⁰ the phenols are found in the phenolate form. Two phenolate ions coordinate to the two Cu(II) ions of the copper(II) acetate dimer, reducing them to the copper(I) oxidation state. Next, the reaction of dioxygen with the copper(II)-phenolate complex afforded a Cu₂–O₂-phenolate adduct. The latter undergoes oxygen–oxygen bond scission simultaneously with the hydroxylation of the substrate. Finally, the acetate group can change its mode of coordination from a bidentate to a monodentate type as a result of providing the dioxygen adduct (Scheme 48).

Copper(II), nickel(II) and zinc(II) complexes of the amidate ligand 1,2-bis(2-hydroxybenzamido) ethane(H₂hybe) (63) were encapsulated into the supercages of zeolite-Y ([Cu(hybe)]-Y) (Scheme 49).¹⁰¹ These complexes catalyzed the liquid-phase hydroxylation reaction of phenol to catechol as a major

product, and hydroquinone as a major product using hydrogen peroxide. Based on the optimized conditions, ([Cu(hybe)]-Y) exhibited the maximum conversion of 40% after 6 hours.

Table 23 shows the results along with the Turnover Frequency (TOF) for the phenol conversion upon 6 hours of reaction time. The selectivity of the catechol construction is comparable (89–91%) in all cases. However, the conversion of phenol changed from catalyst to catalyst. Fascinatingly, this great selectivity of the catechol construction is preserved even with 24 hours of reaction time.

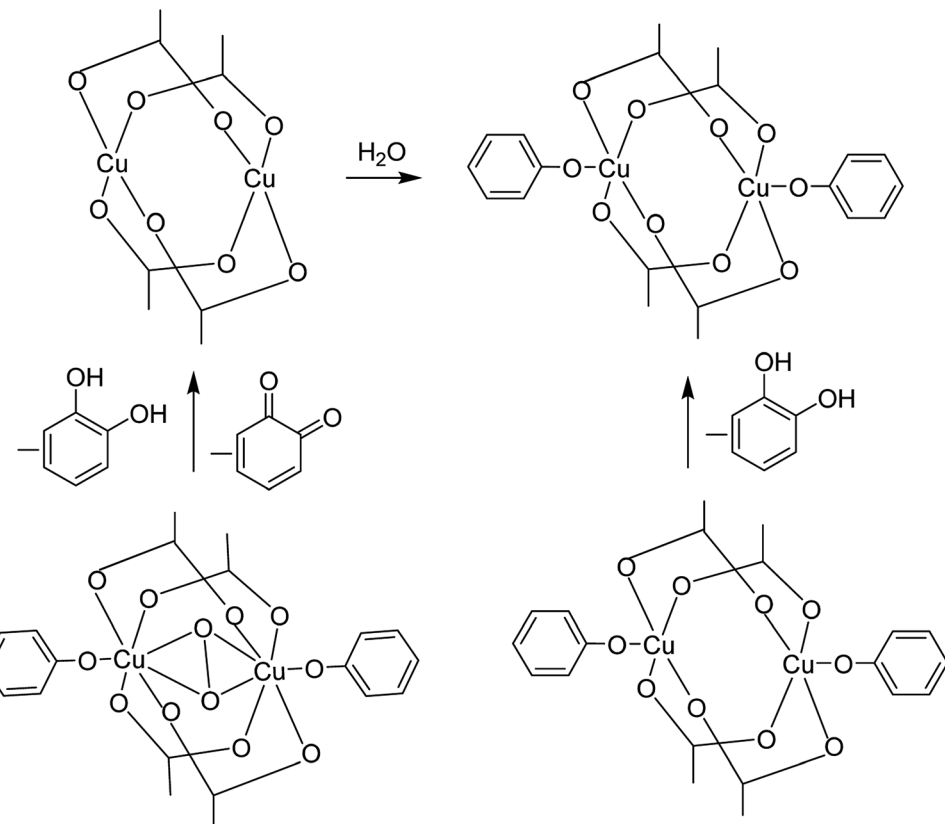
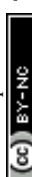
The copper(II) complex of 2,2-(((butane-1,4-diylbis(oxy)) bis(2,1-phenylene)bis(azanylylidene)) bis(methanylylidene) diphenol (H₂L) was encapsulated into the supercages of zeolite NaY (64) *via* the flexible ligand method (Fig. 6).¹⁰² The selective hydroxylation reaction of phenol was accomplished using the free and encapsulated complexes. The catalytic efficacy of Cu(II)-Y was lower in comparison with that of the encapsulated complex. The results showed that the catalytic activity and stability of the complex was increased *via* encapsulation.

To examine the influence of the solvent, various solvents such as CHCl₃, CH₂Cl₂, MeOH, and MeCN were applied. The results demonstrated that for the hydroxylation of phenol, the optimal solvent is MeCN because the great polarity of MeCN provided a completely homogeneous reaction medium.

On the other hand, the concentration of H₂O₂ may affect the conversion of phenol. For this purpose, the hydroxylation of phenol was investigated using various molar ratios of oxidant to phenol. It was found that a 1 : 1 molar ratio was optimal to provide the maximum phenol conversion.

Moreover, atomic absorption spectroscopy demonstrated that no leaching of the encapsulated complex was detected. Remarkably, this catalyst can be recovered and reused, while





Scheme 48 The suggested probable mechanism of oxidation that phenols exist in the phenolate form.

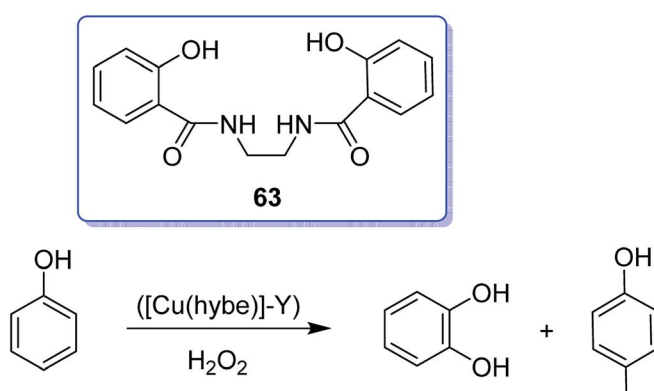
Scheme 49 Hydroxylation of phenol in the presence of $[\text{Cu}(\text{hybe})]\text{-Y}$ and hydrogen peroxide.

Table 23 Selectivity of catechol and hydroquinone formation, and percent conversion of phenol after 6 hours of reaction time

Catalyst	Conversion%	TOF h^{-1}	Selectivity%	
			Catechol	Hydroquinone
$[\text{Cu}(\text{hybe})]\text{-Y}$	40.14	201.5	90.9	9.1

the leaching of the Cu ions from $\text{Cu}(\text{II})\text{-Y}$ is constantly probable during the reaction.

Scheme 50 shows the suggested probable mechanism for the hydroxylation reaction of phenol. It was proposed that an electron transfer between Cu^{2+} and hydrogen peroxide gives M^{3+} and the hydroxyl radical. This high valence for the transition ions is definitely unusual. In addition, the cycle is closed when M^{3+} is reduced to M^{2+} , with the cyclohexadienyl radical obtained from phenol.¹⁰³

$\text{Cu}(\text{II})$ and $\text{Zn}(\text{II})$ complexes of 2-methylbenzimidazol (Mebzlh) were encapsulated into the supercages of zeolite-Y and ZSM-5 through the flexible ligand method.¹⁰⁴ The catalytic activity of the encapsulated complexes was examined for the decomposition of hydrogen peroxide and the hydroxylation of

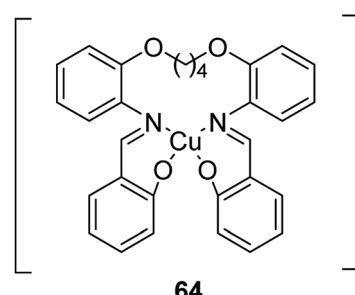
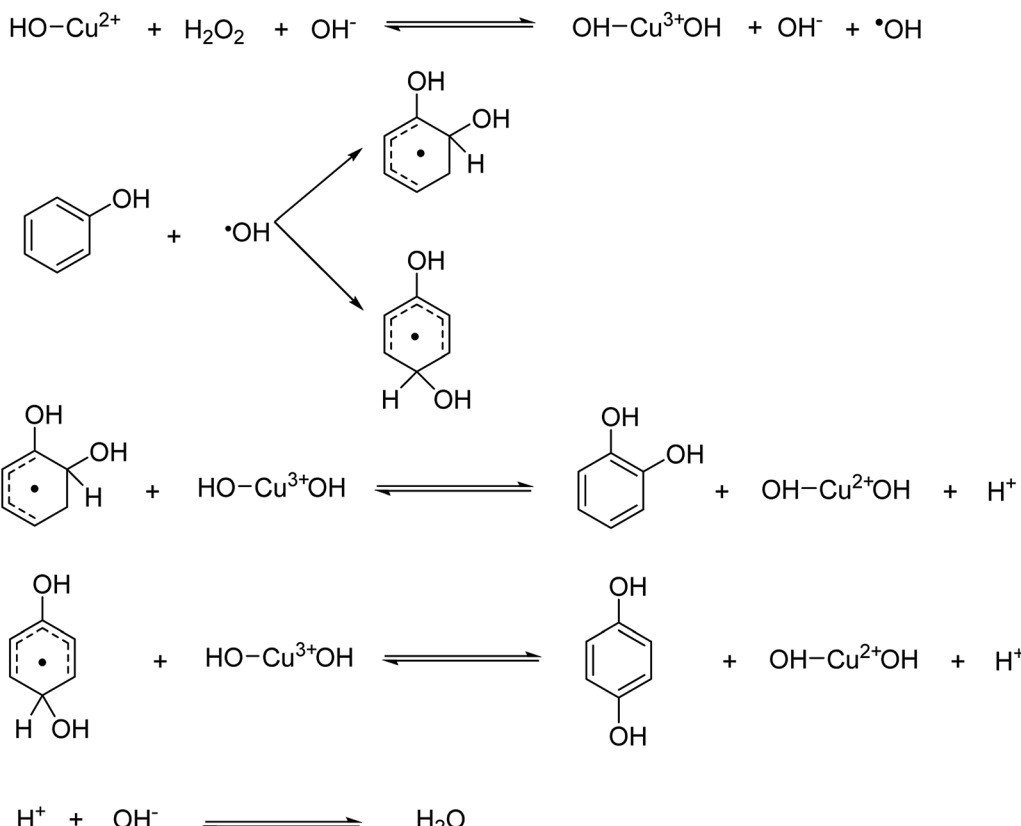
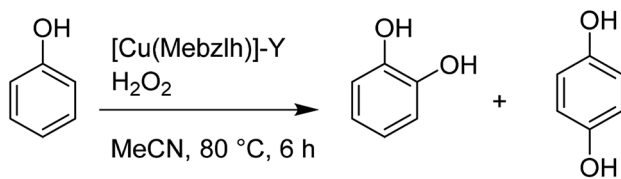


Fig. 6 Proposed structure for the free and encapsulated complexes.



Scheme 50 Suggested probable mechanism for the hydroxylation reaction of phenol.



Scheme 51 Hydroxylation reaction of phenol in the presence of [Cu(Mebzlh)]-Y.

phenol using hydrogen peroxide as an oxidant. Remarkably, the hydroxylation of phenol afforded hydroquinone and catechol as the major products (Scheme 51). A maximum conversion of about 52% was identified using the catalyst, [Cu(Mebzlh)]-Y.

The results demonstrated that the decomposition of hydrogen peroxide is slow at first. However, it increases with time (Table 24). This is because of the fact that this encapsulated complex needs a comparatively prolonged time to show

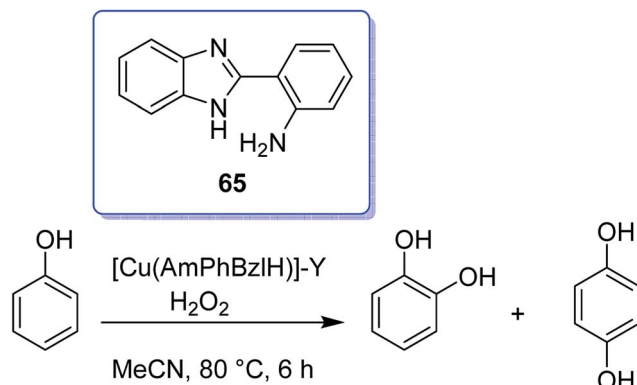
high catalytic activity as the number of metal centres is less than that of the neat complex.¹⁰⁵

Mahendra and co-workers in 2011 reported the encapsulation of the copper(II) complex of 2-(*o*-aminophenyl)benzimidazole (AmPhBzlH) (65) into the supercages of zeolite-Y and ZSM-5.¹⁰⁶ The catalytic activity of the encapsulated complexes was investigated for the hydroxylation of phenol using hydrogen peroxide as an oxidant. The hydroxylation of phenol gave hydroquinone and catechol as the main products. [Cu(AmPhBzlH)]-Y exhibited the maximum phenol conversion with 82% selectivity for the catechol construction. It should be mentioned that the percentage selectivity for the formation of catechol is greater for all types of catalysts provided in comparison with that for hydroquinone. The catalytic hydroxylation reaction of phenol in the presence of various encapsulated complexes was investigated as a function of time using the aqueous hydrogen peroxide solution as the oxidant and MeCN

Table 24 Turnover number for the decomposition of hydrogen peroxide

Catalyst	Percentage of H ₂ O ₂ reacted after 1 hour	TOF (h ⁻¹)	Percentage of H ₂ O ₂ reacted after 2 hours	TOF (h ⁻¹)
[Cu(Mebzlh)]-Y	0.673	159.42	1.360	159.42
[Cu(Mebzlh)]-ZSM-5	0.600	538.89	0.600	269.44





Scheme 52 Hydroxylation reaction of phenol in the presence of AmPhBzI H as the catalyst.

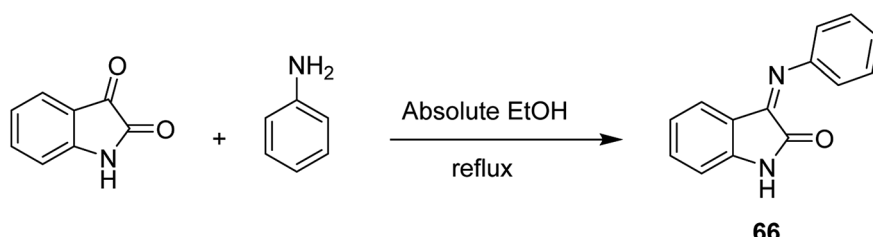
as the solvent. Catechol and hydroquinone were provided as the major products (Scheme 52).

CuBA was linked covalently with APTES, and provided a multifunctional compound that involved both silicon alkoxides and Cu ions. Mostly, the protonated amine substituents

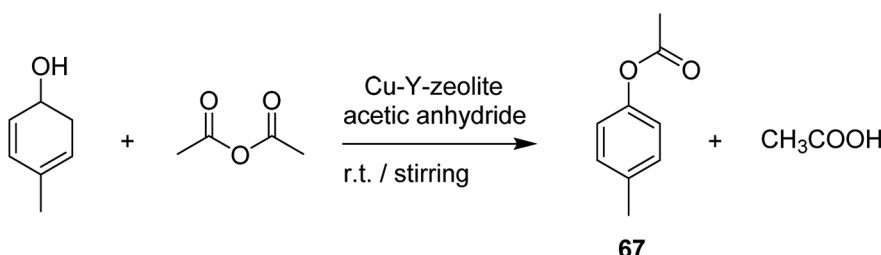
contained the ability to catalyze silica construction. Therefore, the construction of Si-O-Si networks can be induced *in situ* without any additional basic or acidic catalysts. This occurrence assists the protection of the pH-sensitive organic Cu(II) salt. Notably, CuBA was covalently connected to APTES *via* a nucleophilic substitution reaction. This significant chemical bond can guarantee the molecular-level dispersion of Cu ions, which is vital for the generation of ultrasmall sized CuO NPs with a more dispersed spatial distribution. Lastly, Cu ions were transformed into CuO NPs spontaneously under thermal treatment. The encapsulation of the copper(II) complex of 3-phenylimino-1,3-dihydro-indol-2-one **66** into the supercages of zeolite-Y (Cu-Y-zeolite) was accomplished *via* flexible ligand method (Scheme 53).¹⁰⁷

The acetylation reaction of *p*-cresol with several encapsulated complexes was investigated using Ac_2O as the acetylating agent. The *p*-cresyl acetate **67** was provided as the main corresponding products (Scheme 54).

The catalytic activity of the cationic exchanged zeolite, Cu(II) complex of ligand and complex encapsulated inside the zeolite was explored for the decomposition of hydrogen peroxide and for the acetylation of *p*-cresol. The maximum conversion of *p*-



Scheme 53 The formation of **66**.



Scheme 54 Acetylation of *p*-cresol.

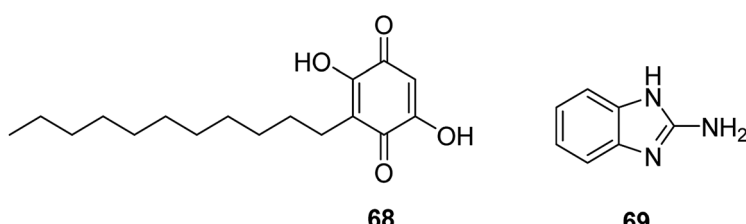
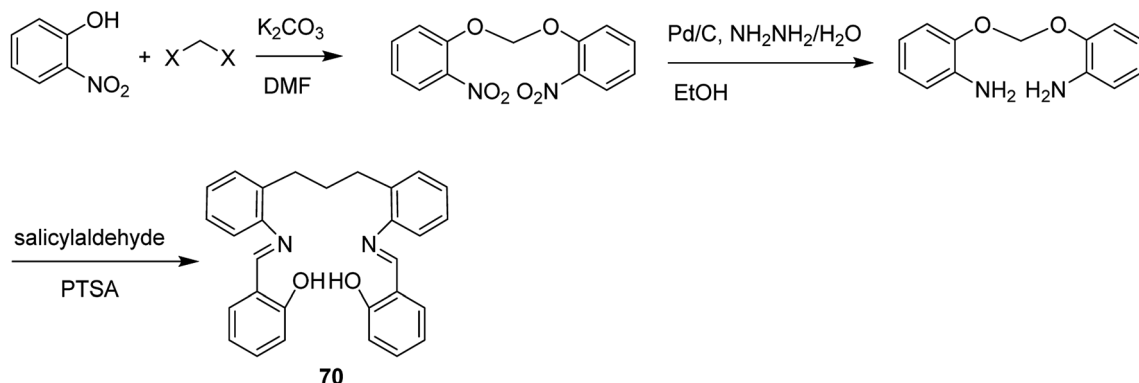
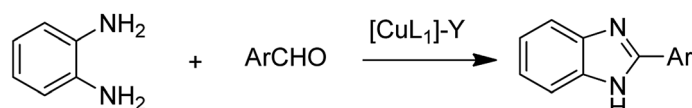


Fig. 7 Copper(II) complexes of two biologically significant ligands, namely embelin (2,5-dihydroxy-3-undecyl-2,5-cyclohexadien-1,4-dione) (**68**) and 2-aminobenzimidazole (**69**).

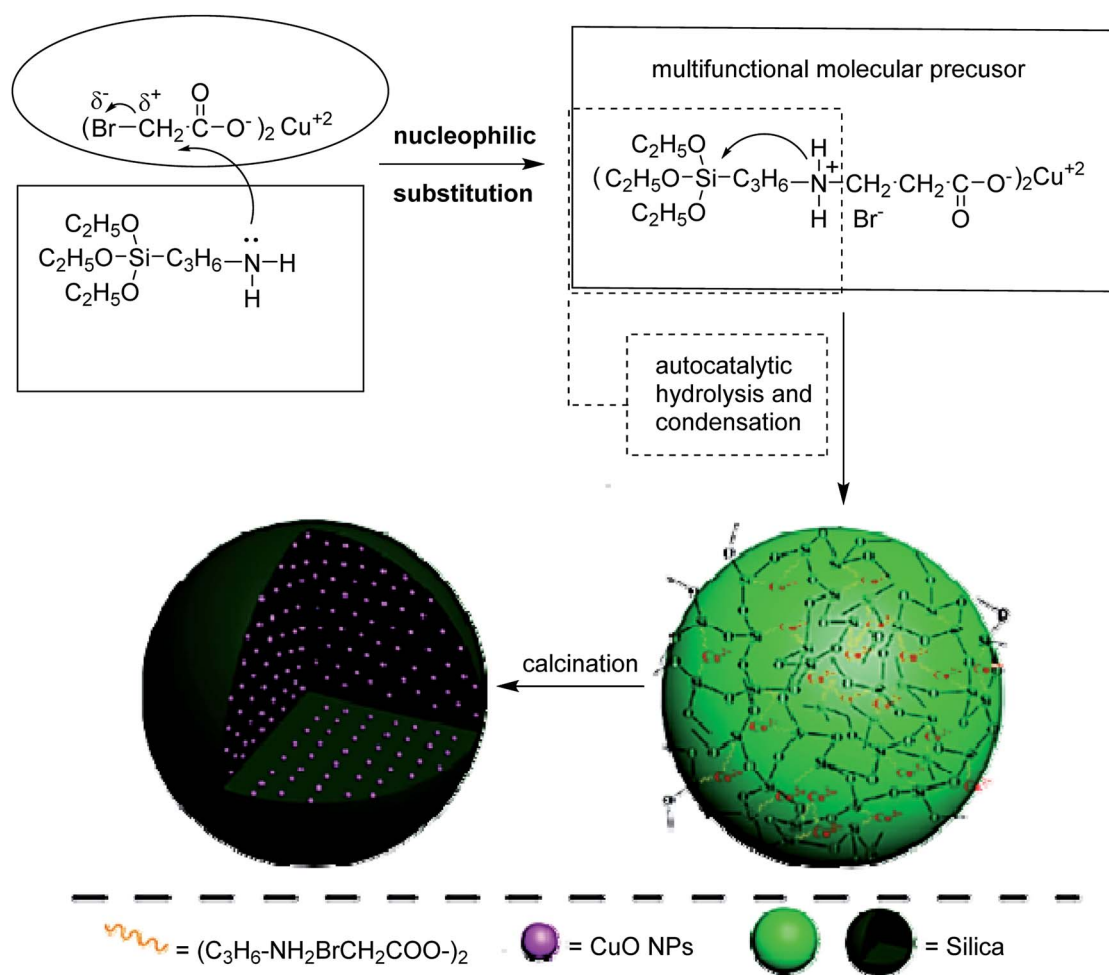




Scheme 55 Synthetic route for the construction of the Schiff base.

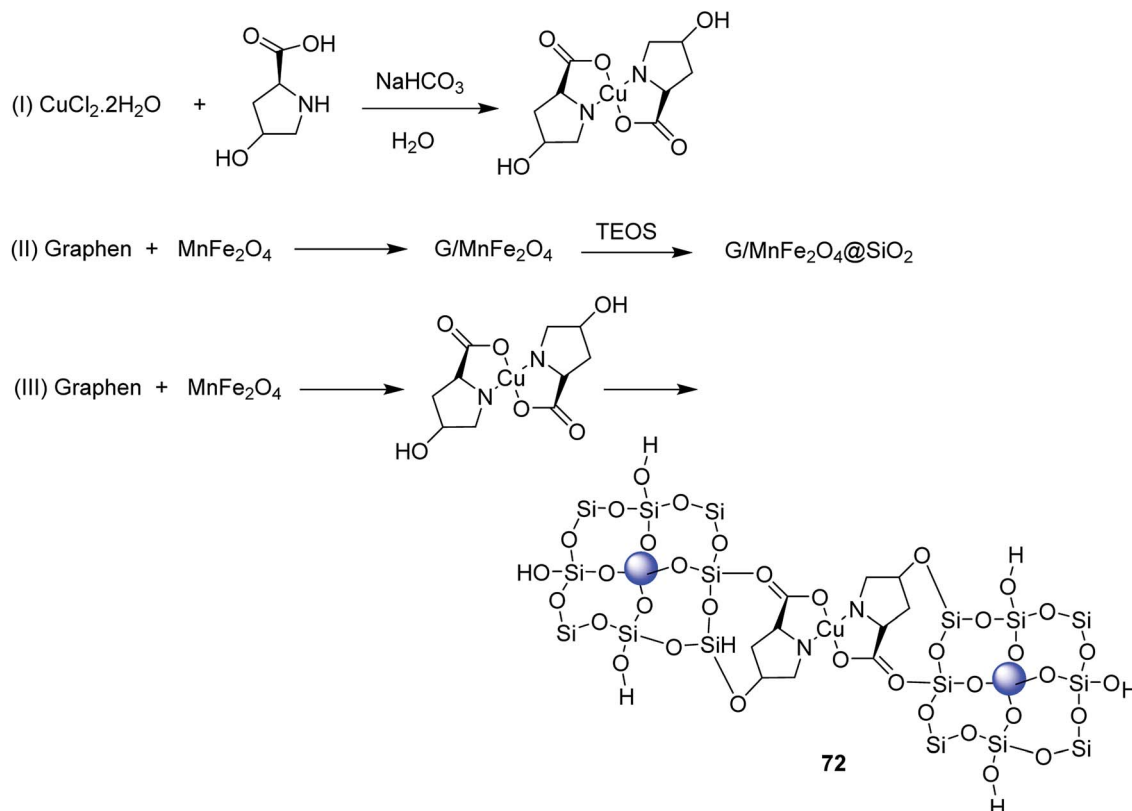


Scheme 56 Synthesis of benzimidazoles.



Scheme 57 The formation of catalyst 71. Reprinted from (ref. 111) with permission of the Royal Society of Chemistry.





Scheme 58 Stepwise construction of 72.

cresol was provided using the zeolite-encapsulated complex in a shorter reaction time in comparison with another catalyst. The order of the catalytic activity for the acetylation reaction of *p*-cresol was found to be as follows: heterogeneous catalyst (75%), $[\text{Cu-Y}]$ zeolite (55%), $[\text{Na-Y}]$ zeolite (50%), homogeneous catalyst (65%) and without catalyst (50%).

In this method, no leaching of metal ions was identified in the solution. The effect of various factors, including temperature, the quantity of catalyst and time, was investigated and these parameters exhibited various catalytic activities in the decomposition of hydrogen peroxide and the acetylation of *p*-cresol. This reaction was performed for all catalysts under the optimal reaction conditions (5 mmol *p*-cresol, acetic anhydride 7.5 mmol and 0.05 g catalyst at ambient temperature). Moreover, the influence of various catalysts on the percentage conversion of *p*-cresol was examined, and the results demonstrated the maximum *p*-cresol conversion using the heterogeneous catalyst.

2.1.3. Reduction. Copper(II) complexes of two biologically significant ligands, including embelin (2,5-dihydroxy-3-undecyl-2,5-cyclohexadien 1,4-dione) (68) and 2-amino-benzimidazole (69) were entrapped in the cages of zeolite Y *via* the flexible ligand method (Fig. 7).¹⁰⁸ These molecules were used as the catalyst in the reduction of oxygen (industrially recognized as deoxo reaction). The results exhibited an improvement in the catalytic activity in comparison with the facile copper ion exchanged zeolite. This is due to the ability of the ligands in increasing the oxygen binding ability of the metal ion. The

ability of the complexes to serve as catalysts for the reduction of oxygen was explored, and the results showed that the complexes are catalytically active. The mechanical and thermal stability increases because of encapsulation. In addition, the copper(II) complex of embelin, YCuEm is a superior catalyst due to its activity and stability. In turn, this shows that embelin is an appropriate ligand in changing the oxygen binding capability of the metal ion.

2.1.4. Carbon bond formation. The copper(II) complex of 2,2'-(methylenebis-(oxy))bis(2,1-phenylene)bis(azanyllylidene)-bis(methanyllylidene) diphenol (H_2L) (70) was encapsulated into the supercages of zeolite NaY *via* the flexible ligand method.¹⁰⁹ Based on this method, the Schiff base was constructed *via* a three-step method (Scheme 55). The resultant encapsulated complex and its relevant free complex were used as significant catalysts for the synthesis of benzimidazoles from the reaction of aldehydes and 1,2-phenylenediamine (Scheme 56). It is noteworthy that the catalytic activity and stability of the complex were both improved using encapsulation.¹¹⁰

In an investigation to increase the yields, various solvents such as EtOH, DMF, MeCN, and CHCl_3 were used for the reaction between benzaldehyde and *o*-phenylenediamine using $[\text{CuL}]$ -Y under reflux. Significantly, polar solvents like MeCN and DMF were appropriate for this reaction, with moderately high yields. However, EtOH demonstrated the lowest yield, maybe due to its coordination to the Lewis acid sites, leading to a decrease in the catalytic efficacy.



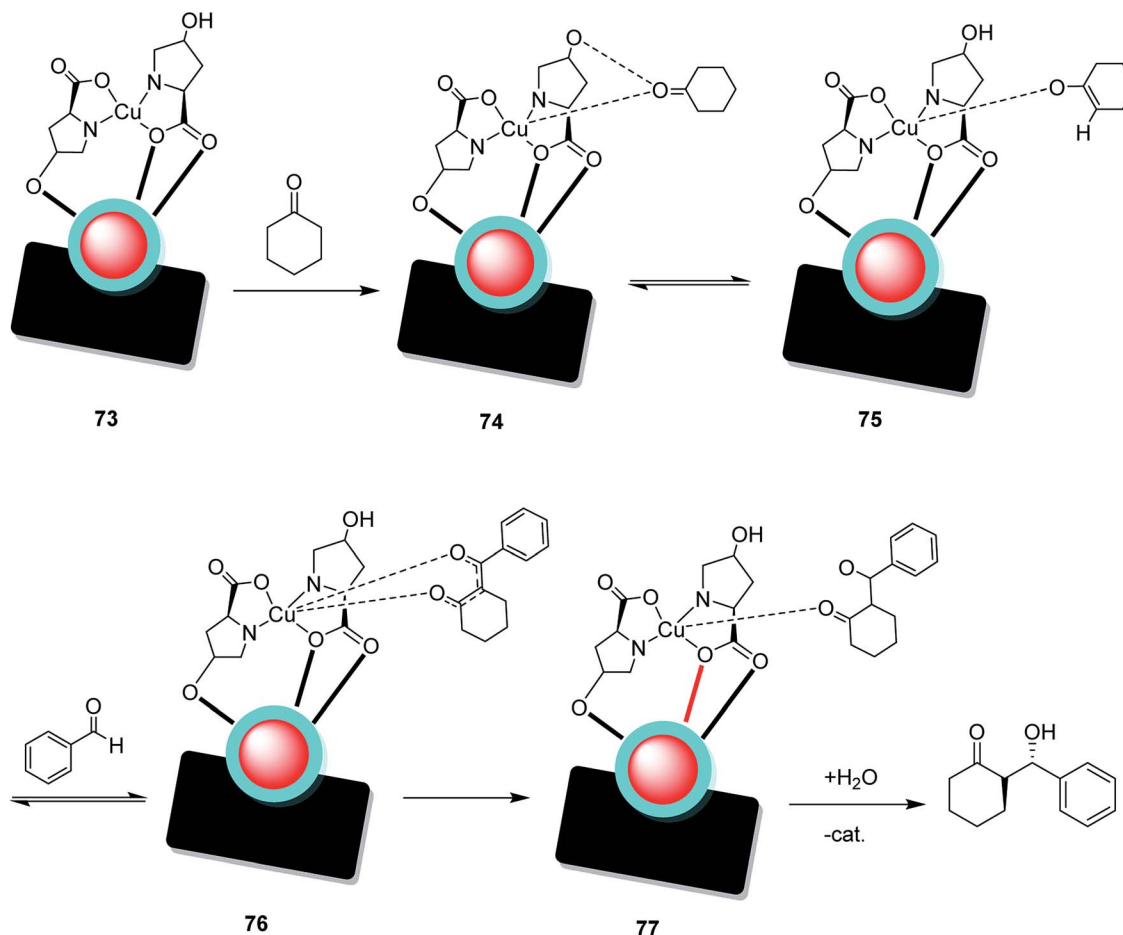
Table 25 Aldol reaction using 72 as a nanocatalyst under a solvent-free condition

Aldehyde	Ketone	Yield	ee% (anti/syn)
4-Nitrobenzaldehyde	Cyclohexanone propan-2-one acetophenone pentane-2,4-dione	30–98%	69/31–95/5
2-Hydroxybenzaldehyde			
Benzaldehyde			
Acetaldehyde			
Formaldehyde			
Cinnamaldehyde			
Hexanal			
Heptanal			
4-Methylbenzaldehyde			
3-Chlorobenzaldehyde			
3-Methoxybenzaldehyde			
2-Methoxybenzaldehyde			
3-Fluorobenzaldehyde			
4-(Dimethylamino)benzaldehyde			
2-Chlorobenzaldehyde			
2-Hydroxybenzaldehyde			

The atomic absorption spectroscopy demonstrated that no leaching was detected using the encapsulated complex as a catalyst, while the moderate leaching of Cu ions happened once the reaction was accomplished using Cu(II)/Y.

2.2. Silica-encapsulated Cu NPs

2.2.1. Carbon–carbon bond formations. Copper(II) oxide nanoparticles (CuO NPs) having an ultrasmall size (~3.6 nm) and a highly-dispersed pattern surrounded in a silica matrix were synthesized *in situ* via calcination of organic Cu salt.¹¹¹



Scheme 59 Suggested possible mechanism for the aldol reaction using 73. Reprinted from (ref. 112) with permission of the Royal Society of Chemistry.



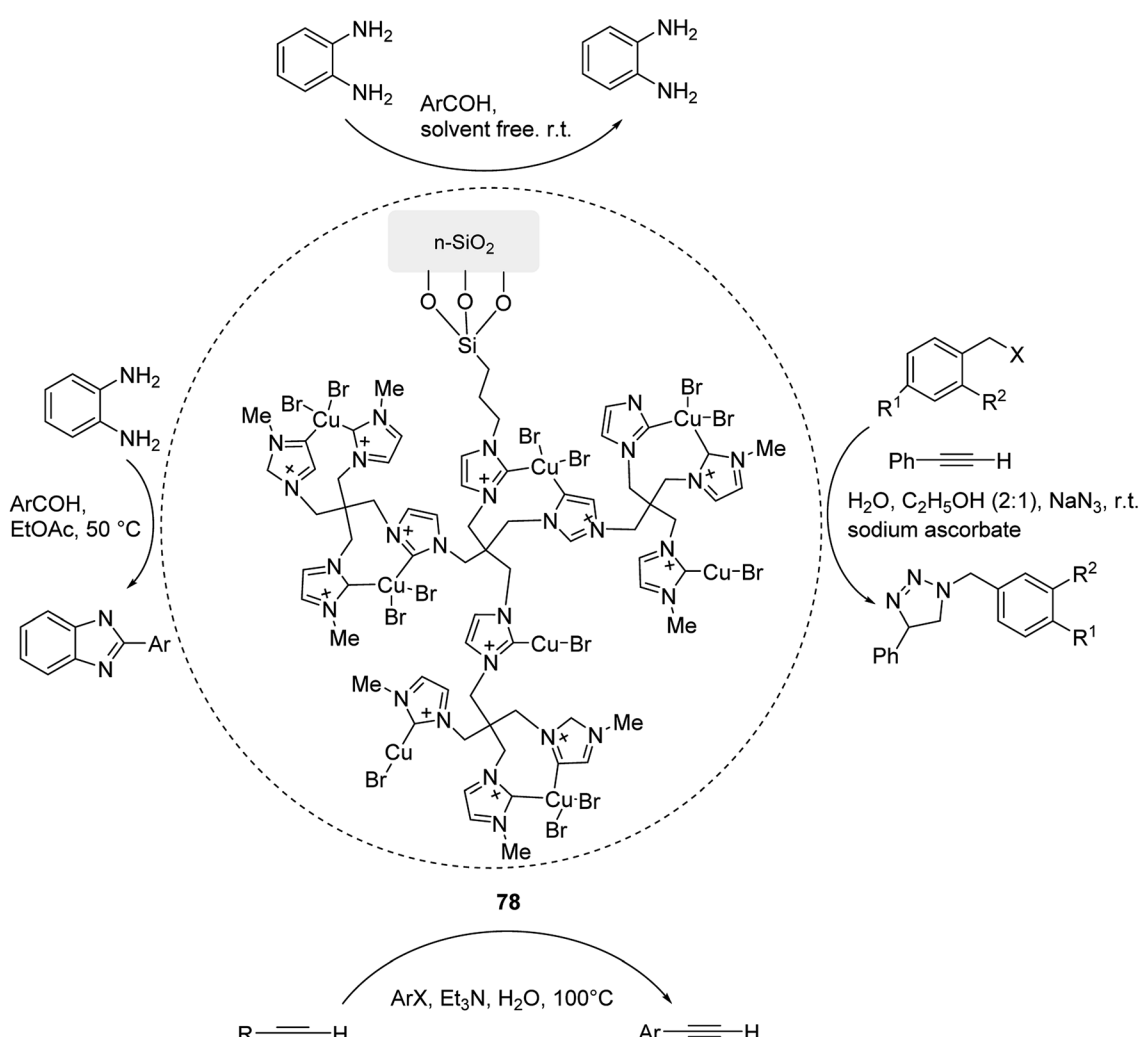
Using the rational selection of reactants, organic Cu salt was inserted into the Si–O–Si networks through the covalent bonding throughout the sol–gel method based on neutral conditions without any additional catalyst. The introduction of the organic Cu(II) salt through covalent bonding and the compact Si–O–Si networks permitted for the construction of highly dispersed and ultrasmall sized CuO NPs. CuO@SiO₂ nanocomposites **71** demonstrated satisfactory catalytic activity on the reduction of an organic dye using sodium borohydride as the reducing agent. An organic Cu salt was covalently introduced into the silica matrix and spontaneously transformed into CuO NPs. An autocatalytic pathway based on the protonated amine group as a catalytic site afforded all required conditions for confirming the complete and identical introduction of the organic Cu salt into the silica matrix. This was important in providing ultrasmall sized and well-dispersed CuO NPs. As a result, in comparison with the common approaches for providing silica-based metal nanocomposites, which need complex multi-stages and very specific pH conditions, this spontaneous construction pathway is simple and effective.

Scheme 57 exhibits the synthetic pathway for the construction of **71**. APTES was selected since it involves both a silanol group and an electron-rich amine group on its unhydrolyzed alkyl chain. On the copper(II) bromoacetate (CuBA) compound, there is an electron-deficient α -C because of the high electronegativity of the bromine group. Therefore, APTES and CuBA were mixed and a nucleophilic substitution reaction happened at room temperature.

Kooti and coworkers in 2019 examined the catalytic activity of the synthesized catalyst through immobilization of the Cu(proline)₂ complex onto the surface of magnetic graphene in the aldol reaction.¹¹²

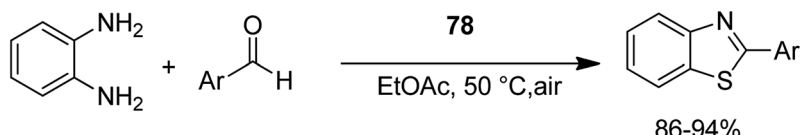
This group demonstrated the formation of a heterogeneous nanocatalyst bearing a Cu(proline)₂ complex immobilized on a silica-coated graphene/MnFe₂O₄ (G/MF) composite. The unique nanocomposite [G/MF@SiO₂@Cu(proline)₂] was used as a significant catalyst for the enantioselective aldol reaction under solvent-free conditions.

The resultant nanocomposite bearing copper(II) center as a Lewis acid was used as a significant catalyst in the



Scheme 60 The formation of 1,2,3-triazoles, benzimidazoles, benzothiazoles, and the Sonogashira–Hagihara cross-coupling reaction in the presence of **78** as an efficient catalyst.





Ar = 2-Me-C₆H₅, 3-Br-C₆H₅, 4-Me-C₆H₅, 4-Cl-C₆H₅
4-OMe-C₆H₅, 2-OMe-C₆H₅, 4-NO₂-C₆H₅, 2-NO₂-C₆H₅

Scheme 61 Synthesis of benzimidazoles in the presence of 78 as the catalyst.

enantioselective aldol reaction to afford the aldol products in excellent yield and high ees (>90%).

By the way, proline was immobilized on different supports, involving metals, mesoporous materials, and layered compounds, to increase its activity for catalyzing asymmetric aldolization.¹¹³ Consequently, this group reported an eco-friendly approach for the one-pot aldol reaction of different aldehydes and ketones using G/MF@SiO₂@Cu(proline)₂ 72 as an efficient catalyst (Scheme 58 and Table 25).

As aforementioned, proline and its derivatives can significantly catalyze asymmetric aldol reactions. The stepwise construction of catalyst 72 is depicted in Scheme 58. This catalyst exhibited high activity in the direct asymmetric aldol reaction. The enantioselectivity values of the anti-isomer, as the major enantiomer, for the reaction of cyclohexanone and aromatic aldehydes under a solvent-free condition in 5 hours were over 90%.

A suggested possible mechanism for the aldol reaction is shown in Scheme 59. At first, the carbonyl group of cyclohexanone is activated with the metal center of the Cu complex in the nanocatalyst. Hence, this interaction gives the α -hydrogen of the ketone more acidity that results in the construction of the metal-enolate complex 75. Then, a nucleophilic attack of the C-C double bond of the enolate scaffold on the carbonyl substituent of benzaldehyde will successively occur to provide intermediate 76. Using the reorganization of bonding pairs,

intermediate 77 is provided, and the protonation of that compound affords the aldol product.

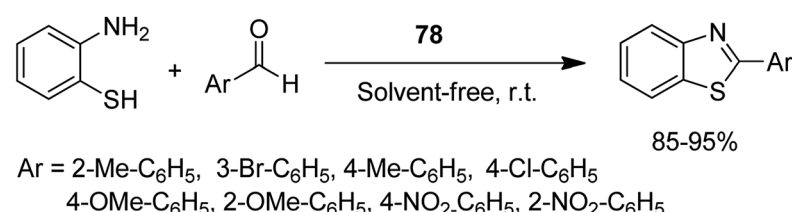
Moghadam and coworkers in 2018 demonstrated the formation of poly (N-heterocyclic carbene copper(II) complex) immobilized on nano-silica, (Cu(II)-NHCs) n@SiO₂ (78). The catalytic activity of 78 was examined for the synthesis of 1,2,3-triazoles, benzimidazoles, benzothiazoles, and the Sonogashira-Hagihara cross-coupling reaction. The suggested probable mechanisms for these reactions is shown in Scheme 60.¹¹⁴

To examine the catalytic activity of 78 in the formation of benzimidazoles, the reactions of the substituted benzaldehydes and 1,2-diaminopropane were examined (Scheme 61). Remarkably, the catalyst showed excellent activity in this reaction and the relevant yields were 86–94%.

To examine the generality of this catalyst, various substituted benzaldehydes were reacted with 2-aminothiophenol to afford the desired 2-substituted benzothiazoles in high to excellent yields (85–95% yield) (Scheme 62).

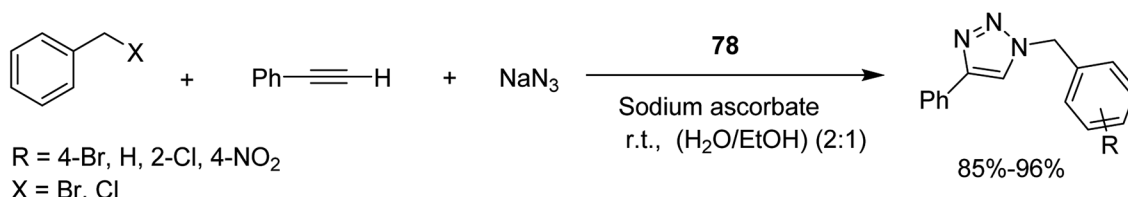
1,2,3-Triazoles were synthesized in the presence of 78 as the catalyst (Scheme 63).

Next, the activity of catalyst 78 was examined in the Sonogashira-Hagihara cross-coupling reaction. Different aryl halides were treated with phenyl acetylene to afford the relevant diphenyl acetylenes in moderate to high yields (85–94%) (Scheme 64). Notably, aryl iodide is more active than aryl chlorides and bromides.



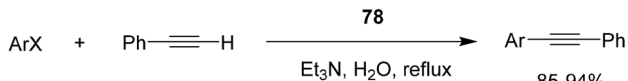
Ar = 2-Me-C₆H₅, 3-Br-C₆H₅, 4-Me-C₆H₅, 4-Cl-C₆H₅
4-OMe-C₆H₅, 2-OMe-C₆H₅, 4-NO₂-C₆H₅, 2-NO₂-C₆H₅

Scheme 62 The formation of benzothiazole derivatives in the presence of 78 as an efficient catalyst.



Scheme 63 Synthesis of 1,2,3-triazoles in the presence of 78 as the catalyst.





ArX = C₆H₅-I, C₆H₅-Cl, C₆H₅-Br, 4Me-C₆H₄I, 4-OMe-C₆H₄I, 4-Cl-C₆H₄Cl, 4-NO₂-C₆H₄Cl, 3-NO₂-C₆H₄Cl

Scheme 64 Sonogashira–Hagihara cross-coupling reaction of aryl halides and phenylacetylene in the presence of **78** as the catalyst.

3. Conclusion

In summary, confinement of zeolite, silica and miscellaneous NPs within the cage of a nanoreactor not only disallowed the NPs from agglomeration, but also increased their consistency. It also facilitated the catalytic accomplishment of the Cu-encapsulated catalyst in terms of its selectivity, reactivity, and leaching of the metal oxide. As a result, this encapsulation significantly improved the catalyst dependability and controlled the Cu species leaching, maintaining its high catalytic originality and selectivity for the oxidation reaction. Different organic, inorganic and hybrid systems can be employed for the encapsulation of zeolites, silica and miscellaneous NPs. Frequently, mesoporous silica, zeolites, MOFs, dendrimers, and carbon materials are used for this purpose. We hope this review describes the merits of encapsulated zeolite, silica and miscellaneous NPs over their bare counterparts in terms of catalyzing different organic transformations.¹¹⁵

Conflicts of interest

There are no conflicts to declare.

Acknowledgements

Financial support of this research from Alzahra University, Iran is gratefully acknowledged. M. M. H. is also thankful for the granted individual research chair given by the Iran National Science Foundation (INSF).

References

- (a) L. R. Cox, *Appl. Organomet. Chem.*, 2003, **17**, 79; (b) X. Lu and S. Ma, *Transition Metal Catalyzed Reactions*, Blackwell Science, Oxford, UK, 1999.
- (a) I. Ojima, M. Tzamarioudaki, Z. Li and R. J. Donovan, *Chem. Rev.*, 1996, **96**, 635–662; (b) M. L. Crawley and B. M. Trost, *Applications of transition metal catalysis in drug discovery and development: an industrial perspective*, John Wiley & Sons, 2012.
- C. Copéret, M. Chabanas, R. Petroff Saint-Arroman and J. M. Basset, *Angew. Chem., Int. Ed.*, 2003, **42**, 156–181.
- (a) W. R. Moser and D. W. Slocum, *Homogeneous Transition Metal Catalyzed Reactions*, American Chemical Society, Washington, DC, United States, 1992; (b) Y. G. Shelke, A. Yashmeen, A. V. Gholap, S. J. Gharpure and A. R. Kapdi, *Asian J. Chem.*, 2018, **13**, 2991–3013; (c) B. Cornils and W. A. Herrmann, *J. Catal.*, 2003, **216**, 23–31; (d) S. Bhaduri and D. Mukesh, *Homogeneous catalysis: mechanisms and industrial applications*, John Wiley & Sons, 2014.
- G. Parshall, *J. Mol. Catal.*, 1978, **4**, 243–270.
- (a) D. T. Genna, A. G. Wong-Foy, A. J. Matzger and M. S. Sanford, *J. Am. Chem. Soc.*, 2013, **135**, 10586–10589; (b) C. Copéret and J. M. Basset, *Adv. Synth. Catal.*, 2007, **349**, 78–92; (c) M. G. Petracci and A. K. Kakkar, *Adv. Mater.*, 1996, **8**, 251–253.
- A. Behr, A. J. Vorholt and T. Seidensticker, *ChemBioEng Rev.*, 2015, **2**, 6–21.
- (a) A. Corma, H. García and F. Llabrés i Xamena, *Chem. Rev.*, 2010, **110**, 4606–4655; (b) C. Baleizao and H. García, *Chem. Rev.*, 2006, **106**, 3987–4043; (c) D. E. De Vos, M. Dams, B. F. Sels and P. A. Jacobs, *Chem. Rev.*, 2002, **102**, 3615–3640.
- C. R. Jacob, S. P. Varkey and P. Ratnasamy, *Microporous Mesoporous Mater.*, 1998, **22**, 465–474.
- R. Raja and P. Ratnasamy, *Stud. Surf. Sci. Catal.*, Elsevier, 1997, vol. 105, pp. 1037–1044.
- K. D. Karlin and Y. Gultneh, *Prog. Inorg. Chem.*, 1987, 219–327.
- Y. Ukiu, A. Kazusaka and M. Nomura, *J. Mol. Catal. B: Enzym.*, 1991, **70**, 165–174.
- A. Hay, H. Blanchard, G. Endres and J. Eustance, *J. Am. Chem. Soc.*, 1959, **81**, 6335–6336.
- K. Kinoshita, *Bull. Chem. Soc. Jpn.*, 1959, **32**, 777–780.
- (a) J. Pritchard, G. A. Filonenko, R. van Putten, E. J. Hensen and E. A. Pidko, *Chem. Soc. Rev.*, 2015, **44**, 3808–3833; (b) A. Sivaramakrishna, P. Suman, E. Veerashekhar Goud, S. Janardan, C. Sravani, T. Sandeep, K. Vijayakrishna and H. S. Clayton, *J. Coord. Chem.*, 2013, **66**, 2091–2109.
- S. Dang, H. Yang, P. Gao, H. Wang, X. Li, W. Wei and Y. Sun, *Catal. Today*, 2019, **330**, 61–75.
- (a) X. Zhao, X. Y. Bao, W. Guo and F. Y. Lee, *Mater. Today*, 2006, **9**, 32–39; (b) P. Barbaro and F. Liguori, *Heterogenized Homogeneous Catalysts for Fine Chemicals Production*, SSBM, 2010, vol. 33.
- L. Cao and R. Schmid, *Application and Design*, Wiley-VCH Verlag GmbH & Co. KGaA, Weinheim, 2006, vol. 10.
- S. Bhattacharyya and B. Basu, *Green Techniques for Organic Synthesis and Medicinal Chemistry* 2018, pp. 269–289.
- M. Meldal, in *Methods in enzymology*, Elsevier, 1997, vol. 289, pp. 83–104.
- J. M. Palomo, *RSC Adv.*, 2014, **4**, 32658–32672.
- Z. Xie, Z. Liu, Y. Wang, Q. Yang, L. Xu and W. Ding, *Int. J. Mol. Sci.*, 2010, **11**, 2152–2187.
- J. A. Cecilia, R. Moreno Tost and M. Retuerto Millán, *Mesoporous Materials: From Synthesis to Applications*, Multidisciplinary Digital Publishing Institute, 2019.
- Z. Wu and D. Zhao, *Chem. Commun.*, 2011, **47**, 3332–3338.
- C. Perego and R. Millini, *Chem. Soc. Rev.*, 2013, **42**, 3956–3976.
- M. Sohmiya, K. Saito and M. Ogawa, *Sci. Technol. Adv. Mater.*, 2015, **16**, 054201.
- O. Pagar, H. Nagare, Y. Chine, R. Autade, P. Narode and V. Sanklecha, *Sci. Technol. Adv. Mater.*, 2018, **6**, 1–12.



28 (a) B. M. Weckhuysen and J. Yu, *Chem. Soc. Rev.*, 2015, **44**, 7022–7024; (b) M. Mishra and S. K. Jain, *Proc. Natl. Acad. Sci., India, Sect. B*, 2011, **81**, 250–259.

29 F. Fajula and D. Brunel, *Microporous Mesoporous Mater.*, 2001, **48**, 119–125.

30 C. Colella and A. F. Gualtieri, *Microporous Mesoporous Mater.*, 2007, **105**, 213–221.

31 S. Bhatia, *Zeolite catalysts: principles and applications*, CRC Press, 1989.

32 Z. Le Hua, J. Zhou and J. L. Shi, *Chem. Commun.*, 2011, **47**, 10536–10547.

33 R. Mirsafaei, M. M. Heravi, T. Hosseinnejad and S. Ahmadi, *Appl. Organomet. Chem.*, 2016, **30**, 823–830.

34 F. Ebrahimpour-Malamir, T. Hosseinnejad, R. Mirsafaei and M. M. Heravi, *Organomet. Chem.*, 2018, **32**, e3913.

35 A. M. Elias and M. Saravanakumar, *IOP Conf. Ser.: Mater. Sci. Eng.*, 2017, **263**, 032019.

36 Y. Suchorski and G. Rupprechter, *Catal. Lett.*, 2018, **148**, 2947–2956.

37 Y. Ukius and A. Kazusaka, *J. Mol. Catal.*, 1987, **43**, 31–33.

38 L. D. Fernández, E. Lara and E. A. Mitchell, *Eur. J. Protistol.*, 2015, **51**, 409–424.

39 (a) L. Guo, X. Zhao, R. Zhang, C. Chen, J. Chen, A. Chen, X. Liu and Z. Hou, *J. Supercrit. Fluids*, 2016, **107**, 715–722; (b) C. Sener, T. Dogu and G. Dogu, *Microporous Mesoporous Mater.*, 2006, **94**, 89–98; (c) Y. Hou, X. Ji, G. Liu, J. Tang, J. Zheng, Y. Liu, W. Zhang and M. Jia, *Catal. Commun.*, 2009, **10**, 1459–1462; (d) V. S. García-Cuello, L. Giraldo and J. C. Moreno-Piraján, *Catal. Lett.*, 2011, **141**, 1659.

40 (a) J. Garcia-Martinez, N. Linares, S. Sinibaldi, E. Coronado and A. Ribera, *Microporous Mesoporous Mater.*, 2009, **117**, 170–177; (b) P. Wang, Z. Wang, J. Li and Y. Bai, *Microporous Mesoporous Mater.*, 2008, **116**, 400–405; (c) Á. Mastalir, B. Rác, Z. Király and Á. Molnár, *J. Mol. Catal. A: Chem.*, 2007, **264**, 170–178; (d) S. Ghosh, R. Dey, S. Ahammed and B. C. Ranu, *Clean Technol. Environ. Policy*, 2014, **16**, 1767–1771; (e) J. N. Park, A. J. Forman, W. Tang, J. Cheng, Y. S. Hu, H. Lin and E. W. McFarland, *Small*, 2008, **4**, 1694–1697; (f) G. Budroni, A. Corma, H. García and A. Primo, *J. Catal.*, 2007, **251**, 345–353; (g) Y. Wan, H. Wang, Q. Zhao, M. Klingstedt, O. Terasaki and D. Zhao, *J. Am. Chem. Soc.*, 2009, **131**, 4541–4550; (h) K. Bendahou, L. Cherif, S. Siffert, H. Tidahy, H. Benaissa and A. Aboukais, *Appl. Catal., A*, 2008, **351**, 82–87; (i) S. Banerjee, V. Balasanthiran, R. T. Koodali and G. A. Sereda, *Org. Biomol. Chem.*, 2010, **8**, 4316–4321.

41 (a) E. Hashemi, Y. S. Beheshtiha, S. Ahmadi and M. M. Heravi, *Transition Met. Chem.*, 2014, **39**, 593–601; (b) M. M. Heravi, S. Sadjadi, H. A. Oskooie, R. H. Shoar and F. F. Bamoharram, *Catal. Commun.*, 2008, **9**, 504–507.

42 S. Sadjadi and M. Heravi, *RSC Adv.*, 2016, **6**, 88588–88624.

43 (a) S. Sabaqian, F. Nemat, M. M. Heravi and H. T. Nahzomi, *Appl. Organomet. Chem.*, 2017, **31**, e3660; (b) T. Baie Lashaki, H. A. Oskooie, T. Hosseinnejad and M. M. Heravi, *J. Coord. Chem.*, 2017, **70**, 1815–1834; (c) M. M. Heravi, H. Hamidi and V. Zadsirjan, *Curr. Org. Synth.*, 2014, **11**, 647–675.

44 K. J. Balkus and A. G. Gabrielov, in *Inclusion chemistry with zeolites: nanoscale materials by design*, Springer, 1995, pp. 159–184.

45 R. Raja and P. Ratnasamy, *J. Catal.*, 1997, **170**, 244–253.

46 A. Corma, *Zeolite microporous solids: synthesis, structure and reactivity*, ed. E. Derouane, F. Lemos, C. Naccache and F. Ribeiro, Kluwer, 1992, vol. 352, p. 373.

47 C. R. Jacob, S. P. Varkey and P. Ratnasamy, *Appl. Catal., A*, 1998, **168**, 353–364.

48 M. R. Maurya, A. K. Chandrakar and S. Chand, *J. Mol. Catal. A: Chem.*, 2007, **270**, 225–235.

49 M. R. Maurya, A. K. Chandrakar and S. Chand, *J. Mol. Catal. A: Chem.*, 2007, **278**, 12–21.

50 Z. Li, S. Wu, Y. Ma, H. Liu, J. Hu, L. Liu, Q. Huo, J. Guan and Q. Kan, *Transition Met. Chem.*, 2013, **38**, 243–251.

51 Y. Yang, H. Ding, S. Hao, Y. Zhang and Q. Kan, *Appl. Organomet. Chem.*, 2011, **25**, 262–269.

52 Y. Yang, Y. Zhang, S. Hao, J. Guan, H. Ding, F. Shang, P. Qiu and Q. Kan, *Appl. Catal., A*, 2010, **381**, 274–281.

53 I. Kuźniarska-Biernacka, M. Carvalho, I. C. Neves, A. M. Fonseca, A. Lisińska-Czekaj and D. Czekaj, *Arch. Metall. Mater.*, 2013, **58**, 1291–1294.

54 M. R. Maurya, A. K. Chandrakar and S. Chand, *J. Mol. Catal. A: Chem.*, 2007, **263**, 227–237.

55 M. R. Maurya, A. K. Chandrakar and S. Chand, *J. Mol. Catal. A: Chem.*, 2007, **274**, 192–201.

56 E. Shilpa and V. Gayathri, *J. Environ. Chem. Eng.*, 2016, **4**, 4194–4206.

57 M. R. Maurya, S. J. Titinchi and S. Chand, *J. Mol. Catal. A: Chem.*, 2003, **201**, 119–130.

58 M. Maurya, S. Titinchi and S. Chand, *Appl. Catal., A*, 2002, **228**, 177–187.

59 I. Kuźniarska-Biernacka, M. M. M. Raposo, R. Batista, P. Parpot, K. Biernacki, A. L. Magalhães, A. M. Fonseca and I. C. Neves, *Microporous Mesoporous Mater.*, 2016, **227**, 272–280.

60 B. K. Kundu, V. Chhabra, N. Malviya, R. Ganguly, G. S. Mishra and S. Mukhopadhyay, *Microporous Mesoporous Mater.*, 2018, **271**, 100–117.

61 B. Xiao, H. Hou and Y. Fan, *J. Organomet. Chem.*, 2007, **692**, 2014–2020.

62 A. Mobinikhaledi, M. Zendehdel and P. Safari, *Transition Met. Chem.*, 2014, **39**, 431–442.

63 R. Raja and P. Ratnasamy, *Stud. Surf. Sci. Catal.*, Elsevier, 1996, Vol. 101, pp. 181–190.

64 G. Endres, A. Hay and J. Eustance, *J. Org. Chem.*, 1963, **28**, 1300–1305.

65 N. Oyama, T. Ohsaka, Y. Ohnuki and T. Suzuki, *J. Electrochem. Soc.*, 1987, **134**, 3068–3073.

66 W. Waters, *J. Am. Oil Chem. Soc.*, 1971, **48**, 427–433.

67 M. Salavati-Niasari, *J. Mol. Catal. A: Chem.*, 2008, **283**, 120–128.

68 B. Fan, H. Li, W. Fan, C. Jin and R. Li, *Appl. Catal., A*, 2008, **340**, 67–75.

69 M. Salavati-Niasari and M. Shaterian, *J. Porous Mater.*, 2008, **15**, 581–588.



70 M. Salavati-Niasari, M. Shakouri-Arani and F. Davar, *Microporous Mesoporous Mater.*, 2008, **116**, 77–85.

71 M. Salavati-Niasari, Z. Salimi, M. Bazarganipour and F. Davar, *Inorg. Chim. Acta*, 2009, **362**, 3715–3724.

72 I. Kužniarska-Biernacka, K. Biernacki, A. Magalhães, A. Fonseca and I. Neves, *J. Catal.*, 2011, **278**, 102–110.

73 H. Figueiredo, B. Silva, C. Quintelas, M. M. M. Raposo, P. Parpot, A. Fonseca, A. Lewandowska, M. Bañares, I. C. Neves and T. Tavares, *Appl. Catal., B*, 2010, **94**, 1–7.

74 M. R. Maurya, C. Haldar, S. Behl, N. Kamatham and F. Avecilla, *J. Coord. Chem.*, 2011, **64**, 2995–3011.

75 M. Lashanizadegan, S. Rayati and Z. Dejparvar Derakhshan, *Chin. J. Chem.*, 2011, **29**, 2439–2444.

76 M. R. Maurya, P. Saini, C. Haldar, A. K. Chandrakar and S. Chand, *J. Coord. Chem.*, 2012, **65**, 2903–2918.

77 M. Lashanizadegan and E. Parvizi, *Synth. React. Inorg., Met.-Org., Nano-Met. Chem.*, 2015, **45**, 1154–1158.

78 A. Banaei and B. Rezazadeh, *J. Coord. Chem.*, 2013, **66**, 2129–2140.

79 A. R. Silva, H. Albuquerque, A. Fontes, S. Borges, Â. Martins, A. P. Carvalho and J. Pires, *Ind. Eng. Chem. Res.*, 2011, **50**, 11495–11501.

80 K. Xavier, J. Chacko and K. M. Yusuff, *Appl. Catal., A*, 2004, **258**, 251–259.

81 K. N. Bhagya and V. Gayathri, *J. Porous Mater.*, 2013, **20**, 257–266.

82 A. Mobinikhaledi, M. Zendehdel and P. Safari, *J. Porous Mater.*, 2014, **21**, 565–577.

83 F. Li, D. Hu, Y. Yuan, B. Luo, Y. Song, S. Xiao, G. Chen, Y. Fang and F. Lu, *Mol. Catal.*, 2018, **452**, 75–82.

84 M. Salavati-Niasari, *J. Mol. Catal. A: Chem.*, 2008, **284**, 97–107.

85 M. Salavati-Niasari and S. Abdolmohammadi, *J. Porous Mater.*, 2009, **16**, 19–26.

86 S. Yamaguchi, A. Suzuki, M. Togawa, M. Nishibori and H. Yahiro, *ACS Catal.*, 2018, **8**, 2645–2650.

87 K. Ebitani, K. Nagashima, T. Mizugaki and K. Kaneda, *Chem. Commun.*, 2000, 869–870.

88 K. Kaneda, T. Itoh, N. Kii, K. Jitsukawa and S. Teranishi, *J. Mol. Catal.*, 1982, **15**, 349–365.

89 M. Salavati-Niasari, *J. Mol. Catal. A: Chem.*, 2004, **217**, 87–92.

90 G. R. Reddy, S. Balasubramanian and K. Chennakesavulu, *J. Mater. Chem. A*, 2014, **2**, 19102.

91 S. Rayati, E. Khodaei and M. Jafarian, *J. Coord. Chem.*, 2017, **70**, 2736–2750.

92 A. Okemoto, K. Ueyama, K. Taniya, Y. Ichihashi and S. Nishiyama, *Catal. Commun.*, 2017, **100**, 29–32.

93 S. L. Hailu, B. U. Nair, M. Redi-Abshiro, I. Diaz, R. Aravindhan and M. Tessema, *Chin. J. Catal.*, 2016, **37**, 135–145.

94 C. Galindo, P. Jacques and A. Kalt, *Chemosphere*, 2001, **45**, 997–1005.

95 J. Prousek, *Chem. Listy*, 1996, **90**, 229–237.

96 (a) H. C. Sutton and C. C. Winterbourn, *Free Radical Biol. Med.*, 1989, **6**, 53–60; (b) M. H. Robbins and R. S. Drago, *J. Catal.*, 1997, **170**, 295–303; (c) A. H. Gemeay, I. A. Mansour, R. G. El-Sharkawy and A. B. Zaki, *J. Mol. Catal. A: Chem.*, 2003, **193**, 109–120.

97 M. Neamtu, C. Zaharia, C. Catrinescu, A. Yediler, M. Macoveanu and A. Kettrup, *Appl. Catal., B*, 2004, **48**, 287–294.

98 O. Legrini, E. Oliveros and A. Braun, *Chem. Rev.*, 1993, **93**, 671–698.

99 S. Chavan, D. Srinivas and P. Ratnasamy, *J. Catal.*, 2000, **192**, 286–295.

100 J. M. Thomas, *Nature*, 1994, **368**, 289.

101 M. R. Maurya, S. J. Titinchi and S. Chand, *Catal. Lett.*, 2003, **89**, 219–227.

102 S. M. B. Hosseini-Ghazvini, P. Safari, A. Mobinikhaledi and M. Zendehdel, *React. Kinet., Mech. Catal.*, 2015, **115**, 703–718.

103 M. Zendehdel, H. Khanmohamadi and M. Mokhtari, *J. Chin. Chem. Soc.*, 2010, **57**, 205–212.

104 B. P. Nethravathi and K. N. Mahendra, *J. Porous Mater.*, 2010, **17**, 107.

105 M. R. Maurya, S. J. Titinchi and S. Chand, *J. Mol. Catal. A: Chem.*, 2003, **193**, 165–176.

106 B. Nethravathi, K. Mahendra and K. R. K. Reddy, *J. Porous Mater.*, 2011, **18**, 389–397.

107 B. Nethravathi, P. Manjunathan and K. Mahendra, *J. Porous Mater.*, 2016, **23**, 1305–1310.

108 R. Abraham and K. Yusuff, *J. Mol. Catal. A: Chem.*, 2003, **198**, 175–183.

109 A. Mobinikhaledi, M. Zendehdel, S. M.-B. Hosseini-Ghazvini and P. Safari, *Transition Met. Chem.*, 2015, **40**, 313–320.

110 A. Mobinikhaledi and M. Jabbarpour, *Res. Chem. Intermed.*, 2015, **41**, 511–523.

111 L. Xu, J. Zhang, Z. Li, Q. Ma, Y. Wang, F. Cui and T. Cui, *New J. Chem.*, 2019, **43**, 520–526.

112 M. Kooti, F. Kooshki and E. Nasiri, *Res. Chem. Intermed.*, 2019, **45**, 2641–2656.

113 (a) Z. An, Y. Guo, L. Zhao, Z. Li and J. He, *ACS Catal.*, 2014, **4**, 2566–2576; (b) S. M. Islam, A. S. Roy, R. C. Dey and S. Paul, *J. Mol. Catal. A: Chem.*, 2014, **394**, 66–73; (c) A. Lu, T. P. Smart, T. H. Epps III, D. A. Longbottom and R. K. O'Reilly, *Macromolecules*, 2011, **44**, 7233–7241.

114 M. Khajehzadeh, M. Moghadam and S. Jamehbozorgi, *Inorg. Chim. Acta*, 2019, **485**, 173–189.

115 (a) A. Zhu, P. Tan, L. Qiao, Y. Liu, Y. Ma, X. Xiong and J. Pan, *Inorg. Chem. Front.*, 2017, **4**, 1748–1756; (b) L. Hu, F. Peng, D. Xia, H. He, C. He, Z. Fang, J. Yang, S. Tian, V. K. Sharma and D. Shu, *ACS Sustainable Chem. Eng.*, 2018, **6**, 17391–17401; (c) B. Sahoo, A. E. Sorkus, M. M. Pohl, J. Radnik, M. Schneider, S. Bachmann, M. Scalone, K. Junge and M. Beller, *Angew. Chem., Int. Ed.*, 2017, **56**, 11242–11247.

